INVESTIGATION OF HYDROGEN STORAGE CAPABILITIES AND RELATED PROPERTIES OF VARIOUS NANO-MATERIALS BY USING COMPUTATIONAL CHEMISTRY METHODS

PhD Thesis

Sinan SAYHAN

Department of Chemistry

İzmir

2019

T.R.

EGE UNIVERSITY

Graduate School of Applied and Natural Science

INVESTIGATION OF HYDROGEN STORAGE CAPABILITIES AND RELATED PROPERTIES OF VARIOUS NANO-MATERIALS BY USING COMPUTATIONAL CHEMISTRY METHODS

Sinan SAYHAN

Supervisor : Prof. Dr. Armağan KINAL

Department of Chemistry

Physical Chemistry Third Cycle Programme

İzmir

2019

Sayın Sinan SAYHAN tarafından Doktora Tezi olarak sunulan "**Investigation of Hydrogen Storage Capabilities and Related Properties of Various Nano-Materials by Using Computational Chemistry Methods**" başlıklı bu çalışma E.Ü Lisansüstü Eğitim ve Öğretim Yönetmeliği ile E.Ü Fen Bilimleri Enstitüsü Eğitim ve Öğretim Yönergesi'nin ilgili hükümleri uyarınca tarafımızdan değerlendirilerek savunmaya değer bulunmuş ve 14.02.2019 tarihinde yapılan tez savunma sınavında aday oybirliği/oyçokluğu ile başarılı bulunmuştur.

Jüri Üyeleri: **İmza**
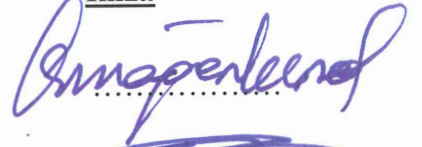
Jüri Başkanı   :Prof. Dr. Armağan KINAL   ....

Raportör Üye   :Prof. Dr. Cenk SELÇUKİ   ....

Üye   : Prof. Dr. Okan ESENTÜRK   ....

Üye   : Doç. Dr. Nursel ACAR SELÇUKİ   ....

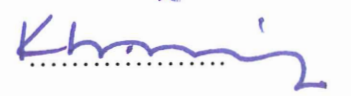**Üye**   : Doç. Dr. Kamil ŞİRİN   ....

EGE ÜNİVERSİTESİ FEN BİLİMLERİ ENSTİTÜSÜ

ETİK KURALLARA UYGUNLUK BEYANI

EÜ Lisansüstü Eğitim ve Öğretim Yönetmeliğinin ilgili hükümleri uyarınca Doktora Tezi olarak sunduğum **"Investigation of Hydrogen Storage Capabilities and Related Properties of Various Nano-Materials by Using Computational Chemistry Methods"** başlıklı bu tezin kendi çalışmam olduğunu, sunduğum tüm sonuç, doküman, bilgi ve belgeleri bizzat ve bu tez çalışması kapsamında elde ettiğimi, bu tez çalışmasıyla elde edilmeyen bütün bilgi ve yorumlara atıf yaptığımı ve bunları kaynaklar listesinde usulüne uygun olarak verdiğimi, tez çalışması ve yazımı sırasında patent ve telif haklarını ihlal edici bir davranışımın olmadığını, bu tezin herhangi bir bölümünü bu üniversite veya diğer bir üniversitede başka bir tez çalışması içinde sunmadığımı, bu tezin planlanmasından yazımına kadar bütün safhalarda bilimsel etik kurallarına uygun olarak davrandığımı ve aksinin ortaya çıkması durumunda her türlü yasal sonucu kabul edeceğimi beyan ederim.

14 / 02 / 2019

Sinan SAYHAN

ÖZET

ÇEŞİTLİ NANO-MATERYELLERİN HİDROJEN DEPOLAMA KAPASİTELERİNİN VE İLGİLİ ÖZELLİKLERİNİN HESAPLAMALI KİMYA METOTLARI KULLANILARAK İNCELENMESİ

SAYHAN, Sinan

Doktora Tezi, Kimya Anabilim Dalı
Tez Yöneticisi: Prof. Dr. Armağan KINAL
Şubat 2019, 110 sayfa

Bu tezde, Bor Nitrür (BN), Alüminyum Nitrür(AlN) ve Silisyum Karbür (SiC) gibi nano yapıların (nanokafes, nanolevha, vs.) hidrojen depolama ve ilgili özellikleri hesaplamalı kimya metotları kullanılarak incelenmiştir. BN, AlN ve SiC nanolevha yapılarında hidrojen molekülü ile en fazla etkileşime giren alanlar bulunur. Bu alanlar hidrojen molekülü için güvenli bölgeler olarak tanımlanabilir. Güvenli bölgelere göre, nanolevha yapıların hidrojen depolama özellikleri belirlenmiştir. Yapılan hesaplamalara göre, SiC nanolevha molekülü diğer nanolevha yapılara göre daha iyi bir hidrojen depolama aracıdır. Ayrıca CCSD(T) referans metoda göre kovalent olmayan zayıf etkileşimlere sahip BN ve AlN nanokafes sistemleri için en iyi Yerel Yoğunluk Teorisi (DFT) metodu ve yarı deneysel metodu belirlenmiştir. Kullanılan DFT metotları ve yarı deneysel metotlar arasında, bu tür sistemler için DFT-ωB97X-D ve PM6-DH2 metodları en iyi metot olarak belirlenmiştir. Ayrıca, PM6-DH2 metodu, DFT-ωB97X-D metodu kadar iyi sonuç verir ve hesaplama zamanı açışından ωB97X-D göre çok daha uygundur. Bunun yanında, bu tür nanokafes yapılar için, hidrojen molekülünün içsel mi yoksa dışsal olarak mı depo edilebileceği incelenmiştir. Yapılan hesaplamalara göre, AlN nanokafes yapısının içerisine hidrojen molekülü depo edilebilirken BN nanokafes yapısına edilemez. Bunun sebebi ise hidrojen molekülü BN nanokafesinin içerisinden geçerken B-N bağını kırar. Bir başka ifadeyle, BN nanokafes yapısı hidrojen molekülünü dışsal olarak depo edebilir. Hidrojen molekülü ilavesiyle AlN nanokafes yapısı, BN nanokafes yapısına göre daha kararlıdır. Bu yüzden AlN nanokafes yapısı BN nanokafes yapısına göre daha iyi bir hidrojen depolama materyalidir.

Anahtar kelimeler: BN, AlN ve SiC Nanoyapılar, Hidrojen Depolama, DFT, PM6-DH2 Yarı Deneysel Metodu.

ABSTRACT

INVESTIGATION OF HYDROGEN STORAGE CAPABILITIES RELATED PROPERTIES OF VARIOUS NANO-MATERIALS BY USING COMPUTATIONAL CHEMISTRY METHODS

SAYHAN, Sinan

PhD Thesis, Chemistry Department
Thesis Supervisor: Prof. Dr. Armağan KINAL
February 2019, 110 pages

In this thesis, hydrogen storage and related properties of nanostructures such as Boron Nitride (BN), Aluminum Nitride (AlN) and Silicon Carbide (SiC) were investigated by using computational chemistry methods. In the structures of the BN, AlN and SiC nanosheets, there are areas that most interact with the hydrogen molecule. These areas can be defined as safe zones for the hydrogen molecule. According to the safe zones, hydrogen storage properties of nanosheet structures have been determined. According to the calculations, the SiC nanosheet molecule is a better hydrogen storage medium than the other nanosheet. In addition, the best density functional theory (DFT) and the semi-empiric method were determined for the BN and AlN nanocage systems having weak non-covalent interactions according to the CCSD(T) reference method. Among the DFT methods and semi-empiric methods used, the DFT-ωB97X-D and PM6-DH2 methods were the best method for those systems. In addition, the PM6-DH2 method gives good results as well as the DFT-ωB97X-D method and it is more suitable in terms of computing time according to DFT-ωB97X-D method. In addition, for those nanocage structures, it has been investigated whether the hydrogen molecule can be stored as endohedral or exohedral form. According to the calculations, hydrogen cannot be stored in the BN nanocage structure while the hydrogen molecule can be stored in the AlN nanocage structure. The reason of this is that the hydrogen molecule breaks the B-N bond as it passes through the BN nanocage. In other words, the BN nanocage structure can store hydrogen molecule as exohedral form. By the addition of hydrogen molecule, the structure of AlN nanocage is more stable than the structure of BN nanocage. Therefore, the AlN nanocage structure is a better hydrogen storage material than the BN nanocage structure.

Keywords: BN, AlN and SiC Nanostructures, Hydrogen Storage, Density Functional Theory (DFT), PM6-DH2 Semi Empiric Method.

PREFACE

In this thesis, I present the hydrogen storage and related properties of various nanostructures by using computational chemistry methods. Because of my special interest in computational chemistry, the results of this thesis all contains theoretical studies. With the increasing industrialization, the consumption of fossil fuels is increasing day by day in the world. Therefore, alternative energy sources that can be used instead of fossil fuels have investigated. One of these alternative energy sources is the hydrogen energy. The biggest problem of hydrogen is the storing problem. Therefore, some nano-structures having hydrogen storage properties were determined and their hydrogen storage properties were compared each other by using computational chemistry methods. The purpose of this thesis is to shed light on the scientists who will work on these issues.

IZMIR   Sinan SAYHAN

14/02/2019

CONTENTS

CONTENTS (Continiued)

CONTENTS (Continiued)

LIST OF FIGURES

LIST OF FIGURES (Continued)

LIST OF FIGURES (Continued)

LIST OF TABLES

LIST OF TABLES (Continued)

SYMBOLS AND ABBREVIATIONS

Symbols	**Explanations**
ξ	Exponent of the Slater type orbital (STO)
$\hbar$	Planck constant
χ_i	i^{th} Atomic Orbital
φ_λ	One-electron wave function
ψ	Wave function
c_{ij}	Coefficient of linear combination
E_o	Ground state energy
f_1 and E_{xc}	Functional of electron density
H_o	Hamiltonian operator of one electron
$I(i)$	Hartree Operator
$J(i)$	Fock Operator
M_a	Mass of nucleus a
R_{ab}	Distance between the ath and b^{th} nucleus
r_{ia}	Distance between the ith and nucleus a
r_{ij}	Distance between the i^{the} and j^{th} electron
S	Overlap matrix

SYMBOLS AND ABBREVIATIONS (Continued)

Symbols	**Explanations**
T_e	Kinetic energy operator of the electrons
T_n	Kinetic energy operator of the nuclei
U	Electron – Electron coulomb interaction Unperturbed energy
V_{ee}	Repulsion energy operator of the electron-electron
V_{ne}	Electron – nucleus attraction energy operator
V_{nn}	Repulsion energy operator of the nucleus-nucleus
W_1, W_2, etc.	First order, second order, and etc. order corrections to the Unperturbed energy
Y_{lm}	Angular shape of wave function
Z_a	Atomic number of nucleus a
Z_j	Nucleus charge of the J^{the} atom
α	Exponent of the Gaussian Type Orbital (GTO)
$\alpha_{1/2}$	½ magnetic spin quantum number
$\beta_{1/2}$	-½ magnetic spin quantum number
ε_λ	Lagrange multiplier
ρ	Molecular density
Ψ_1, Ψ_2, etc.	Wave functions

SYMBOLS AND ABBREVIATIONS (Continued)

Abbreviations	Explanations
AM1	Austin Model 1
B3LYP	Becke's Three-parameter Hybrid Methods with Exchange Functional of Lee
BOA	Born-Oppenheimer Approximation
BNNTs	Boron Nitride Nanotubes
CI	Configuration Interaction
CNTs	Carbon Nanotubes
DOE	The US Department of Energy
DFT	Density Functional Theory
DODS	Different Orbitals for Different Spins
ESM	Electronic Structure Methods
DZ	Double Zeta
EC	Electron Correlation
GTO's	Gaussian Type Orbitals
HF	Hartree-Fock
HOMO	Highest Occupied Molecular Orbital
LCAO	Linear Combination of Atomic Orbitals

SYMBOLS AND ABBREVIATIONS (Continued)

Abbreviations	Explanations
LUMO	Lowest Unoccupied Molecular Orbital
MM	Molecular Mechanics
MNDO	Modified Neglect of Diatomic Overlap
MO	Molecular Orbital
MP	Moller-Plesset
MP2, MP3, etc.	Moller-Plesset theory at second order, third order, etc.
ωB97X-D	The latest functional from Head-Gordon and coworkers, which includes empirical dispersion
PBE1PBE	Hybrid Functional of Perdew, Burke ana Ernserhof
PM3	Parametric Method 3
PM6	Parametric Method 6
QM	Quantum Mechanics
RHF	Restricted Hartee-Fock
ROHF	Restricted Open Shell Hartee-Fock
RS-PT	Rayleigh-Schrödinger Perturbation Theory
SCF	Self Consistent Field
STO's	Slater Type Orbital

SYMBOLS AND ABBREVIATIONS (Continued)

Abbreviations	Explanations
TZ	Triple Zeta
UHF	Unrestricted Hartee-Fock
VBT	Valence Bond Theory

1. INTRODUCTION

The fossil fuels derived from the remains of former life are carbon-based organic materials such as coal, petroleum, natural gas. The easiest way to gain energy is to burn fossil fuels with molecular oxygen. Fossil fuels are seen as energy sources. For instance, electricity is produced with burning them or fuel for transportation is obtained when fossil fuels refine. The date of first usage of fossil fuels was in 1759 when beginning of industrialization in England. After that, the fossil fuels have attracted by many organizations to supply world's energy needs. In the last decades, requirement of energy obtained from fossil fuels has extremely increased due to growing industrial companies that produce a plenty of technological things such as mobile, automotive applications, etc. In other words, the world's energy needs are grown dramatically with the developing industrial technology as word's population increase. Therefore, a large amount of fossil fuel will be needed to meet the world's future energy needs. (Figure1.1). Although usage of fossil fuels may be seen advantageous in terms of producing energy, they have plenty of disadvantages in their consumptions. The worst disadvantage of fossil fuel usage is very bad influence for the environment since various harmful and toxic gases is given off when they are burned. These gases, known as CO_2, SO_3 and NO_2 molecules lead to global warming which are considered as slowly heating of north pole, ocean sand atmosphere in the earth. The fundamental reason of global warming is CO_2 gas emission that comes from primary energy sources including fossil fuels. To reduce CO_2 emission, it must be search for new energy sources that provide world's energy requirement instead of using fossil fuels. Therefore, scientists have been looking for an alternative energy sources having clean, renewable, environmental-friendly, namely; secondary energy resources such as wind power, solar energy, biofuels, and geothermal energy. The energy obtained from these secondary energy resources may not be totally enough to satisfy the world's whole energy need, but at least they do not have any hazardous effect to the environment. In other words, they do not emit CO_2 gas leading to global warming.
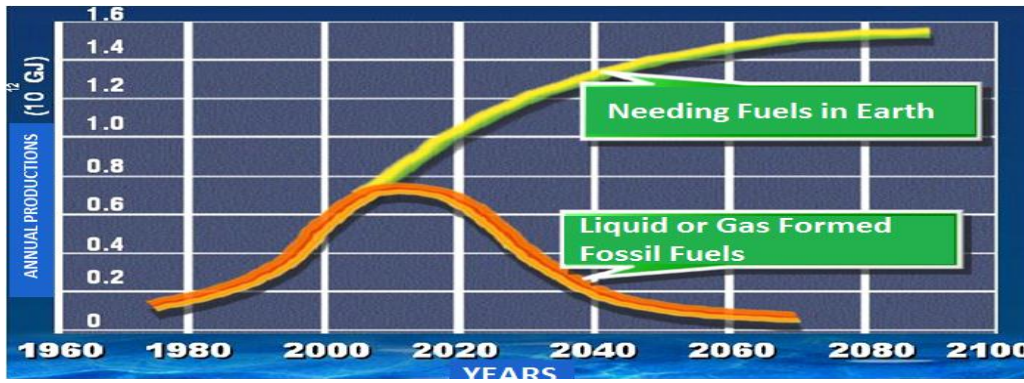
Figure 1.1. The relationship between fossil fuels and annual production according to years.

Wind energy is an alternative energy source where wind turbines captures wind's power and converts it into electricity. Wind energy usage has dramatically increased in years and it reached around 4% of nationwide electric power usage (Fthenakis and Kim, 2009) in UK. The solar energy is produced by converting sunlight into electricity with the use of solar materials namely; solar cells, solar panels, photovoltaics, some of nanomaterials, etc.(Chen et al., 2009). There are plenty of studies (Cook et al., 2010; International Energy Agency IEA, 2011; Lewis and Nocera, 2006; Solangi et al., 2011) about solar energy published by a lot of scientists from different countries in the world since it is the fastest growing renewable energy source (Figure2.1) (Gtz, 2010).
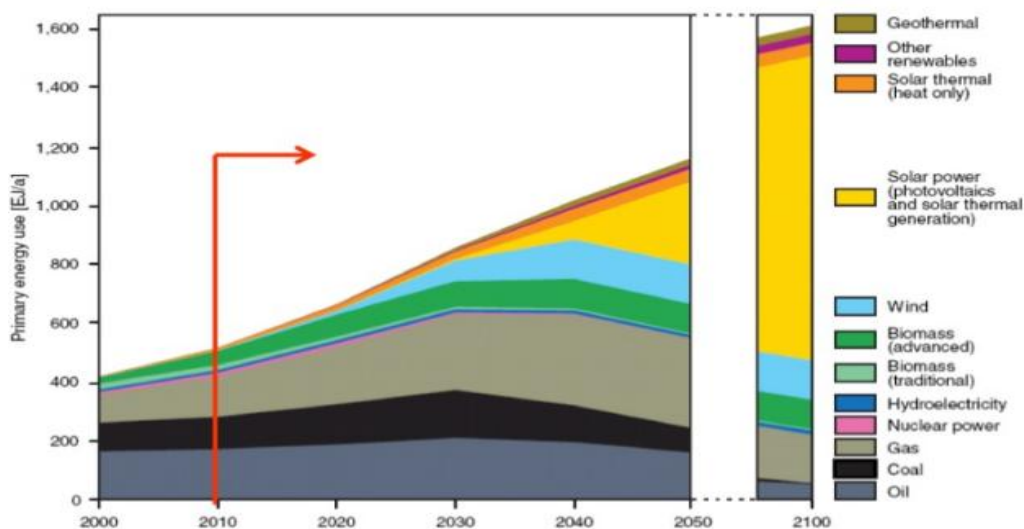
Figure 1.2. The transforming global energy mixture exemplary path until 2050/2100.

Biofuel is an alternative energy produced from materials derived from biological sources namely; plants, woods, vegetable oils, seeds, etc. Therefore, there are many of type of biofuels that are commonly known as biodiesel (e.g. bioethanol). However, none of them can take place of petroleum for mobile applications due to having their low productions capacity (Hassan and Kalam, 2013). The geothermal energy, which is also known as heat energy, is produced from the difference in temperature between the core of the planet and its surface. However, it cannot be produced everywhere; so, the resource of this energy has the limit. Besides these secondary energy resources mentioned above, hydrogen energy is also another important energy source since it is the cheapest and the cleanest of all other secondary energy resources. Moreover, hydrogen energy may be considered as the best alternative energy source because hydrogen is not only conventional fuel for transportation with its high energy content (Figure 1.3) but also it is used as the energy carrier in fuel cells (Cheng et al., 2001). To produce hydrogen energy, there are various hydrogen sources such as water, ammonia, hydrazine, etc.
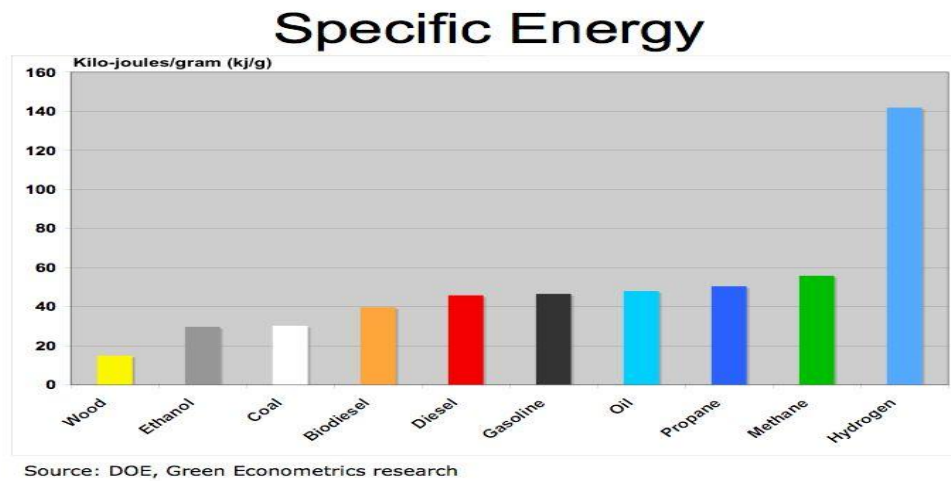
Figure 1.3. The specific energy produced from the energy sources materials per kj/g.

Some kinds of algae, for instance, such as Cyanobacteria can produce molecular hydrogen with the help of the hydrogenase enzyme shown in equation 1. The efficiency of molecular hydrogen for the following reaction is found to be %10-20 percentage by Gaffron (Algae and Rubin, 1942) and his coworkers.

$$2H^+ + 2X_{reduced} \rightarrow 6H_2 + 2X_{oxidised} \tag{1.1}$$

Molecular hydrogen is produced by electrolysis of water and the energy required for this process is provided by wind power. Instead of proton exchange electrodes (PEM), alkaline electrodes (KOH) can be used for enhancing capacity of hydrogen obtained from the electrolysis of water (Barbir, 2005), but this technique has some limitations such as discontinuous and variable wind velocity, cost of electrolysis. Hydrogen is the most abundant element in the universe. However, most of the earth's hydrogen is found as in the form of water rather than the molecular form (two hydrogen atoms are bound to the oxygen atom of the water). Hydrogen gas (energy) can be released from the water when it is heated to elevated temperatures. This method is known as thermolysis of the water. The electrolysis of water is the other hydrogen source where the water splits into hydrogen and oxygen molecules by using the electricity. Although this technique can be applied easily, obtaining hydrogen from the water is not efficient due to costly electricity consumption (Hofmann and Kreuter, 1998). In other words, it is not logical to consume electricity for producing hydrogen energy instead of using molecular hydrogen. The reaction of the electrolysis of water is summarized with the following reaction:

$$\text{Cathode(Reduction): } 2H_2O_{(l)} + 2e^- \rightarrow H_2(g) + 2OH^- \tag{1.2}$$

$$\text{Anode(Oxidation): } 2H_2O_{(l)} \rightarrow O_2(g) + 4H^+ \text{ (aq)} + 4e^- \tag{1.3}$$

$$\text{Overall Reaction: } 2H_2O_{(l)} \rightarrow O_2(g) + 2H_2(g) \tag{1.4}$$
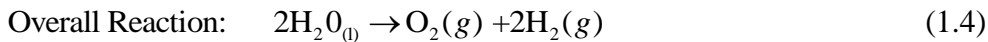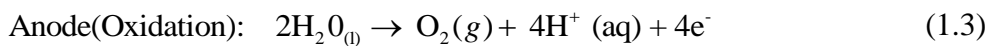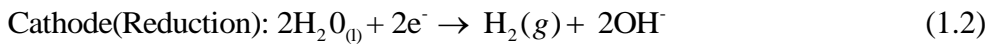
Hydrogen energy can be produced from the Solar energy by using Ru complex, namely $[Ru(bpy)3]^{+2}$ as a photosensitizer(Li et al., 2009). The general process of producing hydrogen is to excite Ru cationic complex. This process makes Ru cationic complex stronger oxidant and reductant. In conclusion, molecular hydrogen is separated from the Ru cationic complex. The photo splitting reaction of the water by using the $[Ru(bpy)3]^{+2}$ complex is summarized with the following reaction.

$$2\left[\,^{*}\mathrm{Ru(bpy)_3}\right]^{+2} \rightarrow \left[\mathrm{Ru(bpy)_3}\right]^{+3} +2\mathrm{OH^-} +\mathrm{H_2} \qquad 0.45\mathrm{V} \qquad (1.5)$$

$$2\left[\,^{*}\mathrm{Ru(bpy)_3}\right]^{+2} +\mathrm{H_2O} \rightarrow 2\left[\mathrm{Ru(bpy)_3}\right]^{+2} +\frac{1}{2}\mathrm{O_2} +2\mathrm{H^+} \quad 0.44\mathrm{V} \qquad (1.6)$$
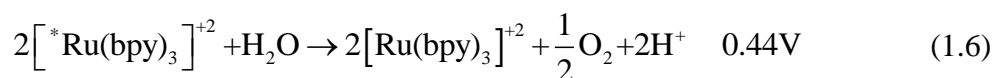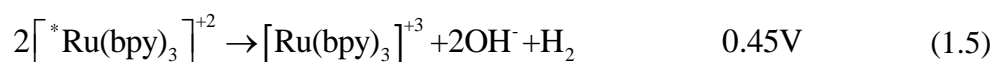
Addition, the water can photochemically dissociate into molecular hydrogen and oxygen by using semiconductors that are also known as photo catalysts, such as TiO_2 and Pt added into the TiO_2(Kudo and Miseki, 2009) molecule. The most common hydrogen production in the world are provided by fossil fuels such as methane gas or oil. The products produced in this way are hydrogen molecule, and carbon dioxide gas leading to global warming (Izquierdo et al., 2012). Therefore, hydrogen source of this type is not desirable due to destructive environmental effect.

$$\mathrm{CH_4} +\mathrm{H_2O} \rightarrow \mathrm{CO_2} +3\mathrm{H_2} \qquad (1.7)$$

Methanol production from biomass is another technique for hydrogen production nevertheless this method must be developed to reduce environmental damage (Galindo Cifre and Badr, 2007). In other words, there is requirement of carbon based materials in methanol production, so, this is undesirable situation.

Yang and his coworkers(Yang et al., 2010) also showed that 48% percent of hydrogen need in the earth is provided by using natural gas, 30% from oil, 18% from coal. In addition, the small percentage of hydrogen production (about 2%) is ensured by the electrolytic incidents.

The Department of Energy (DOE) has announced that percentages of gravimetric and volumetric density of hydrogen by 2020 are 5.5wt% and 4.0 v%, respectively. If the energy consumption increases in the world, the demand of oil will reduce nearly from 90% to 60% for the automotive industries by the year 2040 (Kruger, 2001). Although hydrogen has many advantages such as clean, renewable and non-destructive for environmental, main problem of the hydrogen energy is that it cannot be effectively stored in some materials at desired conditions. The hydrogen storage materials must have unique properties such as high storage capacities,

favorable thermodynamic properties, fast H_2 uptake and H_2 release rates, etc. Therefore, new hydrogen storage materials are still being investigated along with the conventional storage methods.

1.1 Hydrogen Storage Materials

Currently employed hydrogen storage materials are divided into two groups namely; mechanical and chemical hydrogen storage materials (FAKIOLU, 2004) However, scientists are still investigating new hydrogen storage materials since currently known materials are not very economical and sufficient, yet.
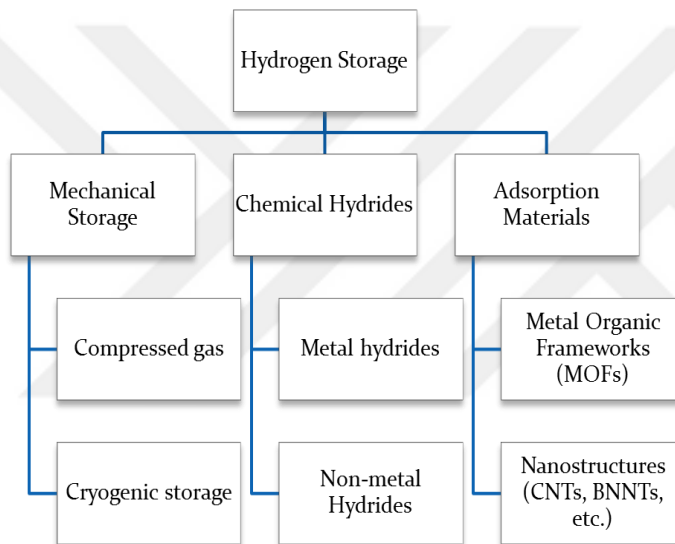
Figure 1.4. Hydrogen storage methods as schematically.

The mechanical storage, in which hydrogen molecules are stored both gas and liquid forms by utilizing pressure and temperature, are split into two types. Compressed hydrogen storage method is a method where hydrogen gas is being kept under high pressure inside the pressure-resisting cylinder tanks. Hydrogen gas can be stored physically at least 345 atm pressure. Therefore, they need pressure-resisting tanks. Nowadays, hydrogen can be stored under higher pressures (>345 atm) inside newly discovered high pressure-resisting cylinder tanks produced from some composite materials such as aluminum, steel and stainless steel etc. This increasing pressure leads to an increase in volumetric hydrogen density inside the tank due to the tensile strength of the material (Züttel, 2004). As pressure increases

the gravimetric density of hydrogen decreases since the thickness of the cylinder tank increases. Therefore, both the gravimetric and volumetric densities depend on the stamina of the material at the elevated pressures (Figure 1.5).

Although hydrogen storage with compressed hydrogen gas may be seen a reasonable method to reach the DOE's target, indeed, the probability of capturing the target is quite low.
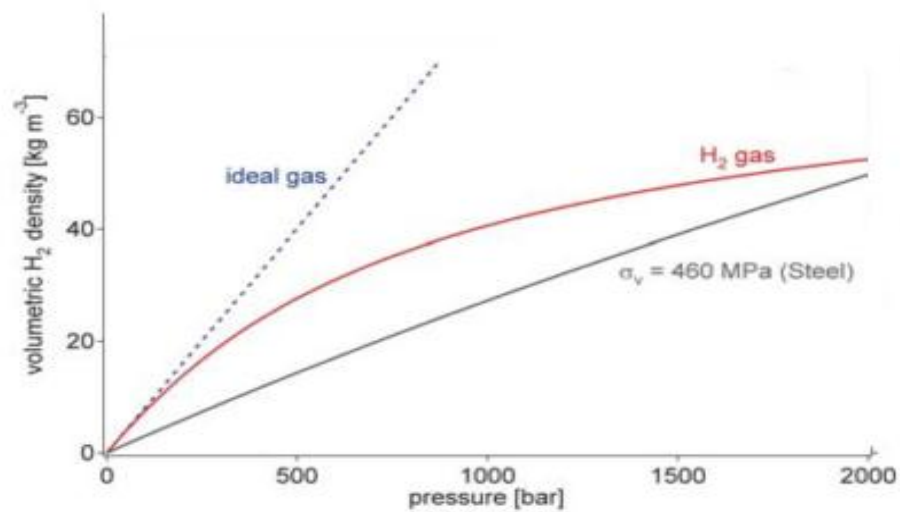
Figure 1.5. Volumetric density of hydrogen as a functional of gas pressure.

The boiling point of hydrogen is 20 K under which hydrogen is in the form of liquid. In other words, the hydrogen molecule turns into liquid form when it is cooled under its critical temperature (33K) where there is an equilibrium between vapor and liquid forms. Thus, liquid hydrogen can be stored in cryogenic tanks that converts any gas to the liquid phase. The rate of liquid hydrogen storage in the cryogenic tanks is the highest. For instance, the gravimetric density of hydrogen in cryogenic tanks (0.070 kg L^{-1}) is slightly higher than that of hydrogen in compressed tanks (0.030 kg L^{-1})(McCarty, 1981). Although the highest storage density is in cryogenic tanks, the most important thing for this kind of storage method is to avoid heat exchange between tanks and their environment. In other words, the cryogenic tanks must be isolated from their environment because of hydrogen's low critical temperature. The liquefaction process of hydrogen is based on the weak binding between hydrogen atoms or molecules and the cryogenic tanks.

Therefore, the new isolated and strong cryogenic tanks have been investigated for liquid hydrogen storage (Satyapal et al., 2007). This method is seen to be very useful for the hydrogen storage due to having high-efficiency storage. However, in a study by Hirscher it is shown that there are some issues that can be faced during the liquefaction of hydrogen. These problems are the high price of the tank, need of a large amount of energy for the process and the difficulty of reversible hydrogen release (Hirscher and Borgschulte, 2010). For example, hydrogen molecules exhibit two forms namely para and ortho hydrogen due to its electronic configuration. While the para hydrogen is known that the total antiparallel nuclear spin of hydrogen is zero (S=0) having one quantum state, the ortho hydrogen is known as the total antiparallel nuclear spin of hydrogen is one (S=1) having three quantum states. The energies and physical properties of these two forms are slightly different. For instance; the energy of Ortho hydrogen is bigger than that of para hydrogen. While the 75 percent of normal hydrogen is in the ortho form, 25 percent of normal hydrogen is in the para form at ambient conditions but liquid hydrogen is in almost 100% para form. Ortho hydrogen converts to para form slowly once the hydrogen is cooled to its melting point, and the conversion reaction enthalpy from ortho to para is exothermic. The value of the conversion enthalpy is 0.15 kWh/kg that is greater than the heat of vaporization of hydrogen (0.12 kWh/kg) so huge energy loss will happen during the process. To avoid the extreme amount of energy, some catalysts are employed for the process such as nickel, charcoal, tungsten (Schlapbach and Züttel, 2001).

Generally, gases can be liquefied by one of three general methods: The first is to compress the gas at temperatures lower than its critical temperature. The other is to make the gas work against external pressure. This causes the gas to lose its energy and change its liquid state. The last one is to cause the gas to lose its energy and liquefy by allowing it to work against its internal pressure.

There are many materials can hold hydrogen atom(s) or molecular hydrogen(s) either chemically or physically, or producing hydrogen molecule at desired conditions. Carbon, boron-nitride, silicon-based nanomaterials are among these materials. The chemical hydrogen storage is a method that gives hydrogen molecule during the chemical process. Throughout this process, the energy needed

to release the hydrogen molecule is very important. There are a variety of chemical hydrogen storage materials producing hydrogen atoms such as ammonia (and its derivatives), non-metal hydrides (carbohydrate, formic acid) and metal hydrides.

The ammonia (also known as azane) is a chemical compound that is produced from nitrogen (N_2) and H_2 molecules. The ammonia is a colorless gas with a wizen smell and is used for many areas in industries such as food, pharmaceutical, and cleaning products. For that reason, it is extremely widely produced in the world. Although the consumption of ammonia is huge, it is an extremely hazardous substance when it is concentrated. Green is the first scientist to discover that ammonia is the source of hydrogen (Green, 1982). He suggested that hydrogen produced in a nuclear reactor could be used as a source of ammonia that can be produced from nitrogen in the air with the help of Haber- Bosch process by using a metal catalyst under high temperatures and pressures. In addition, he also claimed that the ammonia can be used as an alternative energy vector. The equation producing ammonia is summarized as follows.

$$N_2 + 3\,H_2 \rightarrow 2\,NH_3 \quad (\Delta H° = -21940 \text{ cal}) \tag{1.8}$$
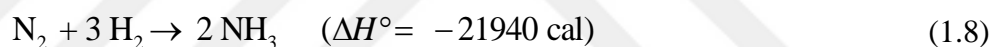
There are several advantages of ammonia as an alternative energy source. These include a simple decomposition that can produce hydrogen, a good hydrogen yield and low cost (Glenn, 2005). Besides, the ammonia usage as a fuel does not produce any CO2 gas because the ammonia does not include carbon atom. The mixture of liquid ammonia and water has the maximum hydrogen capacity. In other words, the hydrogen capacity of the liquid ammonia is 17.6 wt% higher than that of DOE hydrogen target. There are many derivatives of the ammonia that have high hydrogen content such as hydrazine (N2H4), ammonia borane (BNH6), metal ammine complexes, ammonia carbonate (NH4)2CO3 and urea (CH4N2O). For example, the hydrogen content of the hydrazine molecule is nearly 12.5 wt% (Serov and Kwak, 2010). The ammonia borane is the most significant derivative of the ammonia for the direct hydrogen production since its hydrogen content is 12.5 wt% (Chandra and Xu, 2006).

$$NH_3BH_3 + 2H_2O \rightarrow NH_4^+ + BO_2^- + 3H_2 \tag{1.9}$$
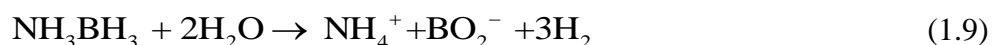
Theoretical calculations of hydrogen storage properties for some metal ammine complexes give good agreement with experimental results (Sorensen et al., 2008). The hydrogen from ammonia is produced with the help of decomposition of ammonia without any catalysts at the extremely higher temperature(Ma et al., 2006). Hydrogen can also be produced from the ammonia at lower temperature (at least 300^0C) by using some catalysts namely, Ru/ZrO_2, Cr_2O_3 and Ce-Ru/Graphite. Among them, the best catalyst for the decomposition is Ce-Ru/Graphite because of having a high hydrogen storage capacity (Lan et al., 2012). On the other hand, There are some nanoparticles that lead to hydrazine decomposition at ambient conditions such as $Rh_{(0)}$, Rh_4Ni, $Ni_{0.93}Pt_{0.07}$, $Ni_{0.95}Ir_{0.05}$(Singh and Xu, 2009). Although the ammonia and its derivatives have a good capacity of hydrogen storage, the safe hydrogen transportation on the vehicles are the main problem. In other words, these problems have same trend with the hydrogen economy's issues. Therefore, the safe transport of hydrogen from ammonia and its derivatives under ambient conditions is still being investigated.

Another hydrogen storage material is the formic acid (HCOOH), known as methanoic acid, which has a pungent odor and it is colorless liquid at room temperature. It is produced in the atmosphere because of forest emissions and it is also found in ants in nature. It is produced from carbon monoxide and sodium hydroxide in the presence of the sulfuric acid catalyst in the laboratory. The formation of formic acid is summarized with the following reaction.

$$CO+NaOH \rightarrow HCOONa \rightarrow HCOOH \qquad (1.10)$$

The gaseous formic acid does not obey to ideal gas laws since it has hydrogen bonds between its molecules in the gas phase. It is a very useful chemical because it is employed in many applications in medicine and industry. Recently, researchers see formic acid as one of hydrogen storage materials(Joó, 2008). Hydrogen can be produced from formic acid in two ways, the first one is the chemical separation of hydrogen from formic acid in fuel cells (CFAFCs), and the second is direct formic acid fuel cells (DFAFCs). The hydrogen efficiency of DFAFCs is better than that of CFAFCs. In addition, DFAFCs are more suitable for vehicles, other energy applications of future and mobile devices. Hydrogen production from DFAFCs is

done by a redox reaction where two electrons are oxidized in the anode and two electrons reduce the O_2 in the cathode. During this process, CO gas may be obtained from formic acid. This is an undesirable situation. In addition, CO can damage to the catalysts in the fuel cell. General reactions will be summarized as follows:

$$\text{Anode: } HCOOH \rightarrow CO_2 + 2H^+ + 2e^- \qquad E^0 \cong -0.25 \text{ V} \qquad (1.11)$$

$$\text{Cathode: } 1/2O_2 + 2H^+ + 2e^- \rightarrow +H_2O \qquad E^0 = 1.23 \text{ V} \qquad (1.12)$$

$$\text{Final: } HCOOH + 1/2O_2 \rightarrow CO_2 + H_2O \qquad E^0_{Cell} \cong 1.48 \text{ V} \qquad (1.13)$$

$$\text{Undesired reaction : } HCOOH \rightarrow CO + H_2O \qquad (1.14)$$
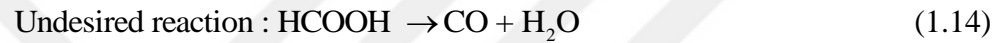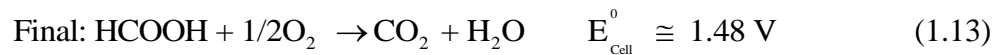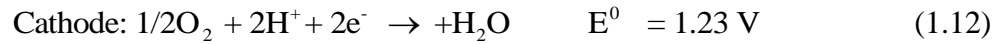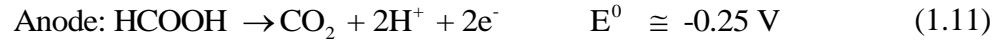
The decomposition of the formic acid includes two main principles for hydrogen production. One of these principles produces CO2 which is a desirable reaction, the other produces CO which is an undesirable reaction (Grasemann and Laurenczy, 2012). Also, the Gibbs Free Energies of these two reactions are very close to each other. The reactions are summarized with the following reactions:

$$HCOOH \rightarrow H_2 + CO_2 \quad \Delta G = -32.9 \text{ kj/mol} \qquad (1.15)$$

$$HCOOH \rightarrow H_2O + CO \quad \Delta G = -28.5 \text{ kj/mol} \qquad (1.16)$$
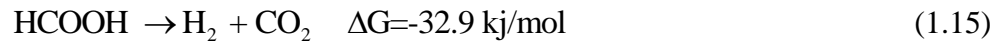
As seen from eq. 15, the formic acid is a hydrogen storage material and its hydrogen storage capacity is 4.4 wt%. The soluble ruthenium catalysts are employed to obtain H_2 and CO_2 molecules (Fellay et al., 2008). The CO_2 emitted can be used to convert back to the formic acid, and this may lead to reducing CO_2 emission. (Singh et al., 2015)(Figure1.6).
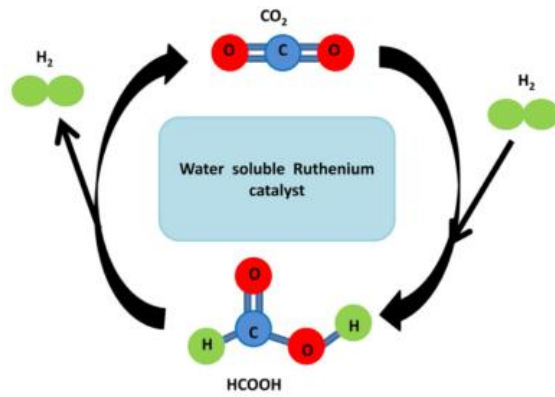
Figure 1.6. Schematic representation of cycle of the formic acid.

One of the hydrogen storage materials is the polymeric carbohydrate with the $C_6H_{10}O_5$ formula. It is also known as bio-resource material having high hydrogen capacity as a liquid form at low-pressure and temperature into the cryogenic tanks. Nowadays, the hydrogen capacity of the polymeric carbohydrate is found 14.8 wt%. The reason for this is that nearly 12 moles of hydrogen are produced from per polymeric carbohydrate water at ambient conditions (Ye et al., 2009; Zhang, 2009, 2011). In other words, the polymeric carbohydrate can be act as hydrogen carrier. The process of hydrogen production from the polymeric carbohydrate is summarized with the following reaction:

$$C_6H_{10}O_{5\ (l)} + 7H_2O_{(l)} \rightarrow 12H_{2\ (g)} + 6CO_{2(g)} \qquad (1.17)$$

Metal hydrides (MHx) are the compounds containing metal atom(s) bonded to a hydrogen atom. Generally, metal hydrides possess the covalent bonds between metal and hydrogen, but some of them have an ionic bond. The hydrogen molecule is absorbed as chemically, known as chemisorption, by the metal hydrides. They are very important compounds for the hydrogen economy because they have high hydrogen storage capacities, nearly 6 wt% (Schulz et al., 1999). The metal hydrides can absorb hydrogen molecules (Figure 1.7) since they have holes between metal and hydrogen atoms. They release hydrogen molecules with the help of heating of tanks (Sakintuna et al., 2007a; Zhou, 2005) at room temperature. Metal hydrides can form two types, namely complex and single hydrides. The single hydrides contain only one metal atom while the complex hydrides contain two or more metal

atoms (M1M2HX). Besides, the single hydrides are generated by Mg, Al and Li atom while complex hydrides are generated by their alanates and alloys. While some of metal hydrides such as NaAlH$_4$ (Bogdanovi et al., 2007; Schüth et al., 2004), AlH3 (Sandrock et al., 2005), and LiBH$_4$ (Zarkevich and Johnson, 2006) reach the gravimetric hydrogen storage target for 2015, (Sakintuna et al., 2007b), LaNi$_5$ (Joubert et al., 2002) cannot reach the target because of its low the hydrogen storage capacity (lower than 2 wt%).

Scientists have shown great interest in magnesium and its metal hydrides due to their hydrogen storage capacities (Grochala and Edwards, 2004). In addition, they have some advantages such as having good thermal resistance and being porous materials for adsorbing hydrogen. Among magnesium and its hydride
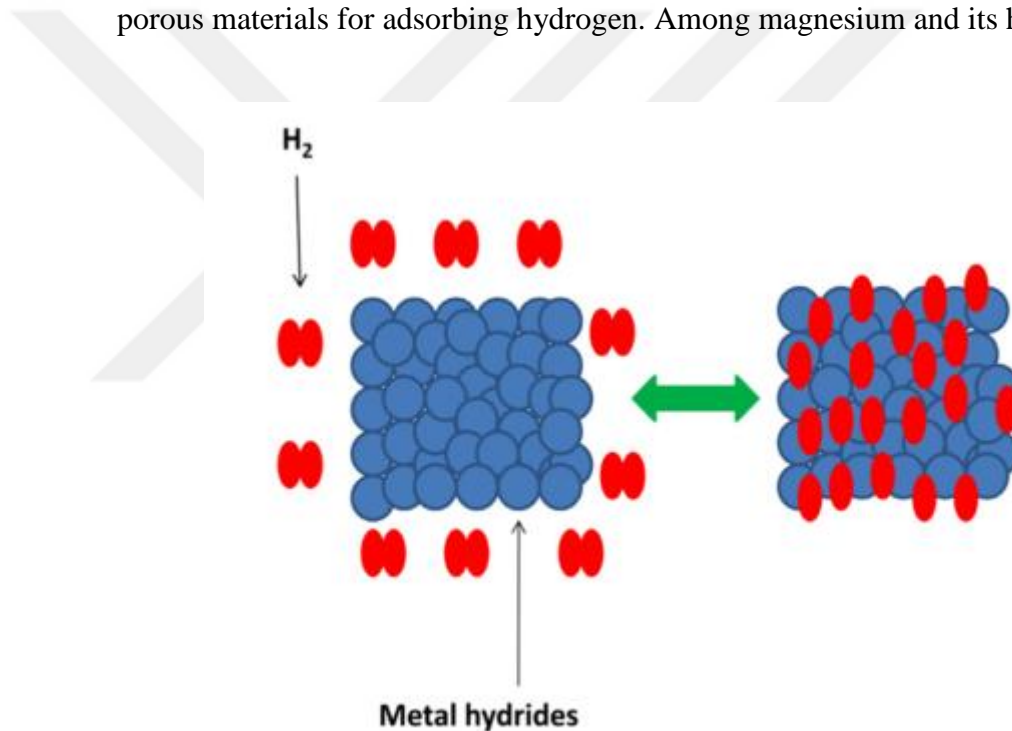
Figure 1.7. Hydrogen adsorption on the metal hydrides.

alloys, the magnesium hydride, MgH$_2$, absorbs more H$_2$ molecules. In fact, the main reason of popularity of Magnesium element is that it is the one of most abundant and cheapest elements in the earth (Zaluski et al., 1997; Zhu et al., 2006). Although MgH$_2$ metal hydrides have excellent hydrogen storage capacity, they have some disadvantages such as a high temperature of hydrogen molecule releasing and irreversible reaction kinetics (Zaluska et al., 1999). In addition, most of the metal

hydrides are highly reactive to the oxygen of the air (Barkhordarian et al., 2004) but, the scientists have managed to produce the metal hydrides and their derivatives for hydrogen storage material at desired conditions. A study published by Chrysler and his co-workers claimed that hydrogen molecule can be produced from the solid sodium borohydride. Then, sodium borohydride was used as hydrogen fuel into the engine of a vehicle invented by a US Company. Besides these, hydrogen can be adsorbed some other materials such as metal organic framework (MOFs), clathrates, carbon (CN_m), boron-nitride $(BN)_m$, aluminum-nitride $(AlN)_m$, silico-carbon $(SiC)_m$ nanomaterials. The hydrogen molecules weakly bind on the surface of these materials because of their porous structures. This weak bond is also known as physisorption. The difference between physisorption and chemisorption is the energy consumption during the hydrogen release from the hydrogen storage materials. In the other way, reversible hydrogen molecules are easily retrieved from the hydrogen storage materials during the physisorption process. Also, there are several advantages of the physisorption. For instance, compressed gas is one of the conventional hydrogen storage methods, but high pressure, leading to hydrogen's safety issues, is necessary for this type of storage. Besides, the huge energy is necessary for liquefaction of hydrogen in cryogenic tanks. Although the metal hydrides seem to be good hydrogen storage material, they release hydrogen molecule at a higher temperature (600°C) and react with the air and oxygen molecules. Therefore, in terms of hydrogen storage, it can be said that the hydrogen physisorption on the surfaces of some materials having higher porosity is much better than their chemisorption.

At the beginning of the 1990s, carbon nanotubes (CNTs) have withdrawn the attention of scientists as the important hydrogen storage materials after they were synthesized by Lijima (Ijiima, 1991). In fact, Dillon(Dillon et al., 1997) and his coworkers found the first experimental evidences where hydrogen molecules can be stored by CNNTs. They, also, suggested that the hydrogen storage capacity of CNTs were extremely higher at the ambient conditions. After their findings, plenty of researchers commenced investigating the hydrogen storage properties of CNTs, experimentally. For instance the article published by Chen (Chen, 1999) was claimed that hydrogen capacity of single wall CNTs extremely enhances by adding alkali metal atom(s) in the carbon nanotubes. According to Chen, the hydrogen

storage capacity of alkali atom doped in CNTs is nearly 14–20 wt% between the 25 $^{\circ}$C and 400°C temperature. This percentage is more than that of metal hydrides. However, Yang (Yang, 2000) disagreed with the Chen's idea because his experimental results showed that hydrogen percentage of alkali metal doped in carbon nanotubes is not accurate because alkali metal reacts with the moisture. Therefore, hydrogen storage percentages of alkali-metal-doped carbon nanotubes are wrong. In other words, the hydrogen storage percentage of alkali-metal-doped carbon nanotubes has a limitation due to having high reactivity of alkali metal. There are several experimental studies about the hydrogen storage properties of different carbon materials such as single wall carbon nanotubes (SWCNT), multiwall (MWCNT) and nanohorns (CNF). Unfortunately, the hydrogen storage capacity of these nanomaterials never passed beyond 0.63 wt% at room temperature at 5 MPa. (Ritschel et al., 2002; Wang and Yang, 2010)(Figure1.8).
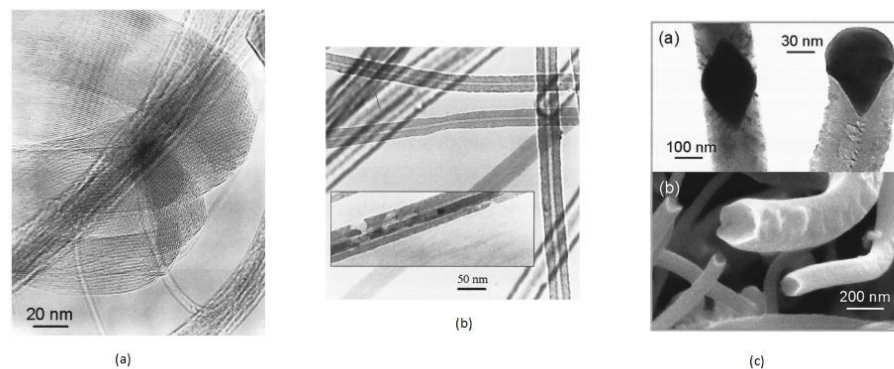
Figure 1.8. Schmatically presentation carbon nanomaterials by using High-resolution transmission electron microscopy, a, b and c donote SWCNT, MWCNT, CNF. respectively.

It is clearly understood that the hydrogen density capacity of pure carbon-nanomaterials could not reach the weight percent determined by DOE due to having weak hydrogen bonding between the hydrogen molecule and the carbon nanomaterial. The reason for this is that the polarity difference between the two carbon atoms is zero. In other words, hydrogen cannot be stored in pure carbon nanomaterials due to having a nonpolar covalent character between the carbon atoms. In fact, there are two plausible ways to enhance weak hydrogen binding at ambient conditions. One of them is doping of a metal (Li, Na, K, Ru, Ni, Ti) on carbon-based material. The other one is to produce new nanomaterials that contain

heteroatoms in carbon-based material. The scientists have initially tried metal atom doping on carbon nanostructures to investigate their hydrogen storage properties instead of producing new nanomaterials. In the article published by Ni (Ni et al., 2010) and coworkers, it is claimed that the hydrogen binding energy of lithium atom doped on charged single walled carbon nanotube ($SWCNT^{+2}$) is higher than that of pure SWCNTs. The maximum hydrogen binding energy of the charged single walled carbon nanotube is 0.26 eV that is considerably appropriative value for the ambient conditions. On the other hand, it was found that Mg-doped MWCNTs (Al-Ghamdi et al., 2012) increase hydrogen binding energy. Also, a new adsorption site was detected by using molecular dynamics (MD) simulations with the quantum chemical calculations. Additionally, the density functional theory (DFT) calculations showed that different graphene structures doped with single calcium atom can hold up to six hydrogen molecules, which makes the hydrogen storage capacity nearly 5 wt% (Lee et al., 2010). It is seen that the reason for the high hydrogen storage capacities in the above-mentioned studies is to change the polarity of the host molecules. While some metals increase the binding energy of hydrogen, doping of the Pt metal does not increase this energy. The hydrogen density capacity of Pt-doped on CNTs produced by using chemical vapor deposition (CVD) is 1.3 wt% (Bhowmick et al., 2011). Additionally, hydrogen can be chemically adsorbed by host molecules due to having stable C-H bond. At this point, there are both experimental and theoretical extremely controversial results about the hydrogen capacity of carbon nanomaterials. The reason for these controversial results is that hydrogen uptake on carbon nanomaterials depends on experimental measurement conditions such as temperature, pressure, etc. The binding energy between carbon nanomaterials and hydrogen molecules is extremely weak since it is about 1 kcal/mole. For reversible hydrogen storage, the binding energy must be nearly 7 kcal/mole at ambient conditions. In other words, the binding energy of hydrogen must be enough for the efficient hydrogen physisorption on the carbon nanomaterials at ambient conditions.

Since carbon materials have low hydrogen binding energies, new alternative hydrogen storage nanomaterials having proper binding energy must be invented. The new alternative hydrogen storage materials can be produced combining heteroatoms with one another. Therefore, our aim in this study is to investigate

hydrogen storage capabilities and related properties of the boron nitride (BN), aluminum nitride (AlN), and silicon carbide nanostructures.

1.2 Boron Nitride Nanomaterials

The boron nitride nanomaterials are the first investigated nanostructures for the hydrogen storage after carbon nanomaterials. While the stability of BN nanomaterials was first theoretically predicted in 1994 (Rubio et al., 1994), they were synthesized with discharge method one year later (Chopra et al., 1995). Boron nitride materials are divided into three groups: a) one dimensional BN molecules consisting of B, N and H atoms. b) Two-dimensional planar graphene type BN nanostructures. c) three dimensional BN crystals and nanotubes. The boron and nitrogen atoms must be equal in all of BN nanomaterials. At the same time, all of the BN nanomaterials are isoelectronic with the carbon nanomaterials such as CNTs, graphene, etc. Compared to carbon materials, the BN nanostructures have marvelous chemical and mechanical properties. For example, all BN nanomaterials
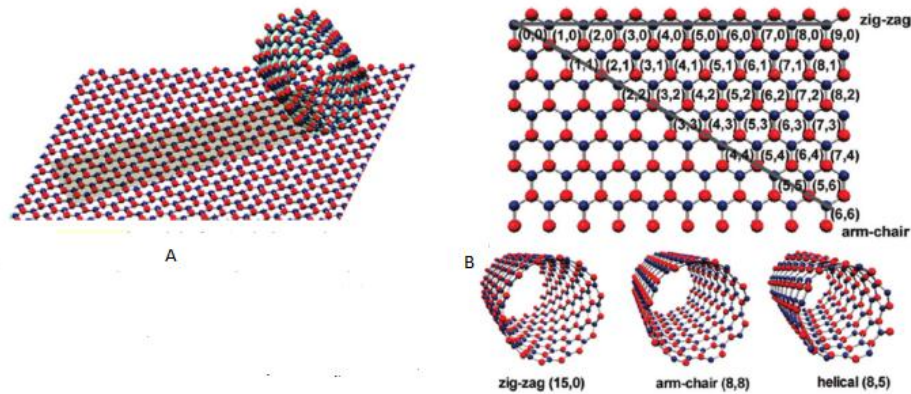
Figure 1.9. Various type of BN nanomaterials, A and B denote nanosheet and nanotubes, respectively.

have an ionic bond between B and N atoms and that bond leads to a stronger binding energy between hydrogen and BN nanomaterials (Wang et al., 2010). In other words, the BN nanomaterials are more suitable hydrogen storage materials than carbon nanomaterials due to having an ionic character between B and N atoms. This unique property of BN nanostructures makes the scientists more curious for their

hydrogen storage properties. Therefore, there is large amount of experimental and theoretical studies on hydrogen storage and related to properties of BN nanomaterials (Chu et al., 2010; Golberg et al., 2010; Hwang and Chung, 2013; Lei et al., 2014; Naresh Muthu et al., 2015; Wu et al., 2012) (Figure 2.1).

Although there are still controversial results for hydrogen properties of BN nanomaterials, many articles were published in the literature. For instance, in the study published Ma and his colleagues(Ma et al., 2002) it is claimed that multi-wall BN nanostructures are suitable hydrogen storage materials, and their hydrogen capacity can go up to 2.6 wt% at room temperature and under 10 MPa. In addition, in another article, Tang et al. (Tang et al., 2002) agree with Ma's findings. They discovered that BNNTs with disrupted structures obtained with the help of a metal-catalyst can store more hydrogen molecules than pure BNNTs, and their hydrogen storage percentage can go up to 4.2 wt%. However, Sun et.al (Sun et al., 2005) was computationally showed that BN nano-cages was not suitable for hydrogen storage because many hydrogen molecules were escaped from the cage at room temperature. They also determined the $B_{36}N_{36}$ structures can store can store up to eighteen H_2 molecules at very low temperatures. Moreover, in another computational study (Zhou et al., 2006) the findings were similar to those in Sun's study. It is clearly seen that there are controversial results for BN nanomaterials. On the other hand, Mananghaya et.al (Mananghaya et al., 2016) claimed that titanium metal doped boron nitride nanotubes (Ti@BNNTs) are better hydrogen storage materials than newly predicted Ni metal-doped carbon nanotubes (CNTs). They found out that the hydrogen storage capacity of Ti@BNNTs is about 7.17 wt% at the room temperature. Rad (Rad and Ayub, 2016) and his coworker suggested that the hydrogen storage capacity of the $B_{12}N_{12}$ nanocage increases when Nickel atoms are doped on its surface, leading to an increase in the hydrogen binding energy of the Ni-doped $B_{12}N_{12}$ nanocage. Tokarev and et.al (Tokarev et al., 2016) presented that the hydrogen storage percentages of pristine BN sheets and oxygen atom doped pristine BN sheets are 1.5 wt% and 1.9 wt% under 5MPa at room temperature, respectively. They also proposed that these materials must be improved doping with the other elements to be able to reach practical hydrogen storage for the applications. On the other hand, it is found that the endohedral hydrogen storage capacities of pure BN nanocages depend on their size (Kinal and

Sayhan, 2016). It is seen that hydrogen storage capacity of the host molecules will increase either element doping on the surface or depending the size of BN nanomaterials. Therefore, it seems that there are still some unclear points in the hydrogen storage of BN nanostructures at desired conditions.

1.3   Aluminum Nitride Nanomaterials

Aluminum nitride with the chemical formula AlN is another material that is thought as a hydrogen storage material. While the date of first theoretical prediction of AlN nanomaterials is in 2003(D, 2003), the first synthesis of the BN nanomaterials with the help of condensation using solid-vapor equilibrium is in 2004(Balasubramanian et al., 2004). AlN nanomaterials have much better hydrogen storage properties compared to BN nanomaterials due to having higher ionic character between Al and N atoms than that of between B and N atoms in BN nanomaterials. In addition, the strain energy of AlN nanotube produced from wrapped AlN nanosheet is lower than those of BN nanotubes, this makes the AlN nanomaterials being more stable structures than the BN nanomaterials. Thus, usage of the AlN nanomaterials in hydrogen storage field has been investigated frequently

(a)   (b)   (c)

(d)
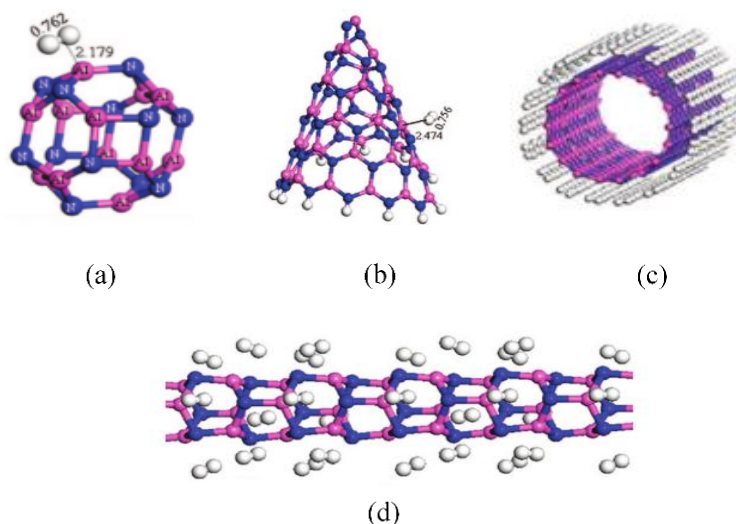
Figure 1.10. Various type of AlN nanomaterials, (a),(b), (c) and (d) denote nanocage, nanocone, nanotube and nanowire, respectively.

with the help of computational tools (Wang et al., 2009)(Figure3.1). For example, Lim and Lin(Lim and Lin, 2008) claimed in their computational study that

hydrogen chemisorption of single-walled AlN nanotubes was nearly 5 wt% and it is energetically favorable, but the hydrogen chemisorption may result in nanocage damage. In addition, Ma(Ma, 2011) showed that the BN nanosheets where B atom sites are substituted by Al atoms (AlB-BN) could easily absorb hydrogen molecules than the BN nanosheets where N atom sites are substituted by Al atoms (AlN-BN) since the bonds of Al in AlB-BN structures was stronger, leading that this material is a suitable one for hydrogen storage. Another article published by Zhang(Zhang et al., 2012) and coworkers indicates that Ni atom decorated $Al_{12}N_{12}$ has relatively high hydrogen storage of 6.8 wt%, but this complex is not stable at 25 ºC because of its positive Gibbs free energy. Addition, each Al atom in bare $Al_{12}N_{12}$ nanocage is capable of storing one hydrogen molecule with the average adsorption energy of -0.165 eV. Wang(Wang et al., 2014) and coworkers also agreed with this idea that having a positive charge of Al atom in $(AlN)m$ where m=12,24,36 can store hydrogen molecules up to 4.7%wt with average binding energies of 0.189, 0.154, 0.144 eV, respectively. In addition, Kuang (Yang and Yang, 2002) and his colleagues suggest that each aluminum atom can adsorb one hydrogen molecule on AlN nanotubes so gravimetrically hydrogen storage reaches to 8.89 wt%. Recently, there are several articles including hydrogen storage of the AlN nano structures. For example, in an article published by Esrafili it is claimed that $Al_{12}N_{12}$ nanocage including formic acid is seen as the hydrogen storage material (Esrafili and Nurazar, 2014). In addition Moradi et.al (Moradi and Naderi, 2014) claim that AlN nanomaterials can adsorb hydrazine molecule for obtaining hydrogen. As clearly seen, AlN nanomaterials are still being investigated as hydrogen storage materials.

1.4   Silicon Carbide Nanomaterials

Silicon carbide (SiC) nanomaterials are made of silicon and carbon atoms that are located at the same group in the periodic table. The silicon carbide as powder was firstly produced in 1891 by heating a mixture of clay and powdered coke in an iron bowl. In addition, SiC materials (figure3.1) have a number of better potential properties compared to carbon nanomaterials. For example, they are very stable at extreme temperatures, they have high power electronic properties, etc. Therefore, these nanomaterials are not only employed for the field of redox and optics but also they are used in the hydrogen storage field (especially the hydrogen adsorption on the surface of SiC nanomaterials because of having more ionic character than carbon-based nanomaterials).
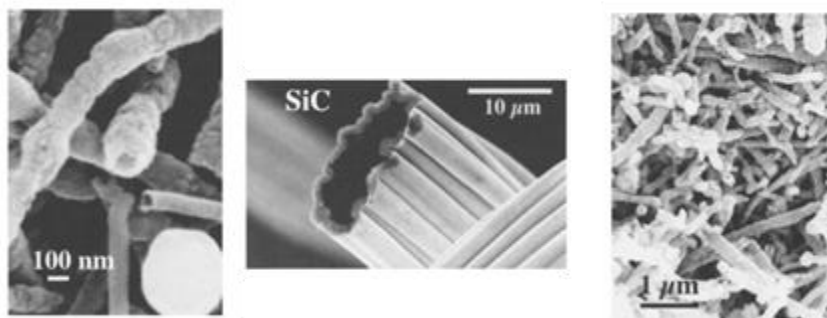
Figure 1.11. Various type of SiC nanotubes in different sides.

A study published by Mpourmpakis (Mpourmpakis et al., 2007) is claimed that hydrogen binding energy of SiC nanomaterial is 20 wt % larger than that of carbon nanomaterials due to polarization of between Si and C atoms. The polarizations of the SiC nanomaterials made them suitable for hydrogen storage. Therefore, there are also many articles including hydrogen storage properties of SiC nanomaterials (Pollmann et al., 2014; Seyller, 2004; Styrov et al., 2005). The interesting article by published Gai(Gali, 2006) indicate that atomic hydrogen chemically adsorbed by SiC nanotube has an amphoteric defect which means atomic hydrogen can act as either donor or acceptor depending adsorption site. Besides, Wang(Wang and Liew, 2012) and his colleagues found that while the binding energy of alkali Li metal doped on SiC nanotube is 0.211eV, the binding energy of pristine SiC nanotube is 0.086 eV. The reason of that is the charge transfer from the tube to Li atom. Similarly, the adsorption interactions of Ca and Li doped on SiC nanosheets also was investigated by Song et.al (Song et al., 2015). Moreover, hydrogen storage properties of titanium metal doped SiC nanomaterials were also investigated by Wang et.al (Meng et al., 2007) and etc. Their findings are that the carbon atom of in Ti-atom-doped SiC nanomaterial is chemically more attractive to hydrogen molecules and could store up to four hydrogen molecules. Also, Javan et.al (Bezi Javan et al., 2016) suggest that Pd-doped-SiC sheet is capable of adsorbing hydrogen both physically and chemically. On the other hand, in an experimental study published by Barghi(Barghi et al., 2014) et al, it is claimed that the percentage of hydrogen adsorption on SiCNT is five times faster than that of CNT. This experimental result also agrees with the theoretical calculations on the hydrogen uptake on SiCNT. It is clearly seen that the hydrogen storage of SiC nanomaterials and its related properties are still being investigated.

2. THEORETICAL METHODS

"The world is given to me only once, not one existing and one perceived. Subject and object are only one. The barrier between them cannot be said to have broken down as a result of recent experience in the physical sciences, for this barrier does not exist"

Erwin Schrodinger

Chemistry is a branch of the science that concerns with particles such as electrons, atoms, molecules. It also investigates properties of matter such as composition, reactivity, and relations with other compounds. In fact, the molecules are combinations of the atoms having the nuclei and electrons. Therefore, the Coulomb interaction that is an only effective physical force for the chemical phenomena will originate between the nuclei and electron. There is a vast number of different molecules having different nuclei at different nuclear positions in nature, so the scientists who intensively deal with the chemistry have chances of the discovery of the new molecules.

Theoretical chemistry is a subdivision of chemistry in which the laws of physics are used to describe chemical processes by means of mathematical methods. The main aim of theoretical chemistry is to find the most stable spatial distributions of the nuclei in a molecule. In addition, the chemical and physical properties of a molecule such as relative energy, dipole moment, hardness descriptor, photochemical properties etc. can be determined with theoretical chemistry.

While an interacting two-body system can be solved analytically many-body systems having more than two electrons cannot be solved exactly. In many-body systems, there are only the numerical solutions found by solving many mathematical equations. These kinds of mathematical equations can be solved by powerful and fast computers. With the development of computers, a new branch of chemistry has arisen, this is the computational chemistry. The main aim of computational chemistry is to obtain results for chemical problems with the known methods instead of developing a new method. Therefore, computational chemistry is seen as the experimental part of theoretical chemistry. Even though

computational chemistry and theoretical chemistry are seen to be different, there is a strong link between them. While some theoretical methods can be developed because of the results obtained by computational calculations, new theoretical methods can help computational problems to be studied.

Although recently one who knows computational chemistry can obtain some results for molecules consisting of a few hundred atoms depending on given accuracy, the biggest problem in computational chemistry is to choose an appropriate theoretical method for the systems to be studied and the evaluation of the results. The computational methodology from the simple to complex theories will be given in the following.

2.1 The Schrödinger Equation

In quantum mechanics, there is a wave function represented as Ψ(r,t) that describes all properties of any system such as stable energy, electron distribution of a particle in a certain volume, dipole moment, etc. The wave function has the two main variables namely r and t. While r is presented as the spatial coordinates of particle, t is presented as time that leads wave function to dynamic. The understanding of wave function including time variable was fully explained by the Schrödinger time-dependent equation:

$$i\hbar \ \frac{\partial \psi(r,t)}{\partial t} = \hat{H}\psi \ (r,t) = E\psi(r,t) \tag{2.1}$$

In this formula, the $\hat{H}$ is called as Hamiltonian operator that is total energy of a particle in terms of kinetic and potential energy. The wave functions of many particles do not include the time variable in most situations. In other words, the time variable of wave function is neglected when many properties of a particle are investigated such as finding of stable coordinates of a particle in space. Therefore, the Schrödinger equation is split into two separate equations, namely time-independent and time-dependent equations, by using variable separation method. Thus, the time-independent Schrödinger equation is summarized with the following reaction

$$\hat{H}\psi(r) = E\psi(r) \qquad (2.2)$$

In this formula, the $\hat{H}$ is given as:

$$\hat{H} = -\sum_{i=1}^{N}\frac{1}{2}\nabla_i^2 - \sum_{a=1}^{M}\frac{1}{2M_a}\nabla_a^2 - \sum_{i}^{N}\sum_{a}^{M}\frac{Z_a}{r_{ia}} + \sum_{i}^{N}\sum_{j>i}^{N}\frac{1}{r_{ij}} + \sum_{a}^{M}\sum_{b>a}^{M}\frac{Z_aZ_b}{R_{ab}} \qquad (2.3)$$

where, i and j are represented as lower bound of N electrons while a and b are represented as lower bound of M atomic nuclei. M_a is defined as the rate of the mass of nucleus a to mass of electron, Z_a is the atomic number of nucleus a. While r_{ij} is the distance between the ith and j^{th} electron, r_{ia} is known as the distance between the ith electron and nucleus a. The first two terms give the kinetic energy of the electrons, T_e, and nuclei, T_n, respectively. The third term is an attractive operator that gives the Coulombic interactions energy between the electrons and nuclei, V_{ne}, while last two terms are the give the repulsive operator that gives the Coulombic interactions of electron-electron, V_{ne}, and nucleus-nucleus, V_{nn}, respectively. $\hat{H}$ is summarized with the following equation:

$$\hat{H} = T_e + T_n + V_{ne} + V_{ee} + V_{nn} \qquad (2.4)$$

2.2 The Born-Oppenheimer Approximation (BOA)

Although the Schrödinger equation explains nearly all chemical properties of a particle, it cannot be fully solved analytically for many-body systems except one-body systems such as $_1H$, $_3Li^{+1}$, etc. because the equations of Schrödinger are too complex to solve analytically. This is the extremely important problem for the quantum mechanics. To solve this problem, many approximations were developed and the most common approximation of which is the Born-Oppenheimer Approximation(Born and Oppenheimer, 1927).

The mass of an electrons is extremely lower than that of nuclei. In any change in spatial coordinates of particle, electrons can move faster than the nuclei. Therefore, it can be said that movements of electron in comparison of nuclei lead

to change the nuclear position of particles. This approximation suggests that kinetic energy of nuclei and nuclear-nuclear columbic interactions are neglected from the full Hamiltonian equations because kinetic energy of electrons are very faster in particle and nuclear-nuclear interactions terms can be seen as constant. The remain terms are also knowns as "Electronic Hamiltonian" that include electronic kinetic energy operator and columbic interactions. The Electronic Schrödinger equation is summarized with the following formula for an isolated N-electron atomic or molecular system:

$$\hat{H}_{elec} \Psi_{elec} = E_{elec} \Psi_{elec} \tag{2.5}$$

In the formula, $E_{elec} = E_{elec}\left(\{R_a\}\right)$ is the electronic energy, $\Psi_{elec} = \Psi_{elec}\left(\{r_i\};\{R_a\}\right)$ gives the wave function which explains movement of electrons and explicitly depends on electronic coordinates and Ψ_{elec} also is parametrically depended on nuclear coordinates. The formula of $\hat{H}_{elec}$ operator is given as:

$$\hat{H}_{elec} = -\sum_{i=1}^{N}\frac{1}{2}\nabla_i^2 - \sum_{i}^{N}\sum_{a}^{M}\frac{Z_a}{r_{ia}} + \sum_{i}^{N}\sum_{j>i}^{N}\frac{1}{r_{ij}} \tag{2.6}$$

In the formula, while the first term is the kinetic energy of electron, the last two terms on the right-side are the attractive energy between electron-nuclei and repulsive energy between electrons, respectively. The constants of repulsive interaction energy of between nuclei, $\sum_{a}^{M}\sum_{b>a}^{M}\frac{Z_a Z_b}{R_{ab}}$, is attached to electronic Hamiltonian at the end of the calculation.

2.3 The Hartee-Fock Theory

With the help of the Born-Oppenheimer approach, the complexity of the Schrödinger wave equation is slightly reduced, but this equation is still complex because of repulsive interactions between electrons. The molecular orbital

approximation (MOT) that is based on obtaining total wave function of a system by using orthogonal molecular orbitals (MOs) is the reasonable solution of this phenomenon. In addition, the Hartee approximation is known as the one of the basic MOT. This idea provided chemists to more attention of investigating electron in orbital. The approximation assumes that each electron in the system moves separately and that each electron is in an "average electric field" created by other electrons. The Hartee wave function for N electron is given as:

$$\Psi = \phi_1(x_1)\phi_2(x_2)\phi_3(x_3)\dots\dots\phi_N(x_N) \tag{2.7}$$

In the formula, ϕ_i having orthonormal is a spin orbital for each electron and ϕ_i function is obtained by two different orbital functions namely; a spatial orbital, $x_i(\vec{r})$ and one of the spin functions, $\alpha(spin\ up)$ or $\beta(spin\ down)$. Therefore, x' is also known as spin-space coordinate including both spatial orbital and spin functions.

The expectation value of Hamiltonian obtained by using variation method of wave function is given as:

$$\left\langle \Psi \middle| H_{elec} \middle| \Psi \right\rangle \tag{2.8}$$

Note that all individual orbitals are orthogonal, as specified,

$$\left\langle \phi_i \middle| \phi_j \right\rangle = \delta_{ij} \tag{2.9}$$

Firstly, the best wave function, ϕ_i, must be found by using variation method, then, Hartee equations are created. Although this approximation encounters many problems, it is a simplest, oldest solution in intensive number of situations. The main failure of this approximation is to accept each electron moving separately and tag electron individually, in fact, these assumptions are completely contrary to quantum mechanics because electrons cannot be tagged and are indistinguishable in quantum chemistry. Electrons are to be part of fermions systems therefore the wave function have to be antisymmetric. The condition of being antisymmetric for the wave function is given as:

$$\Psi(x_1, x_2, x_3, \ldots \ldots x_n) = -\Psi(x_1, x_2, x_3, \ldots \ldots x_n) \tag{2.10}$$

The best approximate produced by Slater for the condition of being antisymmetric of wave function is to solve by putting it into a determinant form. This solvation leads the wave function to being spontaneous antisymmetric form for exchanging of any two electrons. In addition, this determinant is also called 'Slater Determinant'. The Slater Determinant is formulized with the following formula,

$$\psi = \frac{1}{\sqrt{N!}} \begin{vmatrix} \phi_1(x_1) & \phi_2(x_1) & \phi_N(x_1) \\ \phi_1(x_2) & \phi_2(x_2) & \cdot \phi_N(x_2) \\ \vdots & \vdots & \vdots \\ \phi_1(x_N) & \phi_2(x_N) & \cdot \phi_N(x_N) \end{vmatrix} \tag{2.11}$$

The Harttee-Fock Energy is obtained when the determinant wave function (2.11) is employed into the equation 2.8

$$E_{HF} = \sum_i^N h_{ii} + \frac{1}{2} \sum_i^N \sum_j^N (J_{ij} - K_{ij}) + V_{nn} \tag{2.12}$$

In the formula, h_{ii} is presented as the single electron integral and while J_{ij} is the Coulomb integral, K_{ij} is the exchange integral, respectively. These terms are summarized as follows.

$$h_{ii} = \langle \phi_i | h | \phi_i \rangle = \left\langle \phi_i(x_1) \left| -\frac{1}{2} \nabla_1^2 - \sum_a \frac{Z_a}{|R_a - r_i|} \right| \phi_i(x_1) \right\rangle \tag{2.13}$$

$$J_{ij} = \left\langle \phi_i(x_1)\phi_j(x_2) \left| -\frac{1}{|r_1 - r_2|} \right| \phi_i(x_1)\phi_j(x_2) \right\rangle \tag{2.14}$$

$$K_{ij} = \left\langle \phi_i(x_1)\phi_j(x_2) \left| -\frac{1}{|r_1 - r_2|} \right| \phi_i(x_1)\phi_j(x_2) \right\rangle \tag{2.15}$$

Note that the equations of 2.14 and 2.15 are not the same. While the equation 2.14 is represented as Coulombic repulsive interactions between two charge distributions described by ϕ_1^2 and ϕ_2^2, the equation 2.15 is the exchange integral comes from naturally the exchange of the electrons. Besides, the Coulomb operator includes the combining full charged particles as a matrix element with the same orbital including also repulsive terms, but exchange operator includes exchange terms for two electrons. Therefore, Hartee-Fock energy is re-summarized with the following formula,

$$E_{HF} = \sum_i^N \langle \phi_i | h | \phi_i \rangle + \frac{1}{2} \sum_{ij}^N \langle \phi_j | J_i | \phi_j \rangle - \langle \phi_j | K_i | \phi_j \rangle) + V_{nn} \tag{2.16}$$

In the formula, the main purpose is to determine better MOs leading to energy stationary with related to a change in the orbitals. With the determine of the best MOs obtained from the formula, the molecule geometry must have a minimum on the PES. The variation of energy related to changing any orbital into space is the limited(constrain) for the optimization because MOs can be normalized and orthogonal. This limited optimization calculations are solved with the help of Lagrange multipliers method. The condition of applying Lagrange functional on the equation 2.16 is to remain stationary point on the PES related to change any orbital. The utilizing Lagrange function on the equation 2.16 is given the following formula

$$L = E - \sum_{ij}^N \lambda_{ij} \left(\langle \phi_i | \phi_j \rangle - \delta_{ij} \right) \tag{2.17}$$

$$\delta L = \delta E - \sum_{ij}^N \lambda_{ij} \left(\langle \phi_i | \phi_j \rangle + \langle \phi_i | \delta \phi_j \rangle \right) = 0 \tag{2.18}$$

$$\delta E = \sum_i^N \left(\langle \phi_i | F_i | \phi_i \rangle + \langle \phi_i | F_i | \phi_i \rangle \right) = 0 \tag{2.19}$$

$$F_i = h + \sum_j^N (J_j - K_j) \tag{2.20}$$

In the 2.20 formula, the Fock operator, F_i, is represented as an effective one-electron energy operator. It defines as the kinetic energy of an electron, Coulombic attraction to all nuclei and repulsive attraction to all other electrons. Note that Hamiltonian operator cannot be obtained from the sum of these operators since these total operators are obtained from the variation of the energy. The value of total sum of Fock operators are not the equal with Hamiltonian operator including total energy of a systems. Therefore, the final Hartee-Fock equation is summarized with the following formula;

$$F_i\phi_i = \sum_j^N \lambda_{ij}\phi_j \qquad (2.21)$$

In the formula, λ_{ij} is represented as non-diagonal Lagrange multipliers having non zero value. These equations can convert to the matrix diagonal of Lagrange multipliers by using a unitary transformation. In other words, while diagonal terms are the energy of molecular orbitals, ε_i the non-diagonal terms are completely zero. In addition, this type approach of determining MOs is also known as canonical MOs, ϕ' .The canonical MOs can be used into the equation 2.21. Therefore, the new a set of psedo-eigenvalue equations are obtained (2.22) as follows.

$$F_i\phi_i' = \varepsilon_i\phi_i' \qquad (2.22)$$

Note that the equations of 2.22 are not common eigenvalue equations since the terms of Fock operator, F_i, depends on full MOs having exchange and Coulomb integrals. The equation 2.22 is based on *Self-Consistent Field* (SCF) method. In other words, the equation 2.22 is solved by repeating itself; first a suitable spin orbital can be found as initial guess and Fock operator can be employed by using the 2.20 equation and the an improved set of orbitals are generated with the help of equation 2.22. The new orbitals determined from equation 2.22 are again used as new guess orbital in the Fock operator. The procedure keeps going on until the solution of 2.22 is not changed within the specified tolerance.

2.4 The Restricted and Unrestricted Hartee-Fock Wave Functions

Previously, it was mentioned (equation 2.11) that the Slater determinant is the easiest transformation product for the wave functions converting to being antisymmetric wave functions, ϕ_i, having the spin functionals namely $\alpha(spin\ up)$ or $\beta(spin\ down)$. Actually, spin molecular orbitals are to be part of the space molecular orbitals included spin part. The systems are split into two parts in terms of spin functionals namely, '*closed and open shell systems*'. The closed shell system is that all electrons having spin up and spin down are double filled into the space molecular orbital, therefore, the system must be 'singlet' state. If a system has singlet state, the computational time of the system is reduced. The wave function of the system having singlet state is called as Restricted Hartree-Fock (RHF) wave function.

In some systems, not the all electrons can be doubly filled into the space molecular orbital. Such systems are called as 'open shell' systems having different states apart from singlet state namely, doublet, triplet, quartet and so on. For such these systems, RHF wave function cannot be generated. Thus, the wave function can be obtained by using different space molecular orbital for each spin orbital. There is no restriction for the orbitals. For such the wave functional is known as unrestricted Hartee- Fock (UHF) wave functionals. A study is published by Pople(Pople and Nesbet, 1954)is claimed that the system energy obtained from UHF wave function is always lower (or equal) than that of energy obtained from RHF wave function and the reason of this is that UHF wave function has the spin contamination from the higher states namely, triplet, quintet, etc.

There is a special approach for solving the open shells systems. According to this approach, while the core electrons occupy the space molecular orbital as a pair, the other open shell electron(s) fill into different space molecular orbitals one by one. This approach is known as the restricted open-shell Hartree-Fock (ROHF) method.
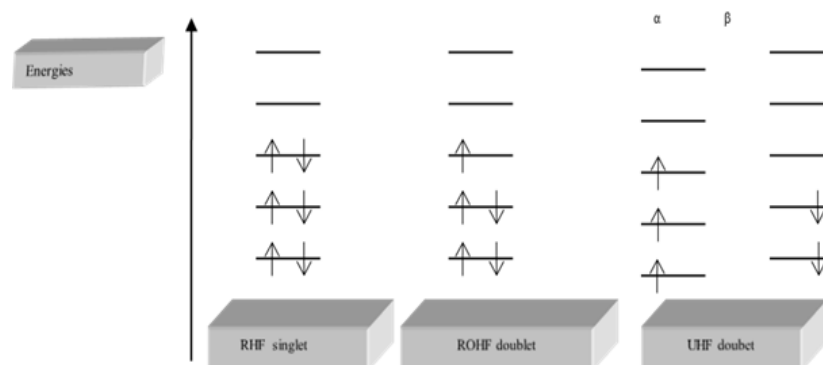
Figure 2.1. Illustrating of RHF, ROHF, UHF, Respectively.

2.5 The Basis Set Approximation

The basis set is a set of functions to explain unknown MOs. The common formula of basis set approximation is summarized with the following formula.

$$\phi_i = \sum_{\alpha}^{K} c_{\alpha i} \chi_a \tag{2.23}$$

In the formula, the basis set function of any system is represented as χ_a. The determining basis set of any system to express its chemical properties is extremely important in computational chemistry. In fact, there are two main criteria for choosing basis set. The first of all is the selection of suitable basis set that can correctly identify any desired problem. For instance, if the selected basis functions go to zero during the calculation, the distance between the nucleus and electrons increases so this is unwanted situation. The second of all is computational applicability. In other words, selected the basis functions must reduce computational time of system while the solving integrals. There are two kind of functions having these criteria namely, Gaussian type orbitals (GTO) and Slater Type Orbitals (STO). The formula of slater type of orbitals is summarized with the following formula;

$$\phi(\xi, n, l, m; r, \theta, \varphi) = N r^{n-1} \exp^{-\xi r} Y_{l,m}(\theta, \varphi) \tag{2.24}$$

While the Gaussian type of orbital is summarized with the following formula,

$$G(\alpha,n,l,m;r,\theta,\varphi) = Nr^{2n-2-1}\exp^{-\xi r^2} Y_{l,m}(\theta,\varphi) \tag{2.25}$$

In the both formulas, the exponential functions are seen as common terms. Actually exponential functions for Slater type orbitals are physically suitable because these terms are very close to solvation of hydrogen atom, but it is very difficult to solve integrals produced by using the Slater type orbital. Although the Gaussian type orbitals are more suitable because of having less computational time, they are not as efficient as the Slater type orbital describing electronic structure of system by using one-to- one basis set. Therefore, linear combination of Gaussian type orbital employs to define electronic structure of system because of having less computational time than that of Slater type orbitals.

A study published by Roothaan (Roothaan, 1951) and Hall(Hall, 1951) is explained that the HF equations can be solved as numerically and unknown molecular orbitals are expanded in the form of linear combinations of unknown atomic orbital sets(equation 2.23). The expansion of molecular orbital functions are accurate when the suitable atomic orbital functions (basis functions), χ_a, are completed. Therefore, the problem of HF molecular orbitals functions is reduced to determine expansion coefficients of basis set functions. Adding equation 2.23 into the HF equation (2.22) thus gives,

$$F_i\sum_{\alpha}^{M} c_{\alpha i}\chi_{\alpha} = \varepsilon_i\sum_{\alpha}^{M} c_{\alpha i}\chi_{\alpha} \tag{2.26}$$

The equation 2.26 can be also shown as the matrix notation formula as follows:

$$FC = SC\varepsilon \tag{2.27}$$

In the formula 2.27, $F_{\alpha\beta} = \langle \chi_\alpha | F | \chi_\beta \rangle$ and $S_{\alpha\beta} = \langle \chi_\alpha | \chi_\beta \rangle$ are the matrix term of Fock and overlap terms, respectively. ε is defined as the MO energies. As it is clearly seen that the new HF formula with the linear combination of atomic orbital is more useful for the SCF calculation. First, the initial guess is generated for atomic orbital coefficients. After that, Fock matrix is obtained by using atomic orbital coefficients and

new atomic orbital coefficients are determined. The procedure keeps going on until the difference between sequential results have the range within the specified tolerance.

2.6 Classification and types of Basis Set

After giving detailed information about the basis set approximation, one of the most important problems for model systems is to assign basis set. In other words, it is to determine the number of basis set functions to be employed for the model systems. If The smallest number of basis set is used to describe for the systems, this is known as 'minimum basis set'. For instance, single basis set function is employed to describe s orbital for one hydrogen atom or two basis set functions are used to define s orbital for the one lithium atom. In most cases, the selected functions in minimum basis set give lesser accuracy for the system in computational chemistry. In order to enhance the accuracy for the system, there are many types of functions in minimum basis set. The one of these is Double Zeta (DZ) type basis set. The meaning of 'Zeta' word comes from the term, ξ, of STO and GTO type basis functions. The DZ type basis set generates double functions for every valance electron. For instance, DZ type basis set describes s-orbital with the two different functions, $(\xi s, \xi s')$ for one hydrogen atom. Actually, in computational chemistry, valance electrons are extremely important than core electrons because the chemical bonding occurs only among valance electrons. The different type of DZ basis set deals with especially valance electrons instead of all electrons into the atom; therefore, the functions for valance electron are produced. This is known as *split valence* basis set. The advantage of split valence basis set is to decrease the computational cost given better accuracy. The other type of function in minimum basis set is to 'Triple Zeta'(TZ) type basis set. Like DZ basis set, TZ type basis set generates three functions for every valance electrons and different type of TZ basis set deals with especially valance electrons instead of all electrons into the atom. This is known as *triple split valence* basis set. For instance, TZ type basis set describes s-orbital with the three different functions, $(\xi s, \xi s', \xi s'')$ for one hydrogen atom.

It is suggested that the functions must be included higher angular momentum terms to define polarization effects while setting of basis set functions. For example,

a basis set function describing p-orbital is added to hydrogen atom in a organic molecule (CH_4), therefore, P_z component of the function can assist to improve the description of C-H bond in the molecule. The p-orbital causes to enhance the polarization of s-orbital. The d- and f- orbital(s) enhance the polarization of p-orbital(s) and d orbital(s) respectively. Besides, the basis function(s) must have small exponential term if the system has weak electrons that can travel out of its own orbit. Such functions having small exponential coefficient are known as '*diffuse functions*'.

The '*contracted* basis set' that is the one of other type basis functions is defined as the functions describing more efficiently core electron(s). Therefore, energy of the system having more accuracy can be obtained by using contracted basis set. The contracted basis set is produced with the help of *primitive* GTOs that is included the all set of functions in the atom. In other words, the smaller set of function(s) is produced by forming fixed linear combinations of GTOs. The resulting functions are described as contracted GTOs, CGTOs. The formulation of CGTOs will summarized with the following equation:

$$\chi(CGTO) = \sum_{i}^{k} \alpha_i \chi_i(PGTO) \tag{2.28}$$

In the formula, α_i(s) is represented as coefficient of CGTO. There are several advantages of using CGTO such as reducing computational effort, describing good core electrons, etc. The energy produced by using CGTO method is always bigger than that of GTO method because restricted parameters of the function are employed for the calculation. However, the computational time is lesser. In other words, the selecting of CGTO basis set is related to the fact that how much loss is acceptable in the accuracy, compared to the take in computational effort. The number of PGTOs is known as such notation gives 'degree contraction'. The presentation of basis set in the way of PGTOs and CGTOs is shown by following notation. $(10s4p1d/4s1p) \rightarrow [3s2p1d/2s1p]$. While it is shown as the number of PGTOs in the parenthesis, the number of CGTOs is represented in the square brackets. In addition, the number of functions belonged to hydrogen atom is the right side of slash in the both representations and the functions of heavy atoms (first row elements) are represented left side of slash in

the both representations. For instance, 4p-PGTOs functions are described by using 2p-CGTOs functions. Note that this illustration does not show how the CTOGs are generated. Although there are number of CGTOs functions in literature, the important thing is to select better and suitable CGTOs for the computational chemistry. The common and suitable contracted basis set is given as follows for the ones used in this thesis.

STO-nG basis sets: The Slater type orbital functions are produced by using (n) number of PGTOs. The STO-nG basis sets are the minimum basis set. The PGTOs are obtained by fitting STOs and the STO-3G is the most common basis set. The illustration of STO-3G basis set is given as $(6s3p/3s) \rightarrow [2s1p/1s]$.

k-nlmG basis sets: This type of basis set is also known as split valance basis set. The k is the number of primitive Gaussian type orbital describing core electron. The *nlm* represents as how many primitive Gaussian type orbital functions describe the valance electrons. The *nl* and *nlm* numbers(values) represent the split valance and triple split valence, respectively. While the s- and p- functions are represented as values before G and polarizations functions comes from after the G. The common k-nlmG basis sets and its notation in terms of PGTOs and CGTOs is shown as following Figure (2.2).

Basis set	Contraction
3-21G	$(6s3p/3s) \rightarrow [3s2p/2s]$
6-31G	$(10s4p/4s) \rightarrow [3s2p/2s]$
6-311G	$(11s5p/5s) \rightarrow [4s3p/3s]$

Figure 2.2. Common k-nmlG type basis sets and their contractions.

Each basis set function expanded by polarization or diffuse functions make the system more accurately. In other words, polarization or diffuse functions are extremely important for the basis set describing the system. In GTOs illustration, s- and p- functions adding only heavy atoms are donated as +, while ++ is the s- and p- functions adding heavy and hydrogen atoms. They accommodate before the letter G. The polarization functions accommodate after the letter G. For instance, for 6-

311++G(d,p) basis set, the 6 is the number of primitive Gaussian orbital describing for the core electron, the 311 is the triples split functions describing valence electrons, ++ is the diffuse functions adding heavy(s- p- orbitals) and hydrogen atom (s-orbital), d and p is represented as polarization functions adding heavy and hydrogen atom, respectively.

The other type of functions improving electron correlation of the valance orbital is the correlation consistent (cc-) basis sets. This basis set is donated as cc-pV(D, T, Q)Z. The cc is the correlation consistent functions for the valance electrons, p is the polarization function, the letters into parenthesis are split functions describing valence electrons. There are various correlation consistent basis sets used by many computational chemists such as cc-pVDZ, cc-pVTZ, cc-pVQZ, so on. The notation of correlation consistent polarized valence triples zeta (cc-pVTZ) employed in this thesis is given with the following notation $(10s5p2d1f/5s2p1d) \rightarrow [4s3p2d1f/3s2p1d]$.

2.7   Electron Correlation Methods

The Coulomb interactions apart from attractive interactions are very important for the movement of electrons. In other words, the repulsive Coulomb interactions provide the motion of electrons therefore, it can be said that the movement of electron is related to the repulsive Coulombic interactions among the electrons. The electron correlation energy is defined as a energy difference between Hartee-Fock energy of the systems and accurate non-relativistic energy.

The one of the aims of HF is to determine the best trial wave function in given basis set by using trail wave functions including more than one Slater Determinant. The formula of best trial function obtained Hartee-Fock and additional Slater determinants is summarized with the following formula.

$$\Psi = \alpha_0 \Phi_{HF} + \sum_{i=1} \alpha_i \Phi_i \qquad (2.29)$$

In the formula, Ψ is the total trial wave function of the system, Φ_{HF} is the HF wave function, Φ_i are the wave functional obtained by additional Slater determinant, the other terms are the coefficients namely, α_0 and α_i, respectively. The Slater determinants can be obtained by using unoccupied MOs replaced with occupied MOs in HF determinant. These determinants provide that Slater determinants are singly, doubly, triply, quadruply etc. excited according to the HF determinant. These determinants are also known as Singles (S), Doubles (D), Triples (T), Quadruples (Q) having maximum excitation of N electrons (N-multiple).

There are many methods having electron correlation namely; Coupled Cluster (CC) Theory, Density Functional Theory (DFT), Configuration Interaction (CI), Multi-configuration Self Consistent Field (MCSCF), Many Body Perturbation Theory (MBPT).

2.8   Configuration Interaction

The simplest method having electron correlations of a system is the '*Configuration Interaction (CI)*' method. The CI employs the wave functions including linear combination of HF wave functions. In other words, the CI is explained that excited Slater Determinants are to generated by using MOs. This is obtained by using HF wave functions and generating new determinants with excited electrons from the occupied to unoccupied molecular orbitals. The formula of wave functions obtained from excited electrons given in equation 2.29.

In CI approach, the expansion coefficients (α_0, α_i)of the trial wave function should be determined under conditions in which the energy is minimal. If the all CI expansion coefficient of a system is determined, the CI gives the exact electron correlation energy of the system. The determining all CI is known as 'full CI'. In other words, The CI calculation having all possible excitations is called a full CI. Although full CI gives the best electronic interaction energy, it is not employed for the big systems apart from the small systems due to having computational effort. The computational effort for CI method is depended on the number of excitation

determinants. In other words, the increasing number of excitation determinants lead to expensive computational time. The number of excitation of determinants is given as follows:

$$\text{\# of Slater Det} = \frac{M!}{N!(M-N)!} \tag{2.30}$$

In the formula, Where M is represented as number of basis functions, N is defined as the expansion length for the number of electron in the system, respectively. The decreasing the number of Slater determinant cutting some order makes the system more efficient for the computational cost. For instance, although first order expansion (Single, S) of CI has better computational cost, it does not give the electron correlation energy because single determinants does not interfere with the HF determinants(Brillouin, 1934). The other definition for the single expansion of CI is that the each determinant obtained by exciting only one electron is known as configuration interaction single-excitation (CIS) calculation. Instead of using CIS method, CISD(Raghavachari et al., 1980)(Singles, Doubles) obtained by the determinants having only singly and doubly excited electrons can be employed for large systems. In addition, CISD not only gives the suitable electron correlation energy but also has not the computational effort for the suitable systems. There are also triple and quadrupole excitation method namely, CISDT and CISTDQ respectively, but they should employ for high accuracy calculations.

2.9 Multi-configuration Self-Consisted Field Theory (MCSCF)

The MCSCF is one of the electron correlation theory that uses the multiple determinants having both coefficient optimizations in front of the determinants (like CI, electron excitation) and molecular orbital optimization. MCSCF methods should not employ for the determining amount of electron correlation energy since this method during calculating the optimization of orbital does not recover the electron correlation energy. In other words, CI methods are the suitable methods for recovering the electron correlation energy than the MCSCF method but it is mostly employed for the systems when RHF wave function has poor quantity. For instance, the RHF wave function of biradicalic molecules has poor therefore; the

MCSCF method should be employed for the determining better HF wave functions of the biradicalic molecules. Though UHF theory is the suitable of the biradicalic molecules, it cannot give better the energy of the system due to having high spin contamination. In addition, the problem of high spin contamination can be solved by using some approximated functions added into an MCSCF expansion. Such of these approximated functions are known as the configurational state functions (CSFs). Therefore, the MCSCF method is the most suitable method for determining the best electronic structure of the system and reliable energy.

In MCSCF theory, the electron correlation is divided into two parts namely, static and dynamic electron correlations. The static electron correlation is known as energy reduction by giving enough flexibility in the wave function to be able to explain the system. This is the allowing of electrons occupying in the orbitals as a single instead of as double occupying. The dynamic electron correlation is known as energy reduction because of having electron movements in the orbitals. The MCSCF methods mostly give the static electron correlation, but they can recover the dynamic electron correlation by using extremely number of configurational state functions(CSFs).

2.10 Complete Active Space SCF Theory (CASSCF)

The one of the biggest handicap about MCSCF is to select which molecular orbital to use because there is no automatically option for the computational chemists into computational software programs to determine which molecular orbitals employ in the MCSCF calculation. The complete active space SCF (CASSCF) method can be mostly used for solve this handicap. In addition, this method is also known as Full Optimized Reaction Space (FORS). In the CASSCF methodology, it can be thought that the MOs split into two spaces namely *active* and *inactive* spaces. While the some of the MOs in active spaces are represented as HOMO and LUMO obtained RHF calculation, the others of MOS in active space are represented as both core (doubly occupied) and empty(virtual) orbitals.

There are many notations representing CASSCF method such as [n,m]-CASSCF, CASSCF(n,m), etc. The n,m are the terms that define the active space

part of molecular orbitals(determinants). The n is the number of active electrons having all configurations in m orbitals selecting active space. The full CI expansion within the active space restricts the number of orbitals and electrons that can be treated by CASSCF methods. The exponential increase of CSFs with increasing constituents of active space limits its dimensions to less than 10-12 electron or orbitals. Therefore, the goal of CASSCF methods is to recover the changes occurring in the correlation energy for the given process, not recovering considerable amount of the correlation. Thus, the aim of CASSCF method is to treated the changing in correlation energy for the given basis set, not to gain full correlation energy. There are many common CASSCF methods namely, CASSCF(4,4), CASSCF(6,6) and CASSCF(8,8) methods, respectively.

The disadvantage of CASSCF methods is to give unstable descriptions for a certain parts of the system interested because this method only recovers the correlation energy in active space, not to recovers correlation energy obtaining either inactive electrons or between the active and inactive electrons. This disadvantage leads to overestimate the correlation energy for the systems especially, biradicalic systems(and and Davidson*, 2000; Staroverov and Davidson, 2001).

2.11 Many Body Perturbation Theory (MBPT)

The one of others theory for the determining electron correlation is the called as *Perturbation Theory* (PT). Mostly, the application of PT to the system having many interactions along the particles is known as many body perturbation theory (MBPT). This method is based on splitting full Hamiltonian into two parts.

$$\hat{H} = \hat{H}_0 + \lambda \hat{H}' \tag{2.31}$$

In the formula, $\hat{H}_0$ is known as reference part or unperturbed part, $\hat{H}'$ and λ are the perturbative part of $\hat{H}_0$ and perturbation parameter showing the strength of the perturbation, respectively. The formula of the solution of reference part is the summarized with the following formula,

$$\hat{H}_0 \Phi_i = E_0 \Phi_i \quad i=0,1,2,3......\infty \qquad (2.32)$$

In the formula, we must assume some following conditions to solve the equation 2.30. These assumptions are given as follows:

    (a) the reference wave function must be non-degenerate,

    (b) perturbation must be time-independent,

    (c) the reference wave function must be in lowest energy state.

Therefore, the perturbation equation is the summarized with the following formula:

$$\hat{H}\Psi = W\Psi \qquad (2.33)$$

Note that if the perturbative parameter must be zero, $\lambda = 0$, then W, $\hat{H}$ and Ψ will be E_o, $\hat{H}_0$ and Φ_0 respectively. If the perturbative parameter expands to infinite, new energies and wave functions will be occurred as inherently. However, to solve equation 2.32, the Taylor expansion must be employed around the perturbation parameter:

$$W = \lambda^0 W_0 + \lambda^1 W_1 + \lambda^2 W_2 + \lambda^3 W_3 +.......... \qquad (2.34)$$

$$\Psi = \lambda^0 \Psi_0 + \lambda^1 \Psi_1 + \lambda^2 \Psi_2 + \lambda^3 \Psi_3 +......... \qquad (2.35)$$

When the perturbative parameter must is the zero, $\lambda = 0$, W_0 and Φ_0 are called as unperturbed zero order energy and wave function. The W_1, W_2, W_3 and etc are called as first, second, third and other energy corrections for unperturbed energy. Similarly, W_0, W_1, W_2 and etc. are called as first, second, third and other corrected wave functions for the unperturbed wave function.

If the equations 2.33 and 2.34 add to into the Schrödinger equation (2.32), the last equation must become,

$$(\hat{H}_0 + \lambda\hat{H}')(\lambda^0 W_0 + \lambda^1 W_1 + \lambda^2 W_2 + \lambda^3 W_3 + ...) =$$
$$(\lambda^0 W_0 + \lambda^1 W_1 + \lambda^2 W_2 + \lambda^3 W_3 + ...)(\lambda^0 \Psi_0 + \lambda^1 \Psi_1 + \lambda^2 \Psi_2 + \lambda^3 \Psi_3 + ...)$$

(2.36)

The perturbative parameters, λ, in the equation 2.35 can be gathered with the following formula,

$$\lambda^0 = \hat{H}_0 \Psi_0 = W_0 \Psi_0$$
$$\lambda^1 = \hat{H}_0 \Psi_1 + \hat{H}'\Psi_0 = W_0 \Psi_1 + W_1 \Psi_0$$
$$\lambda^2 = \hat{H}_0 \Psi_2 + \hat{H}'\Psi_1 = W_0 \Psi_2 + W_1 \Psi_1 + W_2 \Psi_0$$
$$...........$$
$$\lambda^n = \hat{H}_0 \Psi_n + \hat{H}'\Psi_{n-1} = \sum_{i=0}^{n} W_i \Psi_{n-i}$$

(2.37)

The equation 2.36 is called as nth-order perturbation equation. Note that if $\lambda^0 = 0$, the equation is perturbative Schrödinger equation.

2.12 Moller Plesset Perturbation Theory

Moller Plesset Perturbation Theory(MPPT)(Møller and Plesset, 1934) is based on adding correlation energy for ground state to zero-order Hamiltonian obtained from HF-SCF method. The one electron Fock operator gives the electronic Hamiltonian and

$$\hat{H}_0 = \sum_i F_i$$

(2.38)

The total of orbital energies give the E_0

$$E_0 = \sum_i \varepsilon_i$$

(2.39)

The eigen functions of $\hat{H}_0$ are obtained from the all slater determinants, thus, the solvation of the matrix obtained from Slater determinants become extremely easy. The perturbative part, $\hat{H}'$, is the difference of the $\hat{H}$ and $\hat{H}_0$. Actually, this assumption

helps to determine the solutions of unperturbed Schrödinger equation although this assumption does not obey the main assumption of the perturbation theory (the value of perturbation must be small).

The correction of correlation energy obtained by using zero-order perturbation theory is not suitable for the systems. If the order of perturbation is increased, then the favorable correction of correlation will be nearly accurate. At least, the proper correction of correlation energy is obtained by the way of the using second order perturbation because the second-order energy correction energy added the electronic energy consists from determinants having two electrons excitation. The formula of second-order perturbation is summarized with the following formula:

$$W_2 = \sum_{i \neq j}^{occ} \sum_{a \neq b}^{virtual} \frac{\left\langle \phi_0 \left| H' \right| \varphi_{ij}^{ab} \right\rangle \left\langle \varphi_{ij}^{ab} \left| H' \right| \phi_0 \right\rangle}{E_0 - E_{ij}^{ab}} \tag{2.40}$$

In the formula, while i and j are represented as doubly electron occupied orbital, a and b are represented as doubly electron occupied orbital, respectively. Addition, the difference energy of molecular orbitals is obtained from the difference of total energy of two Slater determinants. Thus, The second-order MP energy correction E(MP2) is given as follows:

$$E(MP2) = \sum_{i \neq j}^{occ} \sum_{a \neq b}^{vir} \frac{\left[\left\langle \varphi_i \varphi_j \left| \varphi_a \varphi_b \right\rangle - \left\langle \varphi_i \varphi_j \left| \varphi_a \varphi_b \right\rangle \right]^2}{\varepsilon_i + \varepsilon_j - (\varepsilon_a + \varepsilon_b)} \tag{2.41}$$

Also, there are plenty of supplementary information about PT and MPn(n=3,4,6) including the formula of first and second order correction to wave function in many computational books(Leach, 2001; Springborg, 2000).

The MP2 calculation having electron correlation is economically safe compared to CI calculation. In addition, the MPPT is expands to third(n=3), fourth(n=4)-order energy correction, the calculation will have economical cost.

2.13 Couple Cluster(CC) Theory

Perturbations theories having electron correlations deal with the full type of excitation (S,D,T…etc) adding to reference wave function in a given order (2,3,4….) but Couple Cluster (CC)Theory deals with all corrections adding reference wave function from the given order to infinite order. The CC wave function is the summarized with the following formula:

$$\Psi_{cc} = e^{\hat{T}} \Phi_0 \tag{2.42}$$

$$e^{\hat{T}} = 1 + \hat{T} + \frac{1}{2}\hat{T}^2 + \frac{1}{6}\hat{T}^3 + \dotsb = \sum_{k=0}^{\infty} \frac{1}{k!}\hat{T}^k \tag{2.43}$$

In the formula, exponential operator $\hat{T}$ is given as follow

$$\hat{T} = \hat{T}_1 + \hat{T}_2 + \hat{T}_3 + \dotsb \hat{T}_n \tag{2.44}$$

The HF reference wave function applied by using the $\hat{T}_i$ operator creates excited Slater determinants

$$\hat{T}_1 \Phi_0 = \sum_{i}^{occu} \sum_{a}^{virtual} t_i^a \Phi_i^a \tag{2.44a}$$

$$\hat{T}_2 \Phi_0 = \sum_{i\langle j}^{occu} \sum_{a\langle b}^{virtual} t_{ij}^{ab} \Phi_{ij}^{ab} \tag{2.44b}$$

The expansion coefficients are represented as amplitudes. For the exponential operator can be rewritten by combining between 2.42 and 2.43equations:

$$e^{\hat{T}} = 1 + \hat{T}_1 + (\hat{T}_2 + \frac{1}{2}\hat{T}_1^2) + (\hat{T}_3 + \hat{T}_2\hat{T}_1 + \frac{1}{6}\hat{T}_1^3) + \dotsb \tag{2.45}$$

In the formula, the first two terms (1 and $\hat{T}_1$) are the reference HF wave function and single excitations, respectively. The first terms in the parenthesis give the double excitations and the other terms in the second parenthesis are the triple excitations.

If the CC wave function is added into Schrödinger equation, it becomes as follow:

$$\hat{H}e^{\hat{T}}\Phi_0 = Ee^{\hat{T}}\Phi_0 \tag{2.46}$$

In the formula, the energy, E, becomes as follow when this equation is multiplied from the left side with $\Phi_0^{\,*}$

$$E_{cc} = \left\langle \phi_0 \left| He^{\hat{T}} \right| \phi_0 \right\rangle \tag{2.47}$$

In the formula, Hamiltonian obtained by using expandable $e^{\hat{T}}$ operator includes only one- and two-electron operators. In addition, the matrix element having single excited Slater determinants are zero because HF orbital is employed. E_{cc} becomes as follow

$$E_{cc} = E_0 + \sum_{i\langle j}^{occu} \sum_{a\langle b}^{virtual} (t_{ij}^{ab} + t_i^{\,a}t_j^{\,b} - t_i^{\,b}t_j^{\,a})(\left\langle \phi_i\phi_j \middle| \phi_a\phi_b \right\rangle - \left\langle \phi_i\phi_j \middle| \phi_b\phi_a \right\rangle) \tag{2.48}$$

Because of computational cost, the cutting Couple Cluster methods are employed. Note that adding only $\hat{T}_1$ operator energy correction to HF reference wave function does not give accurate result. Therefore, the lowest level of approximation is to employ when $\hat{T}=\hat{T}_2$ is used. Such approximation is known as CCD(Pople et al., 1978). When $\hat{T}=\hat{T}_1 + \hat{T}_2$ is employed to HF reference wave function, this is known as CCSD(Purvis and Bartlett, 1982; Scuseria et al., 1988, 1989) model. In addition, contribution of triple excitation can be added to CCSD method after it can be obtained with the help of perturbation theory. This method is called as CCSD(T) (Pople et al., 1987) known as 'Gold Method'. Also, CCSD(T) method involves full weak interaction of any system. The couple cluster wave function can equal with

the full CI when all cluster operators ($\hat{T}=\hat{T}_1+\hat{T}_2+\hat{T}_3+.....\hat{T}_n$) are added to the reference HF wave function but it is seen as unreachable process due to computational limits. In this thesis, we used CCSD(T) method because it provides best recover to HF reference wave function and also compared to other methods to check its quality.

2.14 Density Functional Theory (DFT)

Although the Density Function Theory (DFT) was tried to explain by studies of Thomas and Fermi(Lieb and Simon, 1977; Pople et al., 1987) before the 1930s, the first completely explanation of DFT was belonged to Hohenberg and Kohn(Hohenberg and Kohn, 1964). Hohenberg and Kohn are showed that the electron density, $\rho(r)$, determines the ground state energy. In other words, there is extremely correlation between the ground state energy of system and its electron density. The reason of why DFT is so famous is that DFT is based on using simpler electron density instead of using the complicated wave function, Ψ, and the associated Schrödinger equation. However, although DFT has many advantages compared to other post-HF method such computational cost, the biggest handicap of DFT is to determine the best functional consisting of correlation between the electron density of system and its ground state energy. Thus, the main purpose in DFT is to determine the suitable functional consisting the energy and electron density.

The process of DFT calculations is extremely similar to the process of HF calculations. Firstly, With the help of equation 2.12, the HF energy is produced for the single determinant wave function. Note that the formula of exchange integrals is summarized with the following formula into the equation 2.12

$$E_x^{HF} = -\frac{1}{2}\sum_i^N \sum_j^N K_{ij} \tag{2.49}$$

The orbitals are determined with the help of equation 2.24. In DFT calculations, the exchange terms in HF are defined as exchange-correlation functional. The formula of energy in DFT method is given as follow:

$$E^{\text{DFT}} = \sum_i^N h_{ii} + \frac{1}{2}\sum_i^N \sum_j^N J_{ij} + E_{xc}[\rho(\text{r})] \tag{2.50}$$

In the formula, the formula of electron density, ρ, is assumed as follow:

$$\rho(\text{r}) = \sum_i^N \phi_i^*(r)\phi_i = \sum_i^N \phi_i^a(r)\phi_i^a + \sum_i^N \phi_i^b(r)\phi_i^b = \rho(a) + \rho(b) \tag{2.51}$$

For closed shell systems, the electron density having alpha spin electrons equals the electron density having beta spin electrons, $\rho(a) = \rho(b)$, and $\phi_i^a = \phi_i^b$ but for the open shell systems, electron densities of both alpha and beta spins do not equal because spin densities must be independent.

With the help of Kohn-Sham equations(Kohn and Sham, 1965), the orbital must be determined

$$\left(-\frac{1}{2}\nabla^2 + V_{ne}(r) + \int \frac{\rho(r')}{|r - r'|}dr' + V_{xc}\right)\phi_i = \varepsilon_i \phi_i \tag{2.52}$$

In the formula, the first two and third terms are one electron (kinetic energy, potential energy between nuclei and electron) and Coulomb parts defined into Fock matrix, respectively. The last term that is represented as functional of derivative of E_{xc} is called as one-electron potential. The formula of one-electron potential is the summarized with the following formula,

$$V_{xc} = \frac{\delta E_{xc}}{\delta \rho} \tag{2.53}$$

In the formula, the exact value of V_{xc} is not known therefore there is no expression of exact $E_{xc}[\rho(\text{r})]$ value in DFT calculations, but there are various approximate descriptions for E_{xc} and the all descriptions are assumed that electrons do not interact with each other (non-interacting, homogenous electron gas) in the ground state. The approximate method is to split two parts into E_{xc} and V_{xc} equations, namely exchange and correlation.

$$E_{xc}[\rho]=E_x[\rho]+E_c[\rho] \tag{2.54}$$

$$V_{xc}[\rho]=V_x+V_c \tag{2.55}$$

The functionals assumed according to various approximate descriptions are divided into 3 groups namely, Local Density Approximation (LDA), Generalized Gradient Approximation(GGA) and Hybrid Methods.

It can be thought that the density of electron can be formed as an homogenous electron gas and related to only equations of E_x and E_c have the density, ρ. According to LDA, the formula of E_x is the summarized with the following formula:

$$E_x^{LDA}=[\rho_a,\rho_b]=-2^{\frac{1}{3}}c_x\int(\rho_a^{\frac{4}{3}}+\rho_b^{\frac{4}{3}})\,dr \tag{2.56}$$

In the formula, the $c_x=\dfrac{3}{4}\left(\dfrac{3}{\pi}\right)^{1/3}$ is the term obtained from in the Fermi-Dirac-Thomas model. In addition, this expression provides to obtain the exchange potential $V_x^a(r)$,

$$V_x^a(r)=\frac{\delta E_x^{LSDA}}{\delta\rho_x}=-2^{1/3}c_x\rho_a^{1/3} \tag{2.57}$$

For the beta spins, the exchange potential is obtained with the same way,

$$V_x^a(r)=\frac{\delta E_x^{LSDA}}{\delta\rho_x}=-2^{1/3}c_x\rho_b^{1/3} \tag{2.58}$$

In the LDA, the correlation energy, E_c^{LDA}, are obtained by using Monte Carlo methods with different densities and added to the a functional form that can be used in DFT calculations(Vosko et al., 1980). The correlation potentials, E_c^{LDA}, is also donated by E_c^{VWN} (Vosko, Wilk and Nusair). With the help of their findings, the equation 2.50 having V_{xc} term becomes ready for the calculations.

There are several methods to improve LDA. The one is to consider a non-uniform electron gas behavior. In other words, a non-uniform electron gas behavior must be considered to improve LDA. The reason of considering a non-uniform electron gas behavior is that the exchange and correlation energies not only depend on the electron density but also depend on derivatives of the density $E_{xc}[\rho, \nabla \rho]$. The such of this consideration method is known *as Gradient Corrected or Generalized Gradient Approximation(GGA)*. The more popular exchange and correlation functional are given with the following Figure 5.2. The exchange functional in the Figure 2.3 can be employed with any correlation functionals together.

Exchange functionals, E_x^{GGA}	Correlation functionals, E_c^{GGA}
B88 (Becke 88)	LYP (Lee-Yang-Parr)
PW86 (Perdew-Wang 86)	P86 (Perdew 86)
PW91 (Perdew-Wang 91)	PW91 (PerdewWang 91)
	B96 (Becke 96)

Figure 2.3. The popular exchange and correlation functionals in dft.

As it is clearly seen that LDA and GGA deals with the electron density and electron density with derivatives of the density terms, respectively. Also, there are hybrid methods. The method is based on combining LDA and GGA functional with the HF exchange terms. The most popular hybrid functional, is B3LYP consisted form Becker's 3- parameter exchange hybrid functional with Lee, Yang, Parr (LYP)(Becke, 1993a; Lee et al., 1988b) correlation functional. The exchange correlation energy of B3LYP is summarized with the following formula.

$$E_{xc}^{B3LYP} = aE_x^{LSDA} + (1-a)E_x^{HF} + b\Delta E_x^{B88} + c\Delta E_c^{LYP} \tag{2.59}$$

In the formula, $\Delta E_x^{B88} = E_x^{B88} - E_x^{LSDA}$, $\Delta E_c^{LYP} = E_c^{LYP} - E_c^{LSDA}$ and the constants before coming from the energies: a = 0.80, b = 0.72, and c = 0.81

2.15 Semi-empirical Methods

Semi-empirical methods are extremely same to HF calculations because their calculation pose the Hamiltonian and a wave function. In these methods, a certain approximation is accepted or some computational terms are totally omitted. For instance, the core electrons are disregarded and the exchange integrals having two electrons are neglected in the semi-empirical calculations. Because of omitting two electron integrals and disregarding core electrons, the accuracy of semi-empirical methods is weaker than DFT methods. Therefore, the semi-empirical methods must be parametrized in order to fix the errors obtained by neglecting two electron parts of the calculation. The parameters calculated for neglected values are obtained from '*experimental data*' or '*ab initio*' calculations. Generally, the parameters are used instead of omitting two electron integrals.

Although the semi-empirical methods are weaker than ab initio methods, their calculations are extremely faster than that of ab initio methods. In addition, while the number of properties of a system calculated from semi-empirical methods can be erratic only few of them are reliable. For instance, the results will be rich if the molecule being calculated is similar to molecule in the database employed to obtain the parameters, the other way around, the results will be very poor. For instance, the carbon atom in cyclohexane and n-hexane have apparently different bond lengths, angles etc. therefore these molecules cannot be computationally predictable well if they do not exist in the database of semi-empirical methods to be employed. In the meantime, the database of semi-empirical methods is also known as '*parametrization set*' in literature. There are several good semi-empirical methods such as PM6(Stewart, 2009), PM7(Stewart, 2013), PM6-DH2(Fanfrlík et al., 2010) and PM6-D3H4X(Hostaš et al., 2013) to be described in detail result and discussion section.

2.16 The Computational Chemistry Suites Employed

The all calculations in this thesis was mostly employed by utilizing GAUSSIAN (Frisch et al., 2010) chemistry suit package program. In addition, MOPAC(Stewart, 1990) and TURBOMOLE(Steffen et al., 2010) chemistry suites

programs also served in some calculations namely, semi-empirical and DFT including dispersive interactions, respectively. Besides, the graphical interface programs namely, GABEDIT (Allouche, 2012), CUBY4 (Řezáč, 2016) GAUSVIEW (Dennington et al., 2009) and Avogadro(Hanwell et al., 2012) were utilized for collecting and evaluation of output data including computational results.

3. RESULTS AND DISCUSSION

BN, AlN and SiC nanostructures having many unique properties such as hydrogen storage material have been selected as host nanostructures in this thesis. In particular, the properties of these nanomaterials related to the hydrogen storage have been tried to be determined by using computational chemistry methods. Since there are many structural forms of these host materials such as nanocages, nanotubes, nanosheets, etc., we present the computational results related to the hydrogen storage properties of these nanomaterials under several different titles as follows.

3.1 Computational Investigation Hydrogen Storage Capacity of Boron Nitride Nanocages: A Semi-Empirical Study

In this section, the hydrogen storage properties of boron nitride nano-host molecules have been investigated with the help of the PM7 semi-empirical method. This method is a fairly newly developed method and it can account for the weak interactions occurring between the host and hydrogen molecule. In fact, we computationally tried to find out answers to some questions concerning hydrogen storage properties of this materials in this part of the thesis. They are as follows: What are the maximum endohedral hydrogen capacities of the host molecules? In other words, how many hydrogen molecules are stored inside the host molecule before the nano-hosts molecules fracture? Is there a relation between the size of the host molecule and hydrogen molecules additions? How geometric changes of both hydrogen molecules and host molecules take place during the hydrogen addition? Are complexes including endohedral hydrogen molecules thermodynamically stable?

The physical adsorption of hydrogen molecules includes weak non-bonding interactions between the hydrogen and the host molecules. Accordingly, it is very important to select a good computational method in the hydrogen-storage calculations since the selected method have to have the ability to calculate the dispersive effects. Therefore, the PM7 semi-empirical method developed by James J. P. Stewart(Stewart, 2013) was utilized in this part. The reason for selecting the

PM7 method is not only to calculate weak interactions accurately but also to calculate large systems without spending much computational effort. The PM7 method is able to relatively accurately calculate very large systems having non-covalent interaction in a very short time compared to the DFT method In the computational study published by Hobza et.al, it is claimed that the results of the PM7 method are better than those of the PM6 method for the many systems including weak interactions. The PM7 method also gives almost the same results with the modified PM6 methods for the systems not including weak interactions.

All of the host nanocages have only tetragonal and hexagonal connections in their structures. The reason for choosing these types of connections is to prevent the escape of hydrogen molecules through the nanostructure. Initially, all these host structures were optimized and characterized as minima by utilizing harmonic vibrational analysis method at the PM7 level of theory as implemented in MOPAC 2012, semi-empirical quantum chemistry package. Then, hydrogen molecules were added inside each of these nanocages. In addition, their optimizations and frequency calculations were performed with the same method. Each nanocage was filled with hydrogen molecules until it breaks. By doing so, we obtained the hydrogen storage capacities of these nanocages.

To be able to determine thermodynamic stability of the nH_2@host complexes, their formation enthalpies at 298 K were calculated from eqn 3.1

$$\Delta H_f^{complex} = \left[\Delta H_{f(nH_2@host)} - \left(\Delta H_{f(host)} + n\,\Delta H_{f(H_2)} \right) \right] \tag{3.1}$$

where $\Delta H_{f(nH_2@host)}$, $\Delta H_{f(host)}$ and $\Delta H_{f(H_2)}$ are the heats of formation of the complex, host and hydrogen molecules calculated by PM7, respectively.

Within the process of determining hydrogen storage capacity, we obtained the most thermodynamically stable BN-hydrogen complexes for these nanocages. By "stable complex", we mean the complex that has a formation enthalpy lower than the sum of formation enthalpies of individual hydrogen molecules and boron nitride nanocage located at infinite separation from each other. In other words, a

Table 3.1 Maximum number of H$_2$ molecules doped, complex formation enthalpies, enthalpy per added H$_2$ molecule and weight % of hydrogen storage

Nanocage	Max. number of H$_2$ doped	$\Delta H_f^{complex}$ (eV)	$\Delta H_{destability}$ (eV/nH$_2$)	Weight % H$_2$ storage
B$_{12}$N$_{12}$	2	17.88	8.94	1.35
B$_{24}$N$_{24}$	9	35.45	3.94	3.05
B$_{36}$N$_{36}$	22	67.81	3.08	4.96
B$_{48}$N$_{48}$	39	105.25	2.70	6.60
B$_{96}$N$_{96}$	125	229.80	1.84	10.58

complex is thermodynamically stable if it has a negative complex formation enthalpy, $\Delta H_f^{complex}$. The geometries of nH$_2$@B$_m$N$_m$ (m=12, 24, 36, 48 and 96) complexes containing maximum number of H$_2$ molecules are depicted in *Fig. 3.1* while the maximum H$_2$ numbers doped inside the nanocages before they break, the formation enthalpies and gravimetric H$_2$ storage weight percentages (wt%) of these complexes are presented in *Table 3.1*
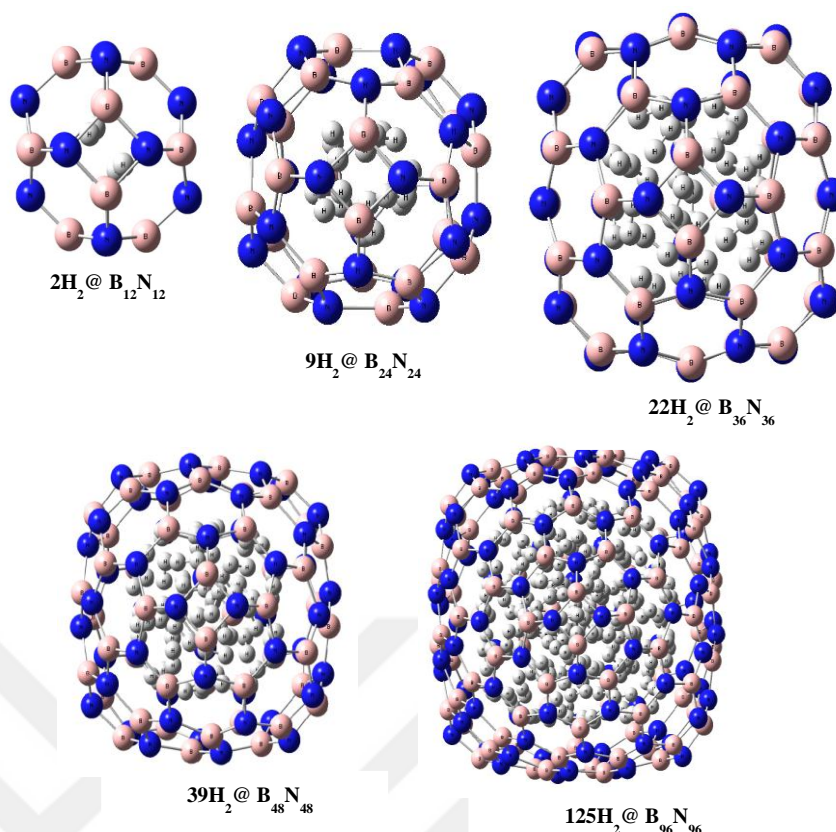
Figure 3.1. Maximum number of H_2 molecule confined B_mN_m nanocages.

The following points about hydrogen storage capabilities of the boron nitride nanocages are to be discussed based on the PM7 results. The variation of complex formation enthalpies, $\Delta H_f^{complex}$, with number of hydrogen molecules are depicted in *Fig.3.2*, revealing several important results. First of all, complex formation enthalpies have quadratic dependence on number of hydrogen molecules. There is no thermodynamically stable complex formation for the smallest two nanocages ($B_{12}N_{12}$ and $B_{24}N_{24}$). In the initial stages of endohedral hydrogen doping, however, there are some thermodynamically stable complexes (having negative complex formation enthalpies) formed up to a certain critical number of hydrogen molecules for the nanocages expect for the smallest two. PM7 predicts these critical numbers as 1, 4 and 25 H_2 molecules for $B_{36}N_{36}$, $B_{48}N_{48}$ and $B_{96}N_{96}$, respectively. After passing these critical numbers, the complexes become thermodynamically unstable but kinetically stable since they cannot overcome the kinetic barrier applied by nanocage inner surface. With continued addition of hydrogen molecules, the repulsive interactions originated from both H_2-H_2 and H_2-nanocage increase so as

to break the weakest B—N bond of nanocage. The kinetic barrier, here, can be considered as the energy necessary to break the weakest B—N bond. In this case the structure of nanocage breaks down. Therefore, hydrogen storage capacity is defined as the maximum number of hydrogen molecules endohedrally doped inside nanocage whose structure is intact. $B_{12}N_{12}$ can accommodate at most two hydrogen molecules.

The $B_{24}N_{24}$ nanocage can be endohedrally doped by nine hydrogen molecules before its structure breaks down, leading to a hydrogen storage capacity of 3.05 wt%. Each endohedral hydrogen molecule addition to $B_{24}N_{24}$ increases formation enthalpy almost linearly. Even if one hydrogen molecule is encapsulated by $B_{24}N_{24}$, the complex becomes thermodynamically unstable with a positive enthalpy of formation. On the other hand, it is not the case for the $B_{36}N_{36}$ nanocage. The complex formed when one hydrogen molecule is encapsulated by the $B_{36}N_{36}$ nanocage becomes thermodynamically stable with a formation enthalpy of -0.19 eV. This shows the endohedral cavity of $B_{36}N_{36}$ applies an attractive force making the resultant complex more favorable. The hydrogen storage capacity of $B_{36}N_{36}$ is 22 hydrogen molecules with a 4.96 wt%. This value is close to the DOE's 2015 target of 5.5 wt%. Oku *et al.*(Koi and Oku, 2004c) reported that maximum 20 hydrogen molecules can be doped inside $B_{36}N_{36}$ nanocage, confirming our findings. The small difference comes from the computational methodology. They used the PM5, earlier version of PM7, method while we employed PM7, a better semi empirical method that can model nonbonding interactions more accurately. Up to four hydrogen molecules can be stored in the $B_{48}N_{48}$ nanocage so that the resulting complexes are thermodynamically stable, and it is revealed that maximum 39 hydrogen molecules can be doped inside $B_{48}N_{48}$. The hydrogen storage capacity of $B_{48}N_{48}$ corresponds to a wt% of 6.60, which is above well above the DOE's 2015 target. The $B_{96}N_{96}$ nanocage, the largest nanocage in this study, has rather huge hydrogen storage capacity of 10.6 wt% since it can endohedrally hold 125 H_2 molecules while keeping its structure intact. As a result, the $B_{48}N_{48}$ and $B_{96}N_{96}$ nanocages can be very promising materials for hydrogen storage.

Fig. 3.3 gives variation of hydrogen storage capacity as wt% with respect to nanocage size (total number B and N atoms in nanocage). The data obtained with

PM7 perfectly fit to a second order polynomial function with a regression value of 0.9991. This function is given in equation 2

$$wt\% = -0.0002k^2 + 0.0948k - 0.917 \qquad (3.2)$$

where k is the total number of B and N atoms in a nanocage. Since the coefficient of second order term is very small and first four data is very close to a linear behavior, one can consider that as hydrogen storage capacity of boron nitride nanocages increase almost linearly with nanocage size. These results point out the possibility of finding highly effective hydrogen storage materials using boron nitride nanostructures.
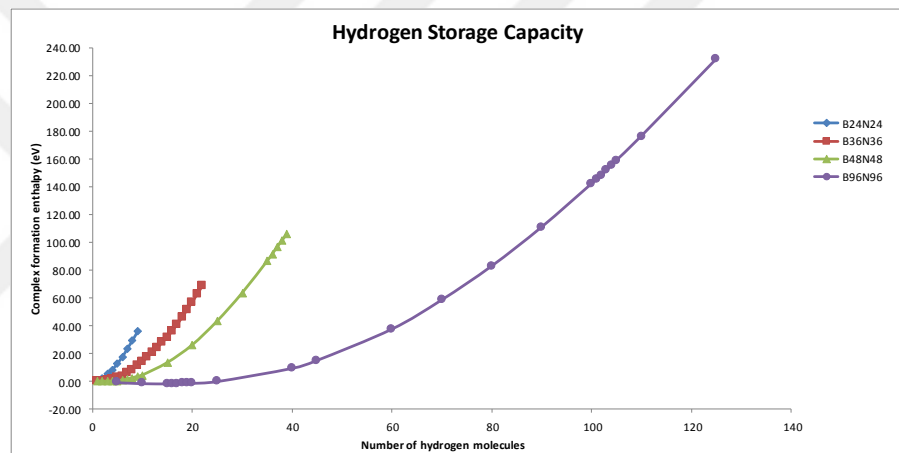

Figure 3.2. Hydrogen capacity of several B_mN_m nanocages.
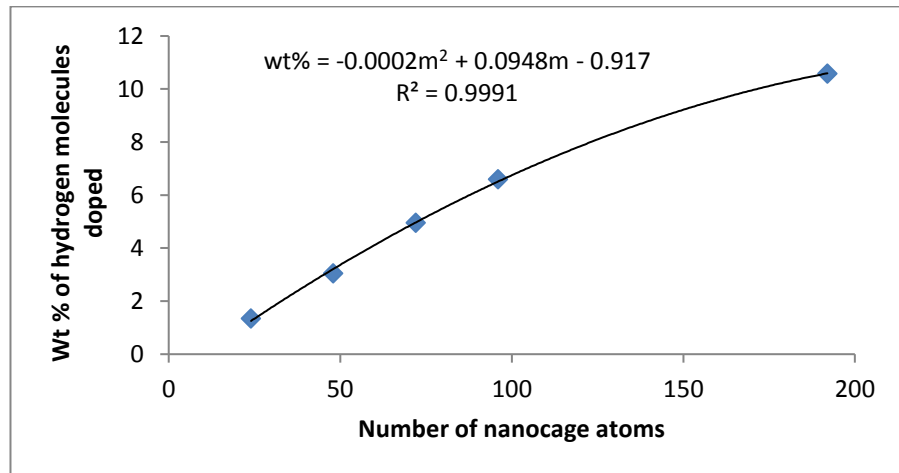

Figure 3.3. Variation of hydrogen storage capacity as wt% with respect to BN nanocage size.

Table 3.2 gives the maximum percent elongation (%elongation) values of B—N and H—H bond lengths, calculated by employing the following average distances. The %elongation values for B—N bonds were obtained by using the difference between average B—N bond distance of the complex having maximum number of H_2 molecules and that of empty nanocages. Similarly, the %elongation values for H—H bond lengths were calculated by exploiting the difference between average H—H bond distances inside the complex containing maximum number of H_2 molecules and the H—H bond lengths of single hydrogen molecule containing nanocages. $B_{12}N_{12}$ is different from other nanocages in that it reaches storage capacity with a sudden 3.3% elongation after two H_2 additions due to having the smallest endohedral surface. On the other hand, the remaining nanocages show gradable trends. As nanocage size increases maximum elongation percent increases. This indicates that larger nanocages become more elastic increasing the storage capability. Upon H_2 addition, increase in H—H bond lengths seem an unexpected result, but this elongation reduces as nanocage size increases.

Table 3.2 Maximum percent elongation values for B-N and H-H bond lengths

| Nanocage | B-N distance | | % elongation |
	Average Bond Distance (full complex)	Average Bond Distance (empty nanocage)	
$B_{12}N_{12}$	1.5578	1.5076	3.33
$B_{24}N_{24}$	1.5514	1.5314	1.31
$B_{36}N_{36}$	1.5567	1.5108	3.04
$B_{48}N_{48}$	1.5659	1.5001	4.39
$B_{96}N_{96}$	1.5751	1.4831	6.20

| Nanocage | H-H distance | | % elongation |
	Average Bond Distance (in full complex)	H_2@nanocage	
$B_{12}N_{12}$	0.7644	0.7594	0.66
$B_{24}N_{24}$	0.7844	0.7594	3.29
$B_{36}N_{36}$	0.7832	0.7594	3.13
$B_{48}N_{48}$	0.7822	0.7594	3.00
$B_{96}N_{96}$	0.7762	0.7594	2.21

3.2 Computational Investigation of Hydrogen storage and properties of Boron Nitride Nanocages by Newly Discovered PM6-DH2 method: A Semi-Empirical Study

In this part, we have different aims in the determination of the hydrogen storage properties of the BN nanostructures. The most important one of these aims is to accurately estimate the hydrogen storage capacity (wt%) of various selected BN nanocage structures namely $B_{12}N_{12}$, $B_{24}N_{24}$, $B_{36}N_{36}$, $B_{48}N_{48}$ and $B_{96}N_{96}$ nanocages. The DFT methods including weak dispersion terms (e.g. ωB97X-D) may be employed for the small BN nanocages such as $B_{12}N_{12}$ and $B_{24}N_{24}$ but they can become useless for large BN nanocages, especially $B_{96}N_{96}$. Therefore, the PM6-DH2 and PM7 semi-empirical methods were tested against ωB97X-D for the small BN nanocages namely, $B_{12}N_{12}$, $B_{24}N_{24}$ nanocages. According to ωB97X-D results, it was determined which semi empirical method is the suitable for BN systems. After finding the suitable semi empirical method, the hydrogen storage capacity of larger BN nanocages and its related properties ($B_{36}N_{36}$, $B_{48}N_{48}$ and $B_{96}N_{96}$) were investigated. The PM6-DH2 results for $B_{24}N_{24}$ are extremely captivating in the way of computational effort because PM6-DH2 results are extremely as same as the ωB97X-D results for the $B_{24}N_{24}$ nanocage. In addition, the PM6-DH2 semi empiric method is approximately ten thousand times faster than ωB97X-D/DFT method.

The optimized host nanocages are depicted in Figure 3.4. Note that the nanocages having tetragonal and hexagonal rings are suitable for the endohedral doping. In other words, the nanocages having octagonal or more connections are not suitable host molecules because hydrogen molecules can escape from inner side of the host molecules. These host nanocages having only tetragonal and hexagonal rings are the thermodynamically most stable structures among their other isomers except for the $B_{24}N_{24}$ nanocage. While the $B_{12}N_{12}$, $B_{36}N_{36}$ and $B_{48}N_{48}$ nanocages are the lowest energy isomers, the $B_{24}N_{24}$ isomer having tetragonal and hexagonal connections does not have the lowest energy among its isomers. Also, the energy of $B_{24}N_{24}$ host nanocage was found 2.4 kcal /mol above compared to its lowest energy isomer (Wu et al., 2006).
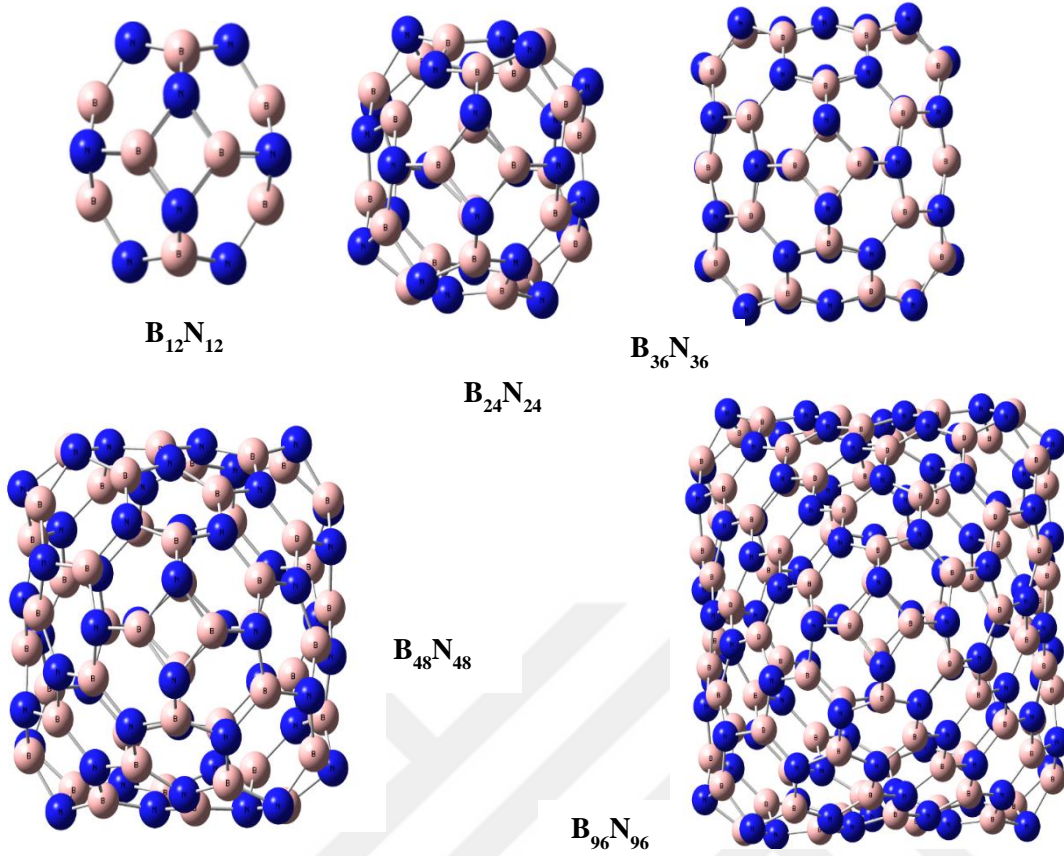
Figure 3.4. The PM6-DH2 optimized geometries of all host B_mN_m nanocages.

Firstly, the optimized geometries and energies of pure $B_{12}N_{12}$ and $B_{24}N_{24}$ nanocages and their hydrogen doped complexes nH_2 @ B_mN_m (m=12 and 24) were determined by employing PM6-DH2, PM7, B3LYP and ωB97X-D methods. The cc-pVTZ basis set was selected for all DFT calculations. In addition, the harmonic vibrational calculations were computed for all optimized BN complexes at their levels of optimization. In other words, there is no imagery frequency value for the BN complexes because they are stable at their levels of optimization.

To be able to determine thermodynamic stability of the nH_2@ B_mN_m (m=12 and 24), their formation enthalpies at 298 K were calculated from eqn 3.3

$$\Delta H_f^{complex} = \left[\Delta H_{f(nH_2 @ host)} - \left(\Delta H_{f(host)} + n\,\Delta H_{f(H_2)} \right) \right] \tag{3.3}$$

where $\Delta H_{f(nH_2 @ host)}$, $\Delta H_{f(host)}$ and $\Delta H_{f(H_2)}$ are the heats of formation of the complex, host and hydrogen molecules calculated by using PM6-DH2, PM7, B3LYP and ωB97X-D methods, respectively. It is known that the ωB97X-D method is suitable for the systems including non-covalent interactions, also, it gives good results. Therefore, the ωB97X-D method is selected as a reference method. When the PM6-DH2 results are compared to with the ωB97X-D results, they give the nearest accurate formation energy of the complexes, especially $B_{24}N_{24}$ complexes, according to the ωB97X-D results. Because $B_{24}N_{24}$ complexes have more dominant non-covalent interactions than $B_{12}N_{12}$ complexes. Due to having high accuracy, the other formation enthalpies of the complexes and their hydrogen storage properties were calculated by utilizing PM6-DH2 method. The semi empirical calculations were performed by using MOPAC2012 computational suite, but the DFT calculations were performed by using Gaussian09. Note that the meaning of 'hydrogen storage capacity' is the maximum number of hydrogen molecules doped into the host molecules. In other words, the hydrogen molecules can be accommodated into the host molecule(s) until the host molecule(s) are broken down. Furthermore, the activation energy that hydrogen molecule passes from hexagonal ring of the biggest host molecule was also calculated with the help of PM6-DH2 method. The activation energy is defined as the difference between single point energy of the largest complex that accommodates hydrogen molecule in the middle of the hexagonal ring and sum of single point energies of both the pure host molecule and hydrogen molecule.

Oku(Koi and Oku, 2004) et.al claims that hydrogen storage capacity of BN nanostructures can be reached up to 4.9 wt%. In addition, they utilized old semi empirical method called PM5.

Table 3.3 Formation heats of $nH_2@B_{12}N_{12}$ and $nH_2@B_{24}N_{24}$ complexes

Complex	n	ΔHf (eV)			
		ωB97X-D	PM6-DH2	B3LYP	PM7
$nH_2@B_{12}N_{12}$	1	0.099	0.139	0.109	0.182
	2	0.392	0.446	0.408	0.663
	3	0.673	0.783	0.697	-
$nH_2@B_{24}N_{24}$	1	0.001	0.007	0.022	0.017
	2	0.051	0.052	0.083	0.082
	3	0.134	0.130	0.175	0.187
	4	0.216	0.217	0.267	0.302

At the ambient condition, the formation enthalpy of the complexes with the first two host molecules estimated by using PM6-DH2, PM7, B3LYP and ωB97X-D methods are presented in Table 3.3, and the hydrogen storage capacity of all host molecules are also depicted in Figure 3.8. Since the dispersive effects of the $B_{12}N_{12}$ and $B_{24}N_{24}$ complexes are quite different, the methods used for each case will be evaluated separately. The one hydrogen molecule addition into the $B_{12}N_{12}$ host molecule is not thermodynamically stable because the formation enthalpy of the complex is estimated nearly 62.3 kcal/mole (0.099 eV) with help of ωB97X-D method. This result is extremely anticipated because the $B_{12}N_{12}$ nanostructure has the smallest internal cavity among all host molecule. Therefore, one and two hydrogen molecule addition make the host molecule more unstable. In other words, the $B_{12}N_{12}$ structure enlarges with the hydrogen molecules addition without breaking its bonds, but the enthalpies of these complexes are higher. The B3LYP method is more suitable than semi-empirical methods because the formation energy of B12N12 complexes obtained from the B3LYP method is slightly higher than those of ωB97X-D method. In addition, the PM6-DH2 method work quite well compared to PM7 that cannot even foresee a stable $B_{12}N_{12}$ complex with the endohedral three hydrogen molecules doping. The reason of this can be sourced from a wide range of core repulsion terms including non-covalent interactions between the host and hydrogen molecules that are compelled to be close to each other because of having the cage restrictions. However, PM6-DH2 method is considerable different than PM7 because it predicts electron-electron repulsion

terms which predominate dispersive interactions good in this system. Consequently, the $B_{12}N_{12}$ nanocage is suitable for neither hydrogen storage material nor testing for computational methods.
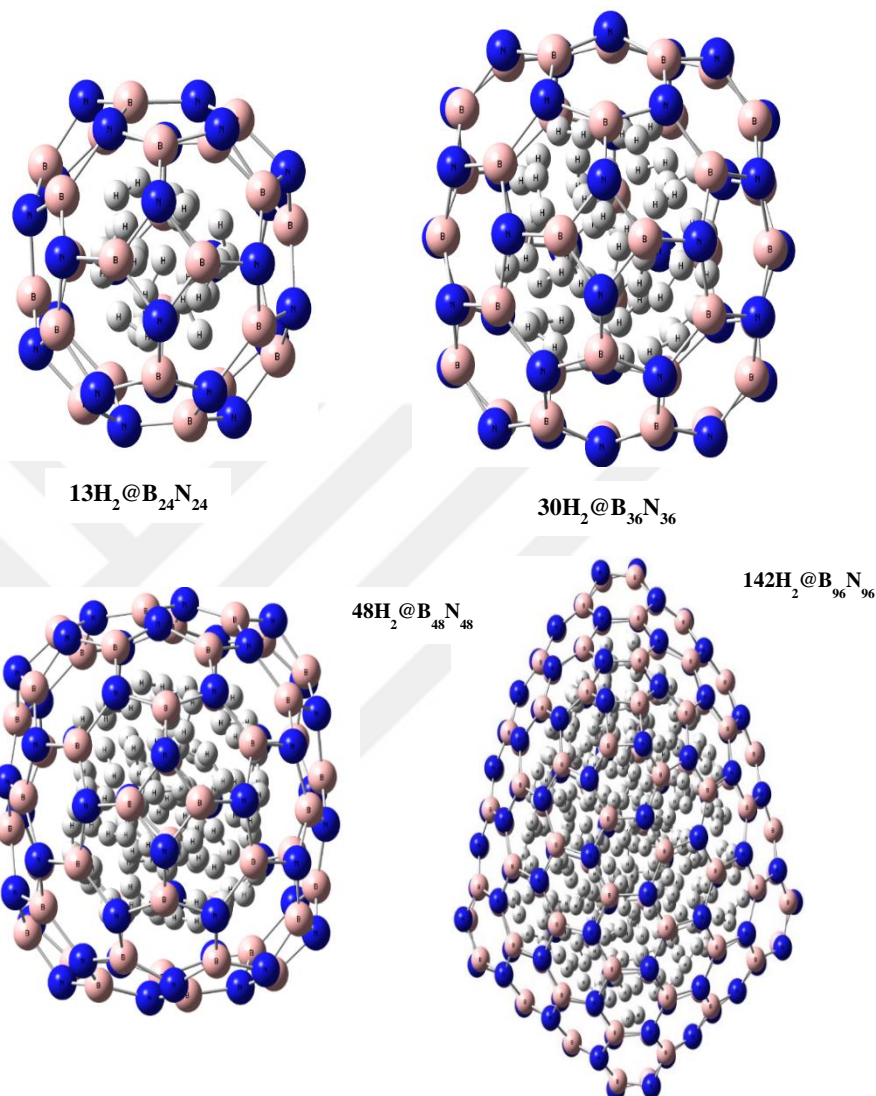
Figure 3.5. The BN host molecules with maximum number of hydrogen molecules estimated by PM6-DH2.

The dispersive effects of $B_{24}N_{24}$ nanocage is higher than that of $B_{12}N_{12}$ nanocage, because the $B_{24}N_{24}$ has larger internal size. Thus, the results obtained by using the $B_{24}N_{24}$ would be more appropriate compared to those of $B_{12}N_{12}$. The formation enthalpy of $B_{24}N_{24}$ nanocage with the one hydrogen molecule obtained by using the ωB97X-D method is 0.5 kcal/mole (0.001 eV). In addition, this result also shows that molecular hydrogen interacts very poorly with the inner atoms of

$B_{24}N_{24}$ nanocage in addition of one hydrogen molecule. In the other way, the formation enthalpy of $H_2@B_{24}N_{24}$ obtained by using PM6-DH2 method is 4.5 kcal/mole (0.007 eV) and this result is the closest to the result obtained by using ωB97X-D method. The formation enthalpy of host nanocage with one hydrogen molecule obtained by the PM7 method is lower than that obtained by the B3LYP method. This result shows that the PM7 method shows better performance than the B3LYP method for our systems, but the deviation of PM7 method considerably increases with the number of hydrogen molecules addition to the system. The PM6-DH2 method shows a good performance increase because the deviation of PM6-DH2 is very low even in the case of encapsulating a hydrogen molecule where the weak interactions predominate. The formation enthalpy values of the other complexes obtained by the PM6-DH2 method are close to the formation enthalpy values of those ($2-4@B_{24}N_{24}$) obtained by the ωB97X-D method. In other words, PM6-DH2 can foresee well the stabilities of BN complexes including endohedrally adding hydrogen molecules as accurately as the ωB97X-D method. In addition, the PM6-DH2 semi empirical method has the best computational cost for BN systems compared to ωB97X-D method. The ωB97X-D/cc-pVTZ level optimization and frequency analysis of the largest system took nearly 3 weeks in a parallel process including 4 CPU while those calculated by PM6-DH2 took several minutes. This result also showed that not only PM6-DH2 method has very as accurate and reliable as ωB97X-D method, but also, it has unique computational cost for the BN systems including non-covalent interactions. Therefore, it is concluded that the endohedrally hydrogen molecule storage capacity of BN nano-host molecules can be investigated by using PM6-DH2.

Table 3.4 Formation heats, destabilization enthalpies and maximum H_2 storage wt% s of the BN nanocages calculated with PM6-DH2 method

Nanocage	Max # of H_2 molecules	ΔH_f (eV)	$\Delta H_{destability}$ (eV)	H_2 storage wt%
$B_{24}N_{24}$	13	53.635	4.126	4.40
$B_{36}N_{36}$	31	100.492	3.242	6.99
$B_{48}N_{48}$	48	126.538	2.636	8.12
$B_{96}N_{96}$	142	240.742	1.695	12.01

The formation enthalpy of the BN complexes, ΔH_f, their endohedral hydrogen storage percent and destability energy per hydrogen molecule adding endohedrally calculated the PM6-DH2 semi empirical method are presented in Table 3.4. The BN host molecules including maximum number hydrogen molecules endohedrally are 13, 31, 38 and 142 while their hydrogen storage percentages are 4.40, 6.99, 8.12 and 12.01, respectively. Therefore, all the host molecules apart from $B_{24}N_{24}$ overrun the revised DOE hydrogen storage target for the year 2015. The formation enthalpy energy of the complexes according to endohedrally adding hydrogen molecules are depicted in Figure 3.6. It is seen from the figure 3.6, all complexes with one molecular hydrogen except $B_{24}N_{24}$ are thermodynamically stable. The formation enthalpies of all complexes increase as the hydrogen molecule is added. The added hydrogen molecules cause the host molecules to swell and this swelling continues until the B-N bonds of the host molecule are broken. The $B_{96}N_{96}$ host nanocage can store the largest number of hydrogen molecules among all nanocages because it becomes slowly unstable with endohedrally adding hydrogen molecule compared to the other host molecules. In other words, its destabilization energy is the lowest among the BN host molecules.
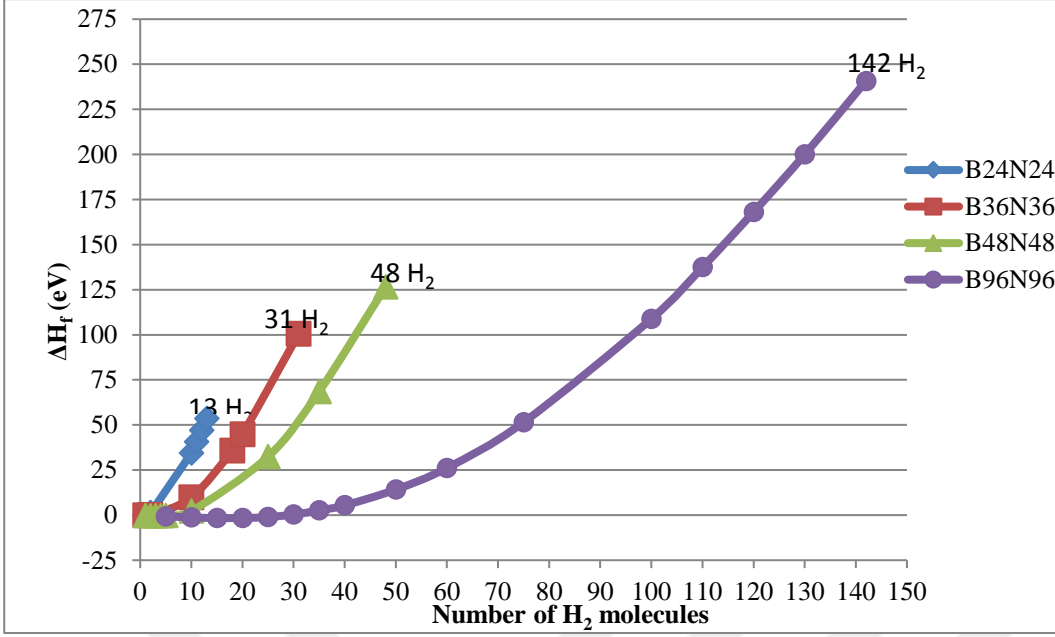
Figure 3.6. The BN host molecules with maximum number of hydrogen molecules estimated by PM6-DH2.

Note that the destabilization enthalpy, $\Delta H_{\text{destability}}$ which is summarized with the following equation 3.4, can be thought as the sum of three different energies obtained from the several interactions namely, destabilization energy generated from cage inflation, $\Delta H_{\text{inflation}}^{\text{cage}}$, destabilization energy generated from contraction of H_2 molecules, $\Delta H_{\text{contraction}}^{\text{H}_2}$ and interaction energy between the cage and hydrogen molecules adsorbed, $\Delta H_{\text{interaction}}^{\text{cage-H}_2}$. In equation 3.4, the first two enthalpies are calculated with following equation 3.5 and 3.6.

$$\Delta H_{\text{destability}} = \Delta H_{\text{inflation}}^{\text{cage}} + \Delta H_{\text{contraction}}^{\text{H}_2} + \Delta H_{\text{interaction}}^{\text{cage-H}_2} \tag{3.4}$$

$$\Delta H_{\text{inflation}}^{\text{cage}} = \Delta H_{f,\text{inflated}}^{\text{empty cage}} - \Delta H_{f,\text{non-inflated}}^{\text{empty cage}} \tag{3.5}$$

$$\Delta H_{\text{contraction}}^{\text{H}_2} = \Delta H_{f,\text{contracted}}^{\text{H}_2} - n\,\Delta H_f^{\text{H}_2} \tag{3.6}$$

where $\Delta H_{f,\text{inflated}}^{\text{empty cage}}$ and $\Delta H_{f,\text{non-inflated}}^{\text{empty cage}}$ enthalpies are the enthalpy of optimized inflated host molecule and pure optimized host molecule, respectively. $\Delta H_{f,\text{contracted}}^{\text{H}_2}$ is the heat of energy generating from contracted hydrogen molecules apart from the cage

and the $\Delta H_f^{\mathrm{H_2}}$ is the heat of formation of single hydrogen molecule. The $\Delta H_{\mathrm{interaction}}^{\mathrm{cage\text{-}H_2}}$ can be easily calculated the difference between destability energy and sum of destabilization energy generating from cage inflation and destabilization energy generating from contraction of H_2 molecules (eqn 3.6). All energy terms mentioned above were calculated by using PM6-DH2 semi empirical method at 298 K. All energy of the complexes including maximum number of hydrogen molecules and their average B-N and H-H distances are also depicted in Table 3.5.

Table 3.5 Destabilization, cage inflation, H_2 contraction and cage-H_2 contraction entalpies (in eV), average B-N and H-H distances (in Å) for the complexes carrying maximum number of H_2 molecules calculated with the PM6-DH2 method

Complex	$^a\Delta H_{\mathrm{destability}}$	$^a\Delta H_{\mathrm{inflation}}^{\mathrm{cage}}$	$^a\Delta H_{\mathrm{contraction}}^{\mathrm{H_2}}$	$^a\Delta H_{\mathrm{interaction}}^{\mathrm{cage\text{-}H_2}}$	Average B-N distance^b	Average H-H distance^b
$13H_2@B_{24}N_{24}$	4.126	4.636	2.556	-3.066	1.67	0.54
$30H_2@B_{36}N_{36}$	3.242	0.883	1.130	1.229	1.60	0.80
$48H_2@B_{48}N_{48}$	2.636	2.627	1.868	-1.859	1.68	0.57
$142H_2@B_{96}N_{96}$	1.695	0.488	0.844	0.364	1.56	0.79

(^{a}in eV. ^{b}in Å.)

When 13 hydrogen molecules become very close to each other in the $B_{24}N_{24}$ nanocage, inflation of the host molecule becomes maximum. Therefore, the interaction energy between the cage and hydrogen molecule is negative. In other words, when the cage endohedrally adsorbs the maximum number of hydrogen molecules, the interaction energy between the cage and a hydrogen molecule become very attractive. The other cage having attractive interactions between hydrogen molecules and the cage atoms is $B_{48}N_{48}$ because average B-N and H-H bond lengths for $B_{48}N_{48}$ nanocage are almost the same as that of $B_{24}N_{24}$ nanocage. The interaction energies of $B_{36}N_{36}$ and $B_{96}N_{96}$ nanocages have positive values (1.229 and 0.364 eV, respectively) and their geometrical properties are the same. These cages cannot be filled with as much hydrogen molecules as $B_{24}N_{24}$ and B48N48 because of having positive $\Delta H_{\mathrm{interaction}}^{\mathrm{cage\text{-}H_2}}$. In addition, these host molecules cannot compress hydrogen molecules hard enough as it is understood from their large H-H bond lengths. Therefore, it can be concluded that these nanocages are not

suitable hydrogen storage materials. On the other hand, the stability of these nanocages increases with increasing host size when their destability energies are considered.

The activation barrier of the hydrogen molecule that passes from the hexagonal ring of the largest host molecule was also investigated by using PM6-DH2 semi empirical method. The reason is to determine whether hydrogen molecule passing from any of hexagonal ring in the host molecule ruptures cage structure or not. In the study published by Koi and Oku(Koi and Oku, 2004b) it is claimed that the energy barrier for $B_{24}N_{24}$ is 15 eV. Note that the energy barrier can be calculated from the single point energy difference for the geometries where hydrogen passes from the center of the hexagonal ring in the host molecule and the geometries where hydrogen in the center of the host molecule. To more accurately estimate the energy barrier of the complex, the transition state (TS) structure of a hydrogen molecule passing from the center of the hexagonal ring of the host molecule was determined by using PM6-DH2 method. According to the PM6-DH2 method, the energy barrier is nearly 9.82 eV that is higher than the destabilization energy of $B_{96}N_{96}$. Therefore, the hydrogen molecule prefers to crack the B-N bond instead of escaping from hexagonal rings of the host. Because the energy of breaking B-N bond in $B_{96}N_{96}$ can be nearly 1.695 eV (its destabilization energy). This energy value is smaller than the energy barrier of the host molecule. In addition, the optimized TS structure of the complex that has the only one imaginary frequency value ($914i$ cm^{-1}) is depicted in figure 3.7.
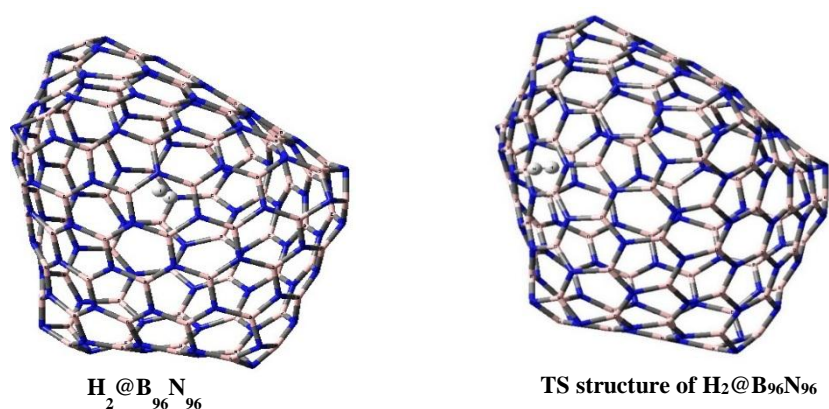

$H_2@B_{96}N_{96}$ TS structure of $H_2@B_{96}N_{96}$

Figure 3.7. Optimized geometries of the TS structure and the $H_2@B_{96}N_{96}$ complex.

3.3 Computational Investigation and Comparison of Hydrogen Storage Properties of $B_{24}N_{24}$ and $Al_{24}N_{24}$ Nanocages

In this part of the study, both endohedrally and exohedrally hydrogen storage properties of $B_{24}N_{24}$ and $Al_{24}N_{24}$ nanocages were investigated by several DFT and ab initio methods. Particularly, we aimed to address the following questions? 1) Which of the DFT methods are suitable for these types of systems where the weak interactions are dominant? 2) Which of the host molecules, $B_{24}N_{24}$ nano-cage or $Al_{24}N_{24}$ nano-cage, is more suitable for hydrogen storage at ambient conditions? 3) Do hydrogen molecules prefer to be adsorbed in or out of nanocages? 4) How important is the effect of B-N and Al-N bond for these type systems? 5) Is hydrogen molecule adsorption on the host molecules is chemical or physical?

It is very important to find out the degree of accuracy of the DFT methods in the calculations of hydrogen doped $Al_{24}N_{24}$, and $B_{24}N_{24}$ nano-cages, which contain weak interactions. Therefore, we focused on the determination of suitable DFT functionals for such systems since some DFT functionals are capable of including dispersive interactions in calculations but some of them cannot include these effects (Zhang and Musgrave, 2007) such as PBEPBE, B3LYP, functionals etc. However, the high level CCSD(T) ab initio method is stated as 'gold standard' and it can be used as the reference method among the computational methods (Zhou et al., 2006) because it does not only give rather accurate results for covalent interactions but also includes dispersive interactions originated from non-covalent interactions. From this point of view, the CCSD(T) method can be used for systems involving weak interactions. However, it demands an enormous amount of computational time and resources so it cannot be used for the systems with a large number of atoms such as 50-60 atoms. Therefore, the host molecules were modelled with smaller structures shown in the Figure 3.8. The most suitable DFT method(s) was determined by exploiting the highly accurate CCSD(T) method for these smaller BN and AlN structures interacting hydrogen molecules. In addition, their edges were filled with atomic hydrogen due to avoid spin contaminations.
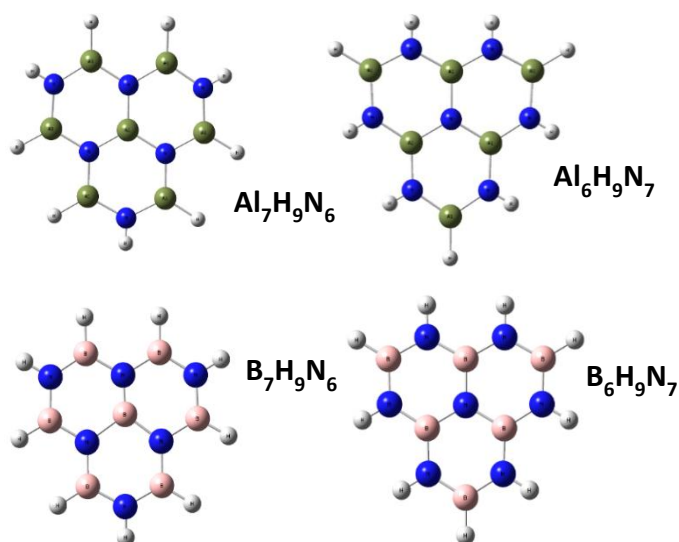
Figure 3.8. Optimized geometries of the smaller host structures namely, $Al_7H_9N_6$, $Al_6H_9N_7$, $B_7H_9N_6$ and $B_6H_9N_7$ molecules.

First of all, hydrogen molecule was approached to center atom of the small host molecules from 10.0 to 2.0 Å with 0.2 Å intervals. Additionally, the hydrogen molecule was placed perpendicular to the plane of the central atom of the host molecule (Figure 3.9). The single point energy of each obtained complex is estimated by using the CCSD(T) method at 6-311 ++G(d,p) basis set. This approach was applied one by one for each geometry of the four systems. In addition, the single point energy of each geometry of the four systems also is estimated by several DFT methods namely, B3LYP, B3P86(Perdew, 1986), B3PW91(Perdew and Wang, 1992),B1LYP(Lee et al., 1988), B1B95(Becke, 1996), BHandH/BhandHLYP(Becke, 1993b), BMK(Boese and Martin, 2004), Cam-B3LYP(Yanai et al., 2004), LC-ωPBE(Vydrov et al., 2006), M06/M062X,(Zhao and Truhlar, 2008) M06HF(Zhao and Truhlar, 2006a), M06l(Zhao and Truhlar, 2006b), PBEPBE(Perdew et al., 1996), TPSSH(Staroverov et al., 2003), ωB97/ωB97X(Chai and Head-Gordon, 2008), ωB97X-D(Chai and Gordon, 2008) and X3LYP(Xu and Goddard, 2004) by utilizing the 6-311++G(d,p) basis set. Furthermore, B3LYP and PBEPBE functionals containing Grimme's dispersive contribution (Grimme, 2006) (DFT-D2) with same basis set were also employed for the same procedure. The DFT-D2 treats the energy of the system including weak interactions by adding the semi empirical dispersive contributions. Finally, we obtained the electronic energy graphs of all four systems relative to electronic energies of the first geometries. The electronic energy graphs obtained by DFT

method are compared to CCSD(T) method. The one which gives the closest to electronic energy graph of each four systems obtained by CCSD(T) is selected as suitable method for BN and AlN systems with H_2 molecules.
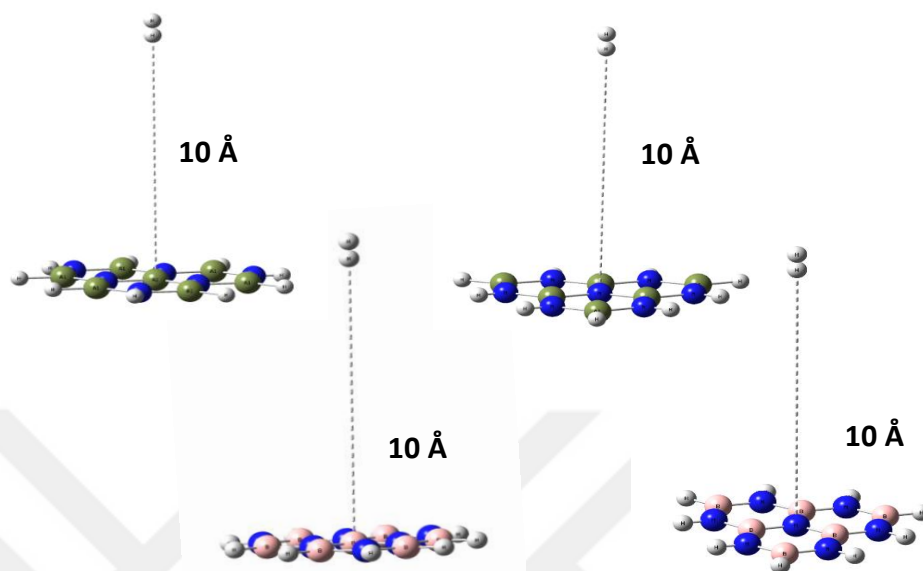

Figure 3.9. Initial geometries of the smaller model system including hydrogen molecule.

After finding the most suitable DFT method, the energies of optimized non-doped real host $Al_{24}N_{24}$ and $B_{24}N_{24}$ nanocages and their hydrogen doped complexes were estimated by employing this method at the same basis set level. The formula of formation energies of the two complexes having endohedral hydrogen molecule doped is shown with the equation 3.7.

$$\Delta H_f^{complex} = \left[\Delta H_{f(nH_2 @ host)} - \left(\Delta H_{f(host)} + n\,\Delta H_{f(H_2)} \right) \right] \tag{3.7}$$

where $\Delta H_{f(nH_2 @ host)}$, $\Delta H_{f(host)}$ and $\Delta H_{f(H_2)}$ are the heats of formation of the complex, host and hydrogen molecules calculated by using the most suitable DFT method. Note that the complex will become more stable if the formation energy has the larger negative value. Furthermore, the exohedrally doped hydrogen molecule on the host molecules (Al, N and B atom sides) was also investigated by using this method with the same basis set. All calculations were estimated by using Gaussian 09 computational chemistry package programme.

The relative electronic energy surfaces of the smaller host molecule including hydrogen molecule approaching to the center atom are depicted in the Figure 3.10.

Distance between H and N atom in $B_6H_9N_7$

(a)

Distance H and B atom in $B_7H_9N_6$

(b)
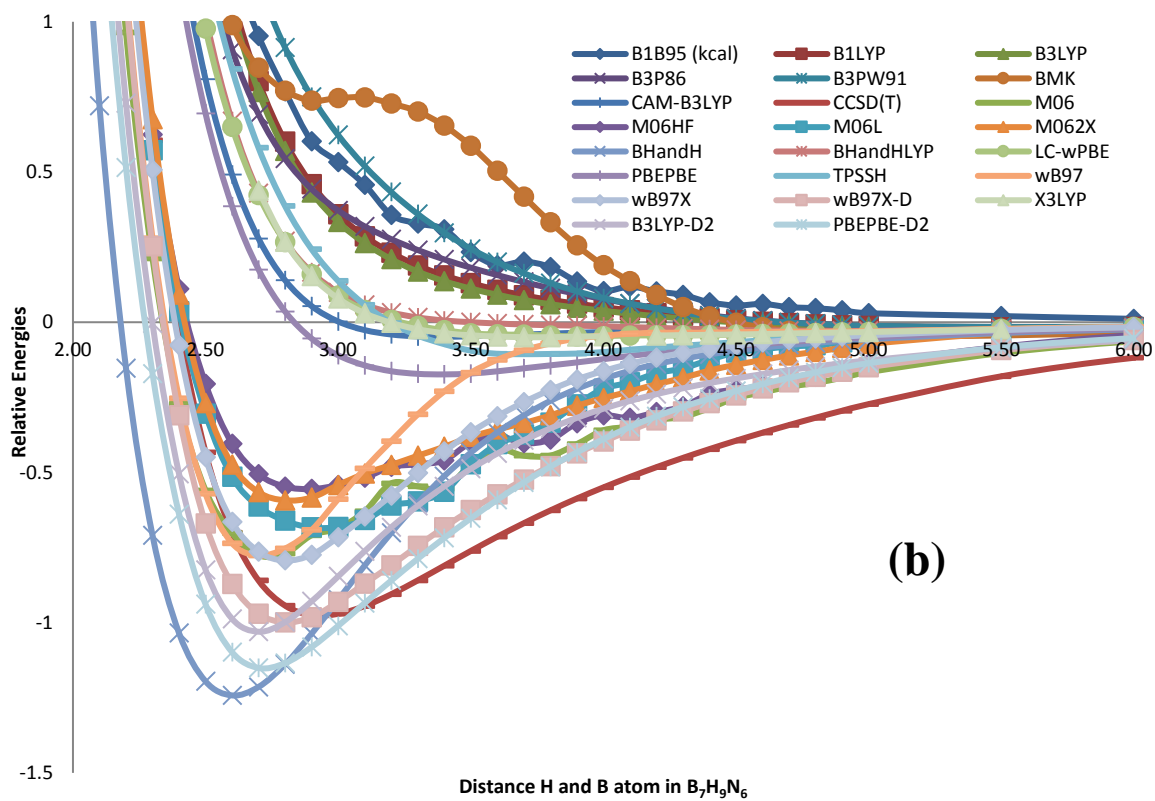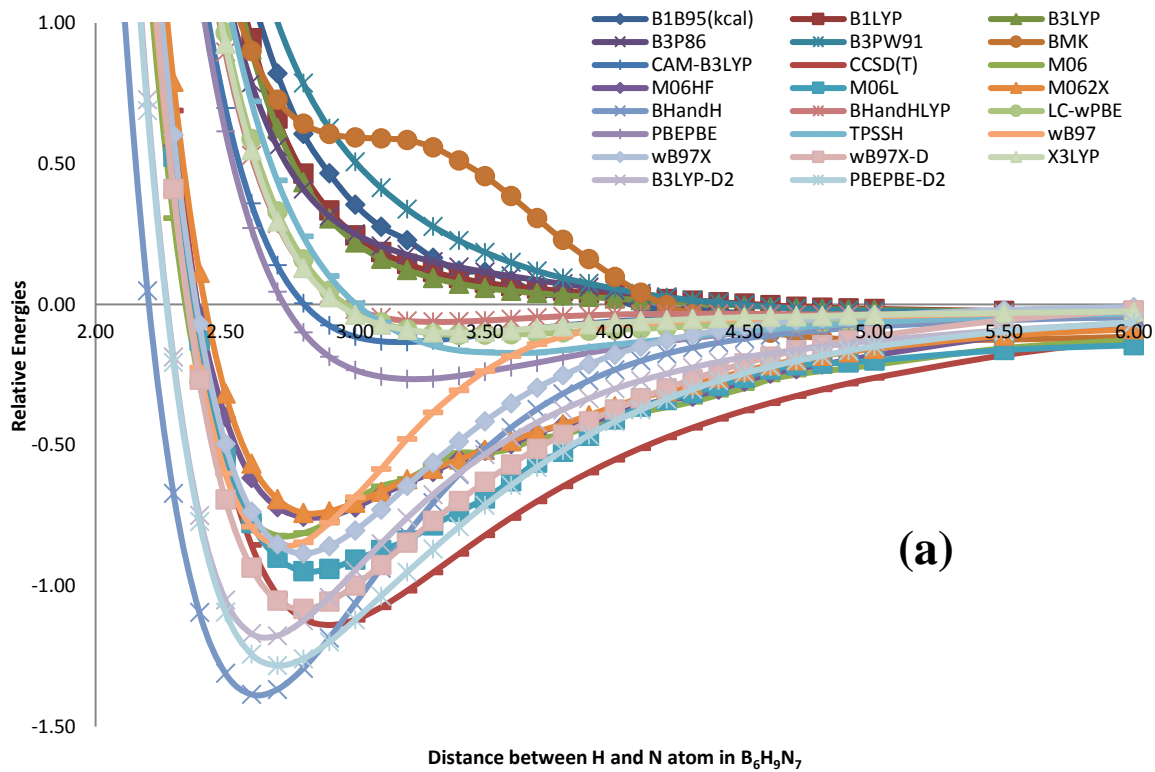
Figure 3.10. The relative electronic energy surfaces of the small model systems obtained by several DFT methods. (where a, b, c and d is represented as $B_6H_9N_7$, $B_7H_9N_6$, $Al_6H_9N_7$ and $Al_7H_9N_6$ model systems approaching H_2 molecule).

The relative electronic surfaces in these small model systems calculated by using the DFT functionals mentioned above are compared to that of CCSD(T) method, which has the ability to calculate the van der Waals interactions. It is clearly seen from the figure 3.10 that the DFT methods employed in these calculations can be divided into two main groups. The first group of electronic graphs obtained by several DFT methods apart from BHandH, ωB97, ωB97X, ωB97X-D, M06, M06L, M06HF, M06-2X, B3LYP-D2 and PBEPBE-D2 do not pass from a proper minimum because of having repulsion interactions against to hydrogen approach. In other words, these small model systems calculated by first group DFT methods are not able to adsorb hydrogen molecule, however, the second group of electronic graphs obtained by some DFT methods namely, BHandH, ωB97, ωB97X, ωB97X-D, M06, M06L, M06HF, M06-2X, B3LYP-D2 and PBEPBE-D2 pass from a well-defined minimum, because the small host structures estimated by these DFT methods can hold to hydrogen molecule. In addition, the small host systems obtained from the second group DFT methods have attractive effect against hydrogen molecule. Therefore, one can say that the second DFT methods are more suitable for BN- AlN systems that include hydrogen adsorption according to the result obtained CCSD(T) method.

The relative electronic graphs obtained by CCSD(T) and second group of DFT methods namely, BHandH, ωB97, ωB97X, ωB97X-D, M06, M06L, M06HF, M06-2X, B3LYP-D2 and PBEPBE-D2 are represented in figure 3.11.

(a)

Distance between H and N atom in $B_6H_9N_7$
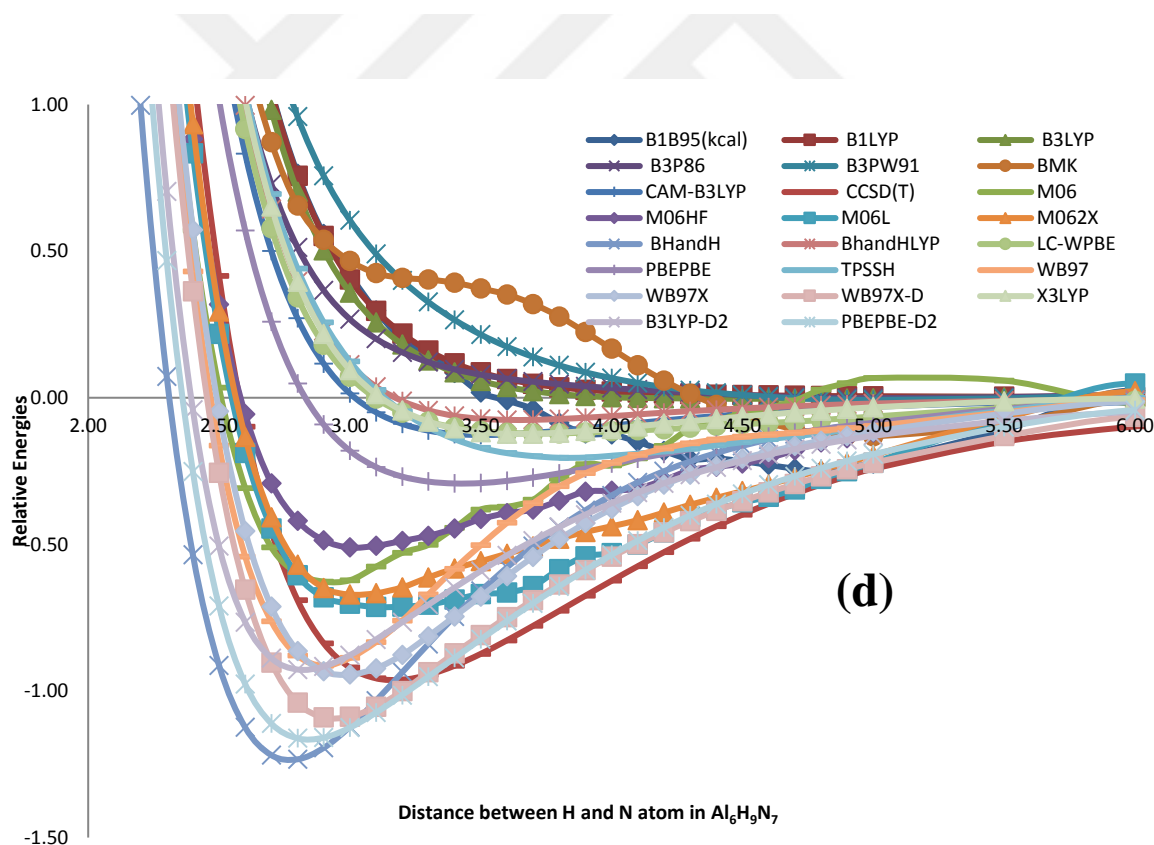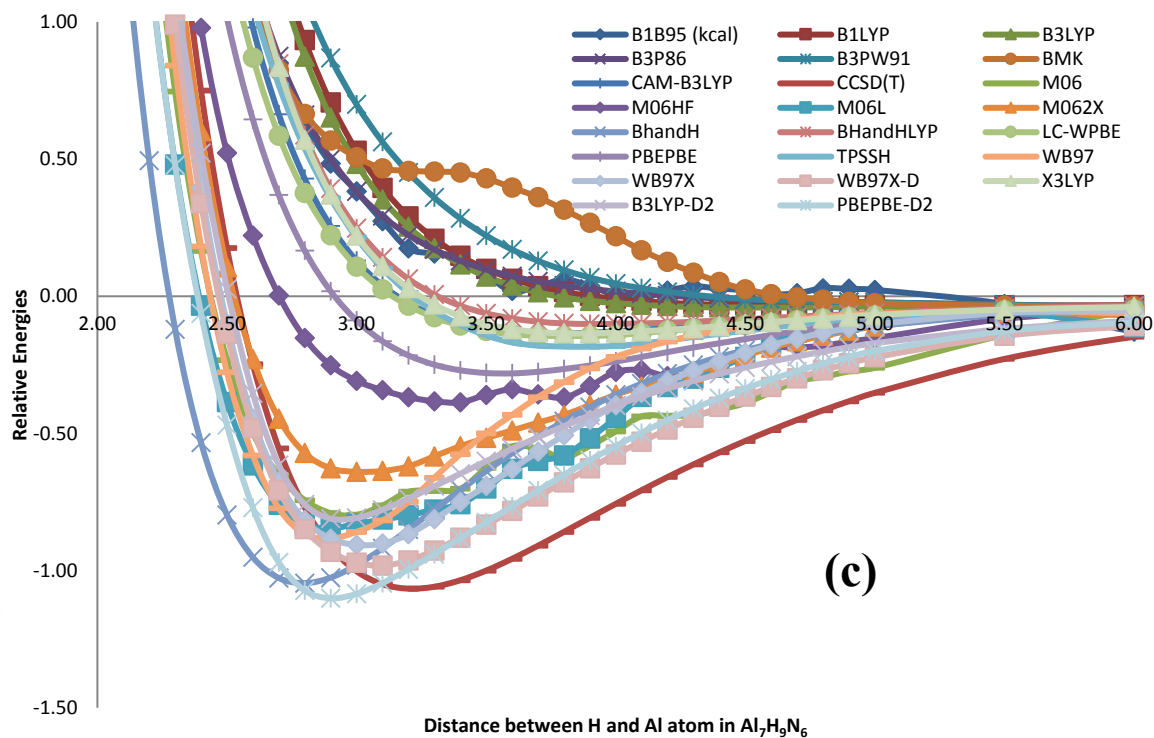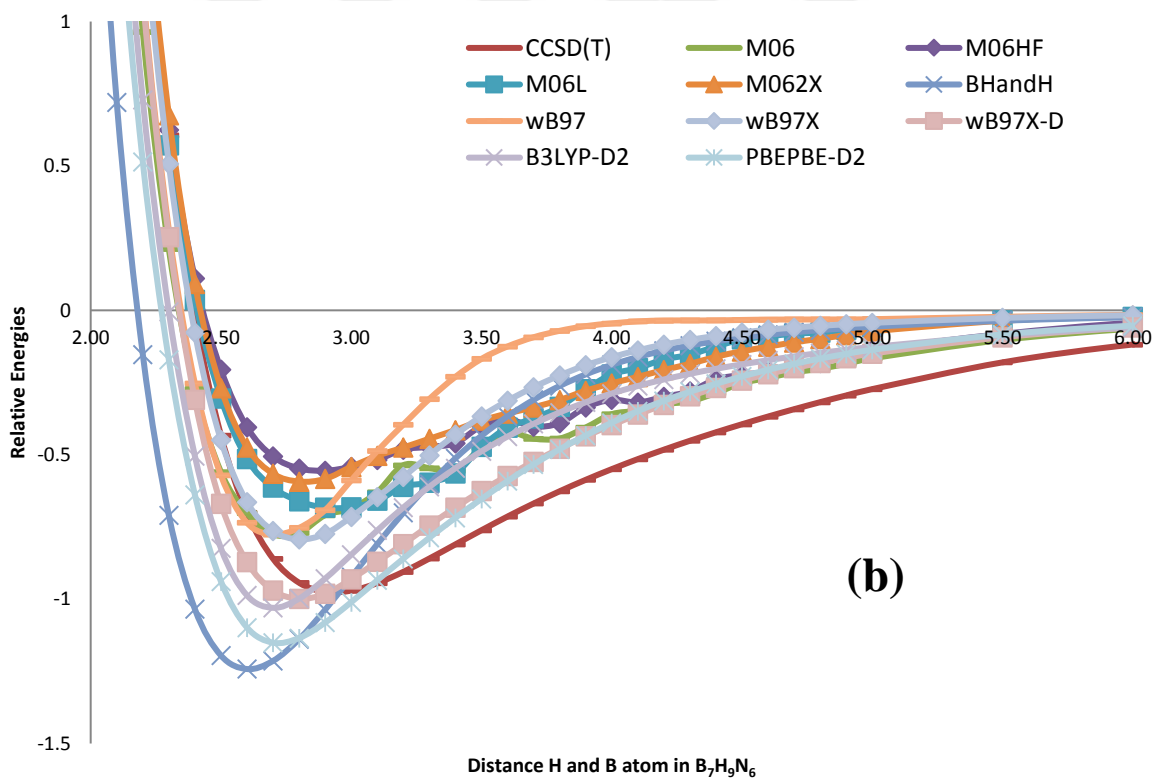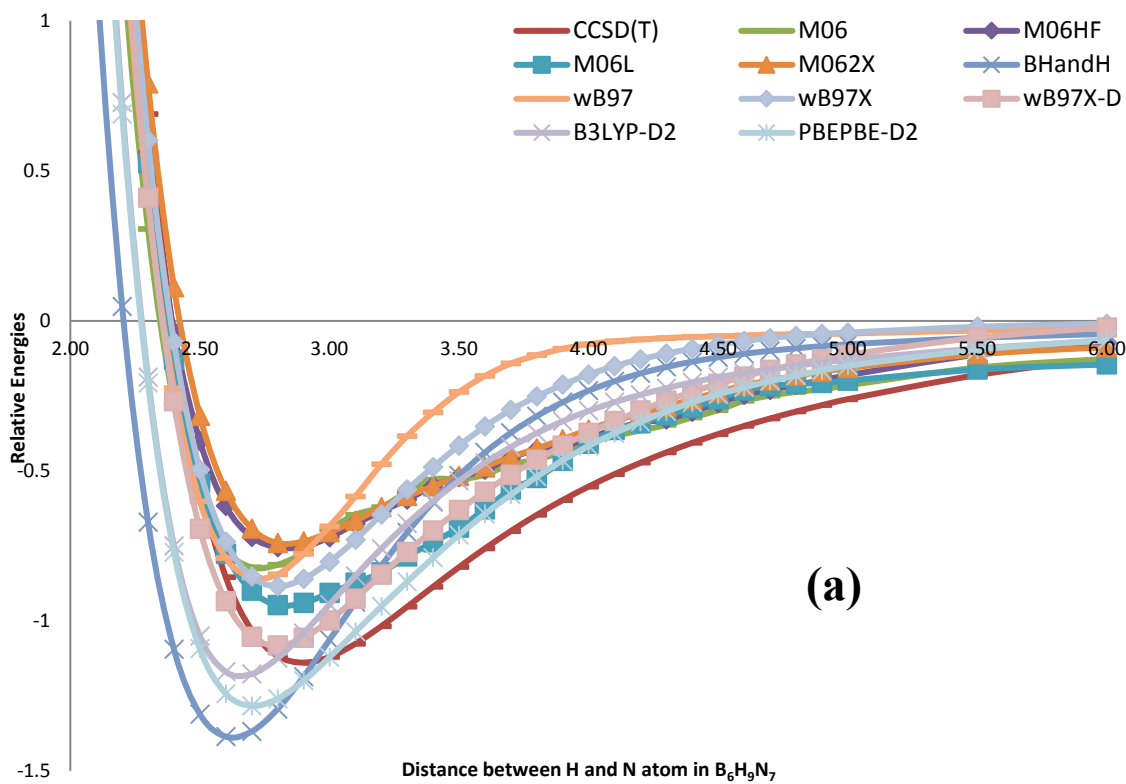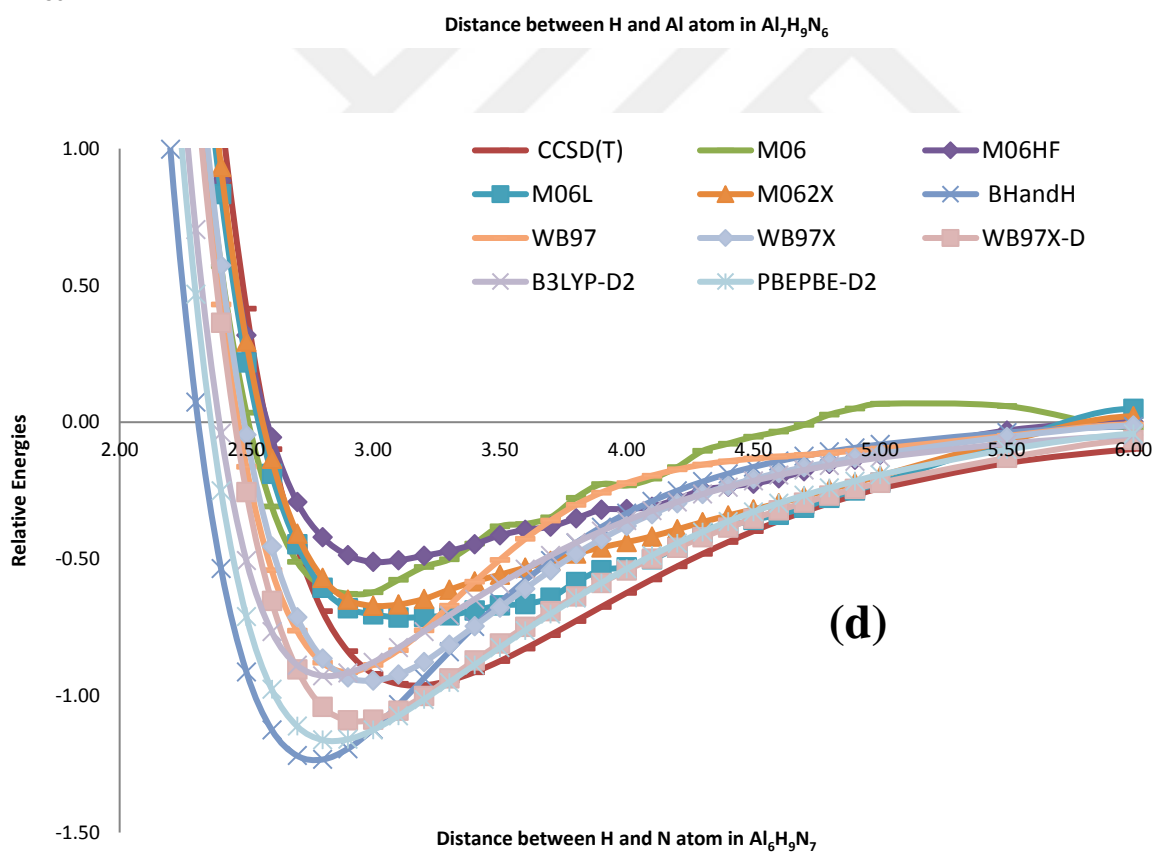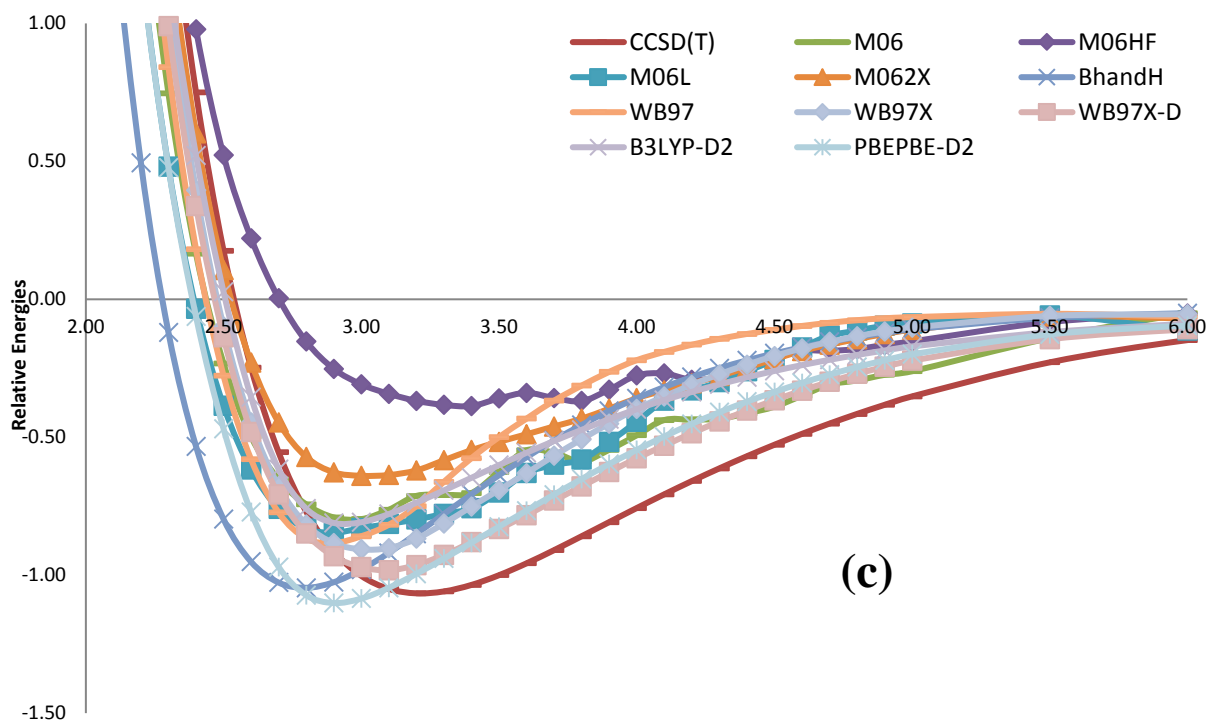
(b)

Distance H and B atom in $B_7H_9N_6$

Figure 3.11. The relative electronic energy surfaces of the small model systems obtained by second group DFT methods. (where a, b,c and d is represented as $B_6H_9N_7$, $B_7H_9N_6$, $Al_6H_9N_7$ and $Al_7H_9N_6$ model systems).

It is clearly seen from the Figure 3.11 that the curves estimated by using second group DFT methods pass from a minima and also their curves are extremely similar to the curve estimated by using CCSD(T) method. Although the M06 family (M06, M06L, M06-HF and M06-2X) is seen as suitable method for BN and AlN systems, the using of one of these method is not suitable when considering all point of electronic energy curve obtained by using CCSD(T) method. Even the result of M06-2X has less wavy among all the M06 method, it can be caused issue of PES.

Table 3.6 Minmum points on relative PES (a) and corresponding H2-surface distances (b) obtained with the DFT ωB97X-D, B3LYP-D2, PBEPBE-D2, BHandH methods and the reference CCSD(T) method

(a)	Minimum points on relative PES			
Method	$B_6H_9N_7$	$B_7H_9N_6$	$Al_6H_9N_7$	$Al_7H_9N_6$
ωB97X-D	-1.08	-0.93	-1.09	-0.98
B3LYP-D2	-1.18	-1.03	-0.93	-0.81
PBEPBE-D2	-1.28	-1.15	-1.16	-1.10
BHandH	-1.39	-1.24	-1.23	-1.05
CCSD(T)	-1.14	-0.97	-0.96	-1.07
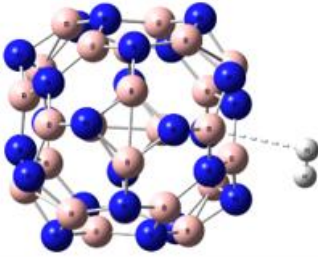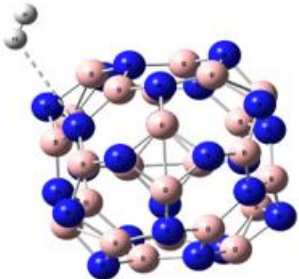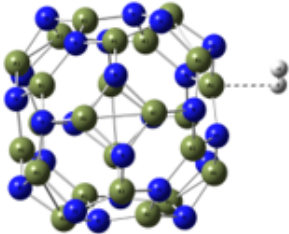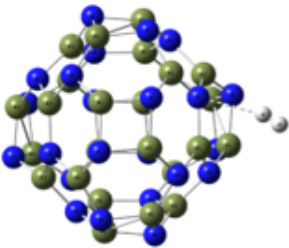
(b)	Corresponding H_2-surface distances (Å)			
Method	$B_6H_9N_7$	$B_7H_9N_6$	$Al_6H_9N_7$	$Al_7H_9N_6$
ωB97X-D	2.8	2.9	3.0	3.1
B3LYP-D2	2.7	2.7	2.8	2.9
PBEPBE-D2	2.7	2.7	2.8	2.9
BHandH	2.6	2.6	2.8	2.8
CCSD(T)	2.9	3.0	3.2	3.2

The energies of electronic energy curves and the distance between hydrogen molecule and center atom of the small host molecule estimated by using ωB97X-D, B3LYP-D2, PBEPBE-D2, BHandH and reference CCSD(T) method in the minimum point are depicted in Table 3.6. The result of ωB97X -D functional is placed in the Table 3.6 because the result of ωB97X -D functional among the ωB97

family is extremely similar to that of the reference method. In the other way, the result of ωB97 and ωB97X functionals in ωB97 series is considerable far away from the that of CCSD(T) method. On the other hand, the energy of all small host complexes located at minima obtained by using BHandH functional generally overestimates according to result of reference method. This may cause that complexes calculated by the BhandH method can be more stable than they should be. The results of B3LYP and PBEPBE functional including dispersive contributions (D2) have a bit better in terms of both energies and distances at minima than that of BhandH functional. However, the among the second group DFT methods, the ωB97X -D functional is the most suitable method for those systems including weak interaction between hydrogen and the small model hosts in terms of both electronic energy and distance located at minima. Therefore, the functional was selected for investigating hydrogen storage and related properties of the real BN and AlN systems namely, $Al_{24}N_{24}$ and $B_{24}N_{24}$, respectively. Note that there are many articles(Oliveira et al., 2016; Wang et al., 2017) claiming the ωB97X -D functional is the suitable for many systems involving weak interactions, but I also found that the method is the most suitable method for BN---H2 and AlN---H2 systems including weak interactions.

After finding the most suitable DFT method for BN and AlN systems, the exohedral hydrogen doped of the hosts molecules were investigated by using the DFT-ωB97X -D method with 6-311++G(d,p) basis set. The distance between hydrogen and the host nanocages, the energies of different adsorption sides (on the B, Al and N atom) of the complexes is presented in table 3.7.
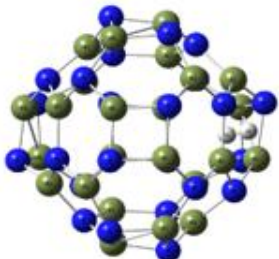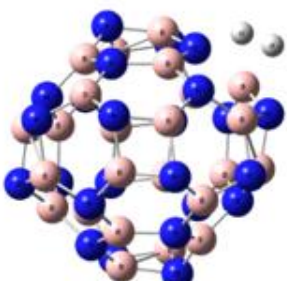
Table 3.7 The distance between hydrogen and the host nanocages, the energies of different adsorption sides (on the B, Al and N atom) of he complexes

$H_{2(exohedral)}$-$B_{24}N_{24}$ complex	Site	dH_2- B(Å)	d_{H-H} (Å)	$\Delta E_{complex}$ (eV)
	B	2.863	0.745	-0.043

$H_{2(exohedral)}$-$N_{24}B_{24}$ complex	Site	dH_2- N(Å)	d_{H-H} (Å)	$\Delta E_{complex}$ (eV)
	N	2.953	0.745	-0.055

$H_{2(exohedral)}$-$Al_{24}N_{24}$ complex	Site	dH_2- Al(Å)	d_{H-H} (Å)	$\Delta E_{complex}$ (eV)
	Al	2.532	0.749	-0.116

$H_{2(exohedral)}$-$N_{24}Al_{24}$ complex	Site	dH_2- N(Å)	d_{H-H} (Å)	$\Delta E_{complex}$ (eV)
	N	2.795	0.750	-0.063

It is clearly seen that the adsorption energy of the $N_{24}B_{24}$ host molecule including hydrogen molecule adsorbed by N atom of the $N_{24}B_{24}$ complex and the distance between hydrogen and nitrogen atom of the host molecule are 0.055 eV and 2.953 Å, respectively, whilst the those of the B atom of the $B_{24}N_{24}$ are -0.043 eV and 2.863Å, respectively. Therefore, it can be claimed that the hydrogen

molecule can prefer to adsorb on N atom of the nanocage instead of B atom, because somehow, the adsorption energy of the N atom side of the nanocage has slightly lower negative energy value than that of the B atom side. In other words, the complex containing hydrogen molecule adsorbed by N atom of the host molecule has a bit more stable than that of by B atom of the host molecule. Furthermore, the hydrogen molecule is adsorbed as being parallel on the B-N bond of the host molecule. In other words, one hydrogen atom of the hydrogen molecule interacts with B atom of the $B_{24}N_{24}$ nanocage, the other interacts with N atom of the $B_{24}N_{24}$ nanocage. Furthermore, the adsorption energy of the $N_{24}B_{24}$ host molecule including hydrogen molecule adsorbed by N atom of the $Al_{24}N_{24}$ complex and the distance between hydrogen and nitrogen atom of the host molecule are -0.063 eV and 2.795 Å, respectively whilst the those of the Al atom of the $Al_{24}N_{24}$ are -0.043 eV and 2.863Å, respectively. In addition, it is extremely shown that the Al atom of the $Al_{24}N_{24}$ nanocage extremely adsorb hydrogen molecule compared to B and N atoms of the host molecules. In other words, the adsorption energy of the $Al_{24}N_{24}$ systems with hydrogen molecule adsorbed by Al atom has largest negative value, this makes the $Al_{24}N_{24}$ complex more stable. The reason of this is to ionic character of Al atom in the host molecule. Therefore, it is seen that the $Al_{24}N_{24}$ host molecule having more ionic strength between hydrogen and Al atom is more suitable hydrogen storage materials than $B_{24}N_{24}$ host molecule. After the determining the exohedrally hydrogen storage properties of the host molecules, the both forward and reverse activation energies of the host molecules while one hydrogen molecule runs through the hexagonal ring of the host molecules, transition state geometries of the complexes and the distance hydrogen atoms estimated by using same method are depicted in Table 3.8. The reason of this investigation is to decide whether endohedrally or exohedrally hydrogen storage of the hosts molecules. The forward activation energy of one hydrogen molecule passing from the hexagonal ring of $Al_{24}N_{24}$ and the distance between Al-N bond of the transition state geometry of $Al_{24}N_{24}$ nanocage are approximately 5.05 eV and 1.96 Å respectively. In addition, the hydrogen molecule does not dissociate into its atoms during the passing from the hexagonal ring of $Al_{24}N_{24}$ nanocage because the distance between the atoms of hydrogen molecule is 0.75 Å.

Table 3.8 The transition state geometries and activation energies of the complexes, the distances between corresponding Al, B and N atoms and H_2 molecules

Nanocage	TS	$E_{a(forward)}$ (eV)	$E_{a(reverse)}$ (eV)	d_{H-H} (Å)	d_{Al-H} (Å)	d_{N-H} (Å)	d_{Al-N} (Å)
		5.054	5.115	0.750	1.870	1.870	1.940
Al$_{24}$N$_{24}$							

		$E_{a(forward)}$ (eV)	$E_{a(reverse)}$ (eV)	d_{H-H} (Å)	d_{B-H} (Å)	d_{N-H} (Å)	d_{B-N} (Å)
		1.674	1.794	1.010	1.350	1.340	1.720
B$_{24}$N$_{24}$							

The reverse activation energy of one hydrogen molecule passing from the hexagonal ring of Al$_{24}$N$_{24}$ is 5.12 eV. The Hydrogen molecule prefers to stay inside the host molecule because the reverse activation energy is bigger than forward activation energy. In addition, the forward activation energy of one hydrogen molecule passing from the hexagonal ring of B$_{24}$N$_{24}$ and the distance between B-N bond of the transition state geometry of Al$_{24}$N$_{24}$ nanocage are approximately 1.67 eV and 1.72 Å respectively. Furthermore, the hydrogen molecule dissociates into its atom when it passes from the hexagonal ring. In other words, hydrogen cannot be endohedrally stored inside the B$_{24}$N$_{24}$ nanocage because the hydrogen-hydrogen bond is broken. The distance between hydrogen atom of distorted hydrogen molecule 1.01 Å. Therefore, After B-N bond is distorted, firstly, one hydrogen atom makes the chemical bound with B atom, the other hydrogen atom makes the chemical bound with N atom.

After determining the activation energies and transition state structures of the host molecules, the endohedral hydrogen storage of the host molecules was

investigated by using DFT-ωB97X -D method with 6-311++G(d,p) basis set. Note that we assume somehow hydrogen molecule(s) is located inside the host molecules. By doing so, we can manage to investigate endohedral hydrogen storage of the complexes. The enthalpies of the complexes and pure host molecules are depicted in table 3.9 and figure 3.12.
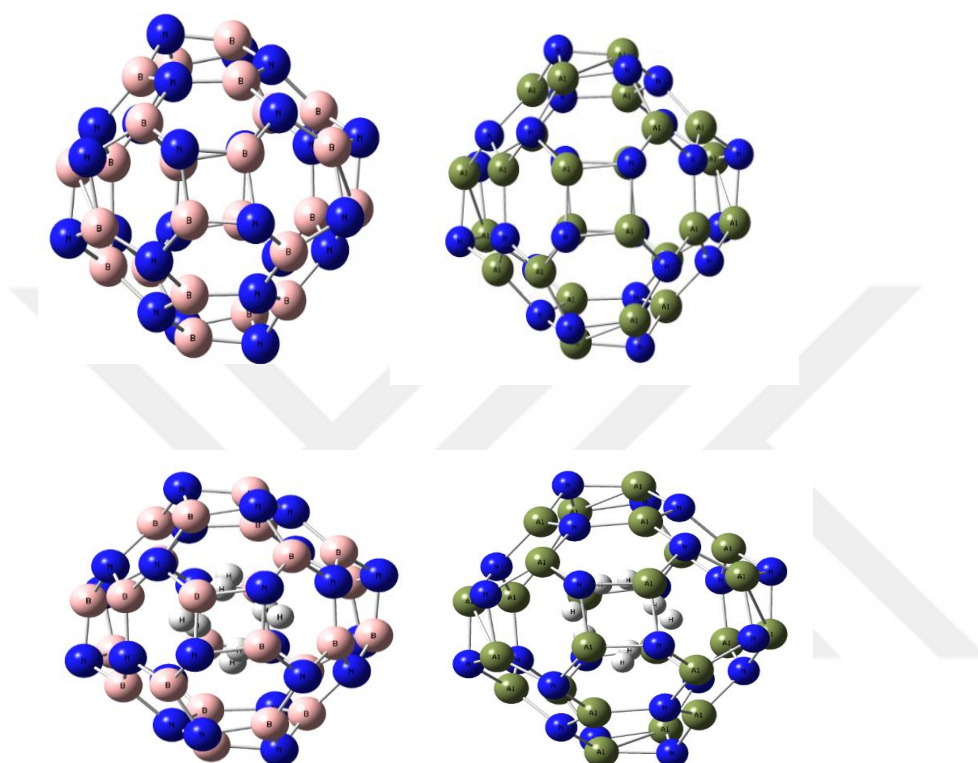
Figure 3.12. The optimized host molecules and their complexes with hydrogen molecules.

Table 3.9 The formation enthalpies of the complexes calculated by wB97X-D/DFT method

Complex		wB97X-D/6-311++G(d,p)				
	n	ΔH_{H2} (a.u)	ΔH_{B24N24} (a.u)	$\Delta H_{complex}$ (a.u)	ΔH_f (a.u)	ΔH_f (kcal/mol)
	1	-1.16	-1912.30	-1913.46	0.00	2.70
	2	-2.33	-1912.30	-1914.58	0.05	32.24
$nH_2@B_{24}N_{24}$	3	-3.49	-1912.30	-1915.66	0.13	84.41
	4	-4.65	-1912.30	-1916.74	0.21	133.61
	1	-1.16	-7134.41	-7135.57	0.00	-1.41
	2	-2.33	-7134.41	-7136.74	0.00	-2.61
$nH_2@Al_{24}N_{24}$	3	-3.49	-7134.41	-7137.87	0.03	15.86
	4	-4.65	-7134.41	-7139.03	0.03	16.77

It is clearly seen from table 3.9 that each formation enthalpy value of the $B_{24}N_{24}$ complex has increased by endohedrally incorporating hydrogen molecule. Therefore, hydrogen molecule is not able to be stored inside the cage. In other words, each formation energy of the complexes is positive value and this leads to each complex is unstable. On the other hand, the $Al_{24}N_{24}$ can thermodynamically store two hydrogen molecules because the binding energy of the cage is negative until adding two hydrogen molecule. The cage becomes unstable after adding two hydrogen molecule because of having positive binding energy.

In addition, considering all the enthalpy values of formation, it can be easily seen that the $Al_{24}N_{24}$ structure is more suitable for the hydrogen storage material than the $B_{24}N_{24}$ structure. In other words, $Al_{24}N_{24}$ nanocage is a promise endohedrally hydrogen storage material because of having the more ionic character between Al and N atoms than B and N atoms.

3.4 The Comparing Hydrogen Storage Properties of $B_{75}N_{75}H_{30}$, $Al_{48}N_{48}H_{24}$ and $Si_{48}C_{48}H_{24}$ Nanoclusters

In this thesis, molecular hydrogen storage properties of various nanolayers, such as $B_{75}N_{75}H_{30}$, $Al_{48}N_{48}H_{24}$ and $Si_{48}C_{48}H_{24}$, were investigated by employing the DFT-B97D method, which is capable of including weak interactions. The $B_{75}N_{75}H_{30}$, $Al_{48}N_{48}H_{24}$ and $Si_{48}C_{48}H_{24}$ clusters were chosen as the model systems to simulate the one-layer hexagonal BN, AlN and SiC nanosheets. The dangling bonds of the cluster edges were saturated with hydrogen atoms to avoid spin contamination during the calculations. The dispersive contributions are extremely important in reasonable DFT calculations for the systems involving weak interactions such as molecular hydrogen adsorbed BN, AlN and SiC nanosheets. Therefore, we employed the DFT-B97D method (Grimme, 2006), which includes dispersive contributions, with the sufficiently large def2-QZVP (split-valance quadruple-zeta) basis set (Weigend, 2006). It is known that the B97D (exchange-correlation functional) is a suitable DFT method for systems having non-covalent (weak) interactions (Frecus et al., 2016; Galindo-Murillo and Barroso-Flores, 2017; Hernández Velázquez et al., 2016; Kuniyil and Maseras, 2017; Nagy, 2016). In addition, we have also added Grime's semi-empiric dispersive corrections (D3)

(Grimme et al., 2010) to the DFT-B97D method to account for the long-range non-bonding interactions between the hydrogen molecule and the host molecules. The molecular hydrogen can be adsorbed from three different sides of the pristine host molecules. These sites are top sites on B, N, Al, Si and C atoms of the host molecules, hollow site of hexagonal rings of the host molecules and bridge sites on the middle of B-N, Al-N, and Si-C bond lengths. The best hydrogen adsorption of host molecules is determined by the binding energy occurring between molecular hydrogen and host molecules.

Figure 3.13. The optimized host molecules calculated at B97D-D3/_def2-QZVP level. Where a,b and c are the $B_{75}N_{75}H_{30}$, $Al_{48}N_{48}H_{24}$ and $Si_{48}C_{48}H_{24}$ nanolayers, respectively. The color blue atoms in (a and b) denote to N atoms, while the colors in (a and b) represents to B and Al atoms. The grey and black color atoms in (c) denote Si and C atoms. respectively.

The binding energies between a hydrogen molecule and the host molecules were estimated by the following formula:

$$\Delta E_b = \left[E_{(nH_2 - hosts)} - \left(E_{(host)} + n E_{(H_2)} \right) \right] \tag{3.8}$$

where $E_{(nH_2 - hosts)}$, $E_{(hosts)}$ and $E_{(H_2)}$ are the electronic energy of the hydrogen adsorbed host molecules, the electronic energy of host molecules and the electronic energy of hydrogen molecules, respectively. The larger negative binding energy makes the complex thermodynamically more stable. The nanolayers employed in this study are not infinite, they have edges that are saturated with hydrogen atoms. Therefore, their electronic properties, especially electron density, are not uniform

the surfaces of these nanolayers. This means that the interactions of the nanolayer atoms with hydrogen molecules adsorbed on their surface will not be the same. However, there are areas having uniform electronic properties such as electron density on these nanolayers. We called these uniform electron density areas as "safe zone". Thus, the hydrogen storage properties of nanolayer were investigated only on these safe zones instead of considering whole molecular surfaces.

The hydrogen storage in terms of g/m^2 on the safe zone is also calculated with the following formula:

$$H_2(g/m^2) = \left[\frac{M_{H_2}}{A} \right] \text{X } 100 \tag{3.9}$$

In the formula, M_{H_2} is the total mass (in gram) of adsorbed hydrogen molecule(s) in the safe zone and A is represented as the area of the safe zone (in meter^2). All calculations were performed by Turbomole program with first principles electronic structure package by using Cuby4 integrative framework. Firstly, it was focused on the determining of the safe zone of each host molecules having the uniform charge density. The following procedure was used to determine the safe zones of the nanolayers. The hexagonal structures of each nanolayer are numbered starting from the center of the sheet (as seen Figure3.14). Therefore, hydrogen molecule perpendicular to the host surface was interacted with center of a certain hexagonal areas of the host molecules. The hydrogen molecule perpendicularly were located with several parts of each hexagonal structure such as the center, the bond (BN, AlN, and SiC) and the atom (B, N, Al, Si). In addition, their hydrogen binding energies were calculated.
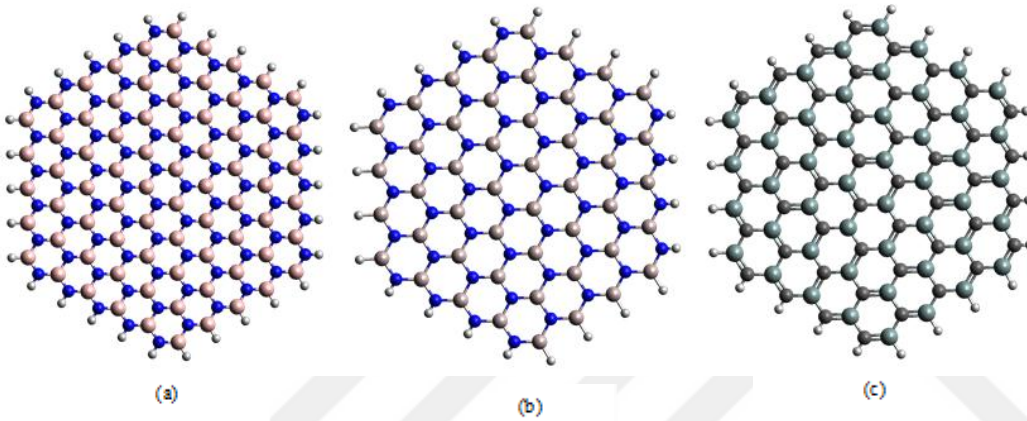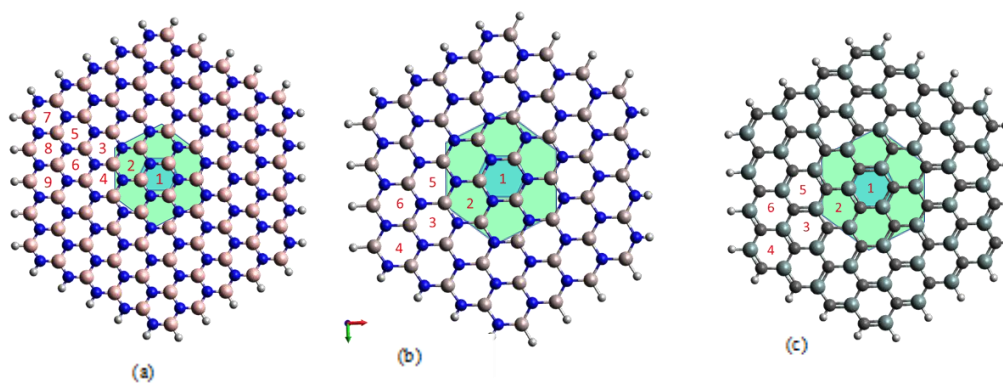
Figure 3.14. The optimized host molecules calculated at B97D-D3/ def2-QZVP level. Where a,b, c are the $B_{75}N_{75}H_{30}$, $Al_{48}N_{48}H_{24}$ and $Si_{48}C_{48}H_{24}$ nanolayers, respectively.

The hydrogen binding energies of the numbered hexagonal rings of the host molecules are given Table 3.10. The most effective area having the largest interaction with hydrogen molecule is the hexagonal area #1. The lowest hydrogen binding energies of the hexagonal rings #1 of the $B_{75}N_{75}H_{30}$, $Al_{48}N_{48}H_{24}$ and $Si_{48}C_{48}H_{24}$ are -1.23, -1.15 and -1.27 eV, respectively. Also, hydrogen binding energies of the hexagonal rings #2 of host molecules are extremely close to that of #1 (see Table 3.10). Therefore, first hexagonal ring and its six adjacent hexagonal rings can be defined as safe zone of the host molecules.

Table 3.10 The hydrogen binding energies of the numbered hexagonal rings of the host molecules

# Hexagonal Area	$E_{binding}$ (eV)		
	$B_{75}N_{75}H_{30}$	$Al_{48}N_{48}H_{24}$	$Si_{48}C_{48}H_{24}$
1	-1.23059	-1.15	-1.27
2	-1.22806	-1.15	-1.26
3	-1.0993	-1.13	-1.23
4	-1.11334	-0.93	-1.29
5	-1.18594	-1.14	-1.25
6	-1.07491	-1.02	-1.11
7	-1.02152		
8	-1.05694		
9	-1.05224		

As it is seen from Table 3.11, the hydrogen molecule prefers to stay on center $B_{75}N_{75}H_{30}$ nanostructure since the binding energy is the lowest at the hollow. Therefore, hydrogen molecule can be adsorbed on the center of each hexagonal ring

of $B_{75}N_{75}H_{30}$, in addition, the safe zone of the host molecule can adsorb up to seven hydrogen molecules. The hydrogen molecule prefers to stay on nitrogen atom of the $Al_{75}N_{75}H_{30}$ host molecule because of high electronegativity of nitrogen atom. The binding energy between nitrogen and hydrogen molecule is the lowest, therefore, the hydrogen molecule can be adsorbed by nitrogen atoms of the $Al_{75}N_{75}H_{30}$ nanocluster. Maximum number of hydrogen molecule capacity of the safe zone in $Al_{75}N_{75}H_{30}$ nanostructure is the twelve hydrogen molecules.

Table 3.11 The hydrogen binding energies of the possible adsorption sites of the host molecules calculated at B97D-D3/ def2- QZVP level

The possible hydrogen adsorption sites				
$B_{75}N_{75}H_{30}$	Hollow	B-N Bond	B	N
$E_{binding}$ (eV)	-1.23	-1.12	-1.1	-1.09
$Al_{75}N_{75}H_{30}$	Hollow	Al-N Bond	Al	N
$E_{binding}$ (eV)	-1.15	-1.03	-0.9	-1.41
$Si_{48}C_{48}H_{24}$	Hollow	Si-C Bond	Si	C
$E_{binding}$ (eV)	-1.27	-1.22	-1	-1.45

(a)   (b)   (c)
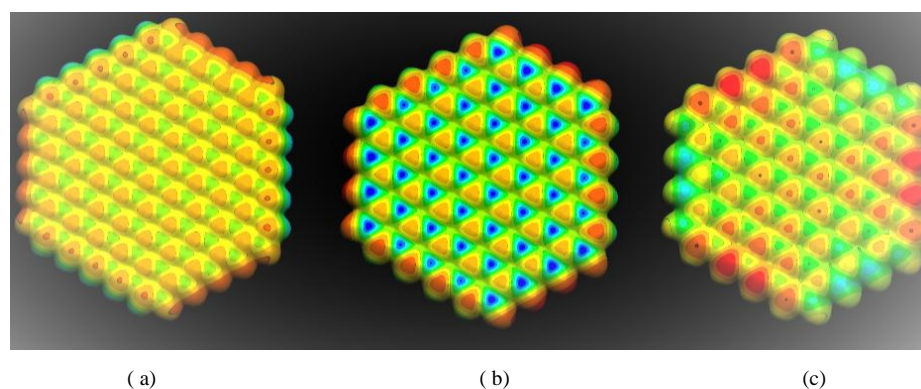
Figure 3.15. The electron density maps of the host molecules where a, b and c are the $B_{75}N_{75}H_{30}$, $Al_{48}N_{48}H_{24}$ and $Si_{48}C_{48}H_{24}$ nanolayers, respectively.

In the $Si_{48}C_{48}H_{24}$ nanostructure, the hydrogen molecule can be adsorbed on the carbon atom of the host molecule due to having largest hydrogen binding interaction. The safe zone of the $Si_{48}C_{48}H_{24}$ nanostructure binds twelve hydrogen molecules. According to all findings, SiC material can be considered the best hydrogen storage material among all of the investigated host molecules in this study.

4. CONCLUSION

In this thesis, the hydrogen storage capabilities and related properties of various nano-material methods have been investigated by using computational chemistry. The all results mentioned above are summarized in detail below.

- The endohedral hydrogen storage capacities of several boron nitride nanocage (B_mN_m where m=12, 24, 36, 48, and 96) structures have been determined by newly developed semi empirical PM7 method. It is shown that the nanocages $B_{12}N_{12}$ and $B_{24}N_{24}$ are inadequate nano structures for hydrogen storage while $B_{36}N_{36}$ might barely fulfill expectations. The $B_{48}N_{48}$ and $B_{96}N_{96}$ nanocages, however, that have hydrogen storage capacities of 6.6 and 10.6 wt%, respectively, can be considered as very promising hydrogen storage materials due to having hydrogen storage wt% considerably higher than the 2015 target value of DOE.

- The endohedral hydrogen storage properties of BN nanocages namely $B_{12}N_{12}$ and $B_{24}N_{24}$ was estimated by using computational methods such as PM6-DH2, PM7 and B3LYP methods to determine the suitable method compared to reference ωB97X-D method. The results of PM6-DH2 semi empirical method is extremely similar to that of reference method. Therefore, the semi empirical method can be selected as suitable computational method for the investigation hydrogen storage properties of BN nanostructures. In addition, the PM6-DH2 is ten thousand times faster than ωB97X-D method in terms of computational time for predicting optimized BN complexes. After selecting the suitable method, the hydrogen storage capacity of the larger BN host molecules namely $B_{36}N_{36}$, $B_{48}N_{48}$ and $B_{96}N_{96}$ were also investigated and their hydrogen percentages are 6.67, 8.12 and 12.01%, respectively. These percentages also show that BN nanomaterials are seen as good hydrogen storage candidates. Also, the resistance of BN host was determined by looking at their destabilization energies. The BN host nanocages apart from $B_{36}N_{36}$ and $B_{96}N_{96}$ have better resistible. The hydrogen molecules located at inside the $B_{96}N_{96}$ nanocage break the B-N bond of the host molecules

instead of passing through hexagonal ring during the escaping of hydrogen molecules.

- The DFT methods including both GGA and LDA were investigated to find the best suitable method for AlN and BN complexes compared to CCSD(T) reference method. According to reference method, the DFT/ωB97X-D method is the most suitable method for BN and AlN systems involving extremely important weak interactions between hydrogen molecule and the host molecules. The endohedral hydrogen molecule doped in the BN nanocage is extremely hard in terms of thermodynamically because the hydrogen molecule is dissociated with its atoms when passing through from the hexagonal ring of BN host molecule. Therefore, one hydrogen molecule is chemically bounded with B atom, the other hydrogen molecule chemically is bounded with N atom during the passing. In other words, the hydrogen molecule can be adsorbed exohedrally instead of endohedrally. The complex including hydrogen molecule exohedrally adsorbed by N atom is slightly stable than that of adsorbed by B atom because of having lower adsorption energy. On the other hand, $Al_{24}N_{24}$ nanocage can endohedrally store hydrogen molecule because the Al-N bond of hexagonal ring is not broken once hydrogen molecule passing into the cage. In addition, two hydrogen molecules can be endohedrally thermodynamically stored in the $Al_{24}N_{24}$ nanocage. Because of having more ionic character between Al an N atom, the AlN host molecules have better exohedrally hydrogen adsorption than BN host molecules. Also AlN complex including hydrogen molecule adsorbed by Al atom has more stable among that of adsorbed by B and N atoms. In other words, the adsorption energy of the $Al_{24}N_{24}$ host molecule including hydrogen molecule adsorbed by Al atom has the negative largest value. Therefore, the AlN nanomaterials are better suitable hydrogen storage materials than BN nanomaterials due to having Al-N ionic character.

- The SiC nano-structures having 2-D structures are suitable hydrogen storage materials among the BN and AlN nano-structures because of

having lowest hydrogen binding energy. In addition, the hydrogen molecule(s) can exohedrally be adsorbed on both Si and C atom in SiC nanomaterials. However, the hydrogen adsorption on C atom in the host molecule is easier than that of on Si atom because the hydrogen adsorption energy of the complex adsorbed by C atom is lower than that of by Si atom. In addition, it was determined the safe zone of the host molecules. Their safe zone areas have the uniform electron density areas, therefore, the hydrogen storage properties of nanolayer were investigated only on these safe zones instead of considering whole molecular surface.

REFERENCES

Al-Ghamdi, A.A., Shalaan, E., Al-Hazmi, F.S., Faidah, A.S., Al-Heniti, S. and Husain, M., 2012, Adsorption sites of hydrogen atom on pure and mg-doped multi-walled carbon nanotubes, Journal of Nanomaterials., 2012.

Algae, O. and Rubin, J., 1942, F e r m e n t a t i v e and photochemical p r o d u c t i o n (From the Department of CkemCztry, The University of Chicago , Chicago) Downloaded from on October 12 , 2016 Methods,219–240pp.

Allouche, A., 2012, Software News and Updates Gabedit — A Graphical User Interface for Computational Chemistry Softwares, Journal of computational chemistry and, V. N. S., and Davidson, E. R. ,2000, Transition Regions in the Cope Rearrangement of 1,5-Hexadiene and Its Cyano Derivatives, American Chemical Society .

Balasubramanian, C., Bellucci, S., Castrucci, P., De Crescenzi, M. and Bhoraskar, S.V., 2004, Scanning tunneling microscopy observation of coiled aluminum nitride nanotubes, Chemical Physics Letters., 383, 188–191pp.

Barbir, F., 2005, PEM electrolysis for production of hydrogen from renewable energy sources, Solar Energy., 78(5), 661–669pp.

Barghi, S.H., Tsotsis, T.T. and Sahimi, M., 2014, Hydrogen sorption hysteresis and superior storage capacity of silicon-carbide nanotubes over their carbon counterparts, International Journal of Hydrogen Energy., 39(36), 21107–21115pp.

Barkhordarian, G., Klassen, T. and Bormann, R.U., 2004, Effect of Nb2O5 content on hydrogen reaction kinetics of Mg, Journal of Alloys and Compounds., 364(1–2), 242–246pp.

Becke, A.D., 1993, Densityfunctional thermochemistry. III. The role of exact exchange Density-functional thermochemistry. III. The role of exact exchange, J. Chem. Phys. Additional information on J. Chem. Phys. Journal Homepage., 98(5648).

REFERENCES (Continued)

Becke, A.D., 1993, A new mixing of Hartree-Fock and local-density-functional theories, J. Chem. Phys., 98(2), 1372–1377pp.

Becke, A.D., 1996, Density-functional thermochemistry. IV. A new dynamical correlation functional and implications for exact-exchange mixing, The Journal of Chemical Physics., 104(3), 1040–1046pp.

Bezi Javan, M., Houshang Shirdel-Havar, A., Soltani, A. and Pourarian, F., 2016, Adsorption and dissociation of H2 on Pd doped graphene-like SiC sheet, International Journal of Hydrogen Energy., Elsevier Ltd, 41(48), 22886–22898pp.

Bhowmick, R., Rajasekaran, S. and Friebel, D., 2011, Hydrogen Spillover in Pt-Single-Walled Carbon Nanotube Composites: Formation of Stable C− H Bonds, Journal of the American Chemical Society., 133(14), 5580–6pp.

Boese, A.D. and Martin, J.M.L., 2004, Development of density functional for thermochemical kinetics, Journal of Chemical Physics., 121(8), 3405–3416pp.

Bogdanovi, B., Eberle, U., Felderhoff, M. and Schoth, F., 2007, Complex aluminum hydrides, Scripta Materialia., 56(10), 813–816pp.

Born, M. and Oppenheimer, J.R., 1927, Born-Oppenheimer approximation, Ann. Phys. (Leipzig)., 84, 457pp.

Brillouin, L., 1934, Les champs self-consistents de Hartree et de Fock, Act. Sci. Ind., 71, 159pp.

Chai, J.D. and Head-gordon, M., 2008, Long-range corrected hybrid density functionals with damped atom − atom dispersion corrections w, Physical Chemistry Chemical Physics., 10(44), 6615–6620pp.

Chai, J. Da and Head-Gordon, M., 2008, Systematic optimization of long-range corrected hybrid density functionals, Journal of Chemical Physics., 128(8).

Chandra, M. and Xu, Q., 2006, A high-performance hydrogen generation system: Transition metal-catalyzed dissociation and hydrolysis of ammonia-borane, Journal of Power Sources., 156(2), 190–194pp.

REFERENCES (Continued)

Chen, H., Cong, T.N., Yang, W., Tan, C., Li, Y. and Ding, Y., 2009, Progress in electrical energy storage system: A critical review, Progress in Natural Science., National Natural Science Foundation of China and Chinese Academy of Sciences, 19(3), 291–312pp.

Chen, P., 1999, High H2 Uptake by Alkali-Doped Carbon Nanotubes Under Ambient Pressure and Moderate Temperatures, Science., 285(1999), 91–93pp.

Cheng, H.M., Yang, Q.H. and Liu, C., 2001, Hydrogen storage in carbon nanotubes, Carbon., 39(10), 1447–1454pp.

Chopra, N.G., Luyken, R.J., Cherrey, K., Crespi, V.H., Cohen, M.L., Louie, S.G. and Zettl, D.,1995, Boron nitride nanotubes., Science (New York, N.Y.)., 269(5226), 966–967pp.

Chu, P. K., Zhi, C., Bando, Y., Tang, C. and Golberg, D., 2010, Boron nitride nanotubes, Materials Science and Engineering: R: Reports., Elsevier B.V., 70(3), 92–111pp.

Cook, T.R., Dogutan, D.K., Reece, S.Y., Surendranath, Y., Teets, T.S. and Nocera, D.G., 2010, Solar energy supply and storage for the legacy and nonlegacy worlds, Chemical Reviews., 110(11), 6474–6502pp.

Zhang, D. and Zhang Q., 2003, Theoretical prediction on aluminum nitride nanotubes, Chemical Physics Letters., 371(3–4), 426–432pp.

Dennington, R., Keith, T. and Millam, J., 2009, GaussView, Version 5., Semichem Inc. , Shawnee Mission, KS.

Dillon, C., Jones, K.M., Bekkedahl, T., Kiang, C.H., Bethune, D.S. and Heben, M.J., 1997, Storage of hydrogen in single-walled carbon nanotubes, Nature.

Esrafili, M.D. and Nurazar, R., 2014, Efficient dehydrogenation of formic acid using Al12N12 nanocage: A DFT study, Superlattices and Microstructures., 75, 17–26pp.

Fakioglu, E., 2004, A review of hydrogen storage systems based on boron and its compounds, International Journal of Hydrogen Energy., 29(13), 1371–1376pp.

REFERENCES (Continued)

Fanfrlík, J., Bronowska, A.K., Řezáč, J., Přenosil, O., Konvalinka, J. and Hobza, P., 2010, A reliable docking/scoring scheme based on the semiempirical quantum mechanical PM6-DH2 method accurately covering dispersion and H-bonding: HIV-1 protease with 22 ligands, Journal of Physical Chemistry B., 114(39), 12666–12678pp.

Fellay, C., Dyson, P.J. and Laurenczy, G., 2008, A viable hydrogen-storage system based on selective formic acid decomposition with a ruthenium catalyst, Angewandte Chemie - International Edition., 47(21), 3966–3968pp.

Frecus, B., Buta, C.M., Oprea, C.I., Stroppa, A., Putz, M.V. and Cimpoesu, F., 2016, Noble gas endohedral fullerenes, Ng@C60 (Ng=Ar, Kr): a particular benchmark for assessing the account of non-covalent interactions by density functional theory calculations, Theoretical Chemistry Accounts., Springer Berlin Heidelberg, 135(5), 1–9pp.

Frisch, M.J., Trucks, G.W., Schlegel, H.B., Scuseria, G.E., Robb, M.A., Cheeseman, J.R., Scalmani, G., Barone, V., Mennucci, B., Petersson, G.A., Nakatsuji, H., Caricato, M., Li, X., Hratchian, H.P., Izmaylov, A.F., Bloino, J., Zheng, G., Sonnenberg, J.L., Hada, M., Ehara, M., Toyota, K., Fukuda, R., Hasegawa, J., Ishida, M., Nakajima, T., Honda, Y., Kitao, O., Nakai, H., Vreven, T., Montgomery Jr., J.A., Peralta, J.E., Ogliaro, F., Bearpark, M., Heyd, J.J., Brothers, E., Kudin, K.N., Staroverov, V.N., Kobayashi, R., Normand, J., Raghavachari, K., Rendell, A., Burant, J.C., Iyengar, S.S., Tomasi, J., Cossi, M., Rega, N., Millam, J.M., Klene, M., Knox, J.E., Cross, J.B., Bakken, V., Adamo, C., Jaramillo, J., Gomperts, R., Stratmann, R.E., Yazyev, O., Austin, A.J., Cammi, R., Pomelli, C., Ochterski, J.W., Martin, R.L., Morokuma, K., Zakrzewski, V.G., Voth, G.A., Salvador, P., Dannenberg, J.J., Dapprich, S., Daniels, A.D., Farkas, ., Foresman, J.B., Ortiz, J.V, Cioslowski, J. and Fox, D.J., 2010, Gaussian09 Revision D.01, Gaussian Inc. Wallingford CT, Gaussian 09 Revision C.01.

REFERENCES (Continued)

Fthenakis, V. and Kim, H. C., 2009, Land use and electricity generation: A life-cycle analysis, Renewable and Sustainable Energy Reviews., 13(6–7), 1465–1474pp.

Gali, A., 2006, Ab initio study of nitrogen and boron substitutional impurities in single-wall SiC nanotubes, Physical Review B - Condensed Matter and Materials Physics., 73(24).

Galindo-Murillo, R. and Barroso-Flores, J., 2017, Structural and Dynamical instability of DNA by high occurrence of d5SICS and dNaM unnatural nucleotides, Phys. Chem. Chem. Phys., 10571–10580pp.

Galindo Cifre, P. and Badr, O., 2007, Renewable hydrogen utilisation for the production of methanol, Energy Conversion and Management., 48(2), 519–527pp.

Glenn, L.A., 2005, Thoughts on Starting the Hydrogen Economy, Physics Today., 58(6), 14–14pp.

Golberg, D., Bando, Y., Huang, Y. and Terao, T., 2010, Boron nitride nanotubes and nanosheets, Acs Nano., 4(6), 2979–2993pp.

Grasemann, M. and Laurenczy, G., 2012, Formic acid as a hydrogen source – recent developments and future trends, Energy & Environmental Science., 5, 8171pp.

Green, L., 1982, An ammonia energy vector for the hydrogen economy, International Journal of Hydrogen Energy., 7(4), 355–359pp.

Grimme, S., 2006, Semiempirical GGA-type density functional constructed with a long-range dispersion correction, Journal of Computational Chemistry., 27(15), 1787–1799pp.

Grimme, S., Antony, J., Ehrlich, S. and Krieg, H., 2010, A consistent and accurate ab initio parametrization of density functional dispersion correction (DFT-D) for the 94 elements H-Pu, Journal of Chemical Physics., 132(15).

Grochala, W. and Edwards, P.P., 2004, Thermal decomposition of the non-interstitial hydrides for the storage and production of hydrogen, Chemical Reviews., 104(3), 1283–1315pp.

REFERENCES (Continued)

Gtz, D.G., 2010, Renewables 2010 Global Status Report, Nuclear Safety., 2010(01.02.2011), 80pp.

Hall, G.G., 1951, The Molecular Orbital Theory of Chemical Valency. VIII. A Method of Calculating Ionization Potentials, Proceedings of the Royal Society A: Mathematical, Physical and Engineering Sciences., 205(1083), 541–552pp.

Hanwell, M.D., Curtis, D.E., Lonie, D.C., Vandermeerschd, T., Zurek, E. and Hutchison, G.R., 2012, Avogadro: An advanced semantic chemical editor, visualization, and analysis platform, Journal of Cheminformatics.

Hassan, M.H. and Kalam, M.A., 2013, An overview of biofuel as a renewable energy source: Development and challenges, Procedia Engineering., Elsevier B.V., 56, 39–53pp.

Hernández Velázquez, J.D., Barroso-Flores, J. and Gama Goicochea, A., 2016, Ab Initio Modeling Of Friction Reducing Agents Shows Quantum Mechanical Interactions Can Have Macroscopic Manifestation, The Journal of Physical Chemistry A., acs.jpca.6b07890pp.

Hirscher, M. and Borgschulte, A., 2010, *Handbook of hydrogen storage: New Materials for Future Energy Storage*, Ceramic.

Hofmann, H. and Kreuter, W., 1998, Electrolysis : the Important Energy Transformer, Int. J. Hydrogen Energy., 23(8), 661–666pp.

Hohenberg, P. and Kohn, W., 1964, Inhomogeneous Electron Gas, Physical Review., American Physical Society, 136(3B), b864–B871pp.

Hostaš, J., Řezáč, J. and Hobza, P., 2013, On the performance of the semiempirical quantum mechanical PM6 and PM7 methods for noncovalent interactions, Chemical Physics Letters., 568–569, 161–166pp.

Hwang, Y. and Chung, Y.C., 2013, Lithium Adsorption on Hexagonal Boron Nitride Nanosheet Using Dispersion-Corrected Density Functional Theory Calculations, Japanese Journal of Applied Physics., 52(6S), 06gg08pp.

Ijiima, S., 1991, IIjima, 1991, Helical microtubles of graphitic carbon.pdf, Nature., 354, 56–58pp.

REFERENCES (Continued)

International Energy Agency, 2011, *Solar Energy Perspectives*, Solar Energy Perspectives.

Izquierdo, U., Barrio, V.L., Cambra, J.F., Requies, J., Güemez, M.B., Arias, P.L., Kolb, G., Zapf, R., Gutiérrez, A.M. and Arraibi, J.R., 2012, Hydrogen production from methane and natural gas steam reforming in conventional and microreactor reaction systems, International Journal of Hydrogen Energy., 37(8), 7026–7033pp.

Joó, F., 2008, Breakthroughs in hydrogen storage\-formic acid as a sustainable storage material for hydrogen, ChemSusChem., 1(10), 805–808pp.

Joubert, J.-M.M., Cerny, R., Latroche, M., Leroy, E., Guenee, L., Percheron-Guegan, A., Yvon, K., Černý, R., Guénée, L. and Guégan, P., 2002, A Structural Study of the Homogeneity Domain of LaNi5, Journal of Solid State Chemistry., 166(1), 1–6pp.

Kınal, A. and Sayhan, S., 2016, Accurate prediction of hydrogen storage capacity of small boron nitride nanocages by dispersion corrected semi-empirical PM6-DH2 method, International Journal of Hydrogen Energy., 41(1), 392–400pp.

Kohn, W. and Sham, L.J., 1965, Self-Consistent Equations Including Exchange and Correlation Effects, Physical Review., American Physical Society, 140(4A), a1133–A1138pp.

Koi, N. and Oku, T., 2004, Hydrogen storage in boron nitride and carbon clusters studied by molecular orbital calculations, Solid State Communications., 131, 121–124pp.

Kruger, P., 2001, Electric power requirement for large-scale production of hydrogen fuel for the world vehicle fleet, International Journal of Hydrogen Energy., 26(11), 1137–1147pp.

Kudo, A. and Miseki, Y., 2009, Heterogeneous photocatalyst materials for water splitting., Chemical Society reviews., 38(1), 253–278pp.

REFERENCES (Continued)

Kuniyil, R. and Maseras, F., 2017, Computational study on the mechanism of the reaction of carbon dioxide with siloxy silanes, Theoretical Chemistry Accounts., Springer Berlin Heidelberg, 136(5), 65pp.

Lan, R., Irvine, J.T.S. and Tao, S., 2012, Ammonia and related chemicals as potential indirect hydrogen storage materials, International Journal of Hydrogen Energy., Elsevier Ltd, 37(2), 1482–1494pp.

Leach, A.R., 2001, *Molecular Modelling: Principles and Applications*, AddisonWesley Longman Ltd.

Lee, C., Yang, W. and Parr, R.G., 1988a, Development of the Colle-Salvetti correlation-energy formula into a functional of the electron density, Physical Review B., 37(2), 785–789pp.

Lee, C., Yang, W. and Parr, R.G., 1988, Development of the Colle-Salvetti correlation-energy formula into a functional of the electron density, Physical Review B., American Physical Society, 37(2), 785–789pp.

Lee, H., Ihm, J., Cohen, M.L. and Louie, S.G., 2010, Calcium-decorated graphene-based nanostructures for hydrogen storage, Nano Letters., 10(3), 793–798pp.

Lei, W., Zhang, H., Wu, Y., Zhang, B., Liu, D., Qin, S., Liu, Z., Liu, L., Ma, Y., and Chen, Y., 2014, Oxygen-doped boron nitride nanosheets with excellent performance in hydrogen storage, Nano Energy., Elsevier, 6, 219–224pp.

Lewis, N.S. and Nocera, D.G., 2006, Powering the planet: Chemical challenges in solar energy utilization, Proceedings of the National Academy of Sciences., 103(43), 15729–15735pp.

Li, C., Wang, M., Pan, J., Zhang, P., Zhang, R. and Sun, L., 2009, Photochemical hydrogen production catalyzed by polypyridyl ruthenium-cobaloxime heterobinuclear complexes with different bridges, Journal of Organometallic Chemistry., 694(17), 2814–2819pp.

Lieb, E. H. and Simon, B., 1977, The Thomas-Fermi theory of atoms, molecules and solids, Advances in Mathematics., 23(1), 22–116pp.

REFERENCES (Continued)

Lim, S. H. and Lin, J.Y., 2008, Ab initio study of the hydrogen chemisorption of single-walled aluminum nitride nanotubes, Chemical Physics Letters., 466(4–6), 197–204pp.

Ma, Q.L., Peng, R.R., Tian, L.Z. and Meng, G.Y., 2006, Direct utilization of ammonia in intermediate-temperature solid oxide fuel cells, Electrochemistry Communications., 8(11), 1791–1795pp.

Ma, R., Bando, Y., Zhu, H., Sato, T., Xu, C. and Wu, D., 2002, Hydrogen uptake in boron nitride nanotubes at room temperature, Journal of the American Chemical Society., 124(26), 7672–7673pp.

Ma, S., 2011, First-Principles Study of Hydrogen Molecules Adsorbed on Al-Doped BN Sheets, Advanced Materials Research., 197–198, 701–704pp.

Mananghaya, M., Yu, D. and Santos, G.N., 2016, Hydrogen adsorption on boron nitride nanotubes functionalized with transition metals, International Journal of Hydrogen Energy., Elsevier Ltd, 41(31), 13531–13539pp.

McCarty, R.D., 1981, Selected Properties of Hydrogen (Engineering Design Data).

Meng, T., Wang, C.Y. and Wang, S.Y., 2007, First-principles study of a single Ti atom adsorbed on silicon carbide nanotubes and the corresponding adsorption of hydrogen molecules to the Ti atom, Chemical Physics Letters., 437(4–6), 224–228pp.

Møller, C. and Plesset, M.S., 1934, Note on an Approximation Treatment for Many-Electron Systems, Physical Review., American Physical Society, 46(7), 618–622pp.

Moradi, M. and Naderi, N., 2014, First principle study of hydrogen storage on the graphene-like aluminum nitride nanosheet, Structural Chemistry., 25(4), 1289–1296pp.

Mpourmpakis, G., Tylianakis, E. and Froudakis, G.E., 2007, Carbon nanoscrolls: A promising material for hydrogen storage, Nano Letters., 7(7), 1893–1897pp.

REFERENCES (Continued)

Baei, M., Soltani, A. and Hashemian, S., 2016, Adsorption properties of hydrazine on pristine and, Phosphorus, Sulfur, and Silicon and the Related Elements., 6507(March 2017).

Nagy, P.I., 2016, Replacement of oxygen by sulfur in small organic molecules. 3. Theoretical studies on the tautomeric equilibria of the 2OH and 4OH-substituted oxazole and thiazole and the 3OH and 4OH-Substituted isoxazole and isothiazole in the isolated state and in solu, International Journal of Molecular Sciences., 17(7), 1–14pp.

Naresh Muthu, R., Rajashabala, S. and Kannan, R., 2015, Synthesis and characterization of polymer (sulfonated poly-ether-ether-ketone) based nanocomposite (h-boron nitride) membrane for hydrogen storage, International Journal of Hydrogen Energy., Elsevier Ltd, 40(4), 1836–1845pp.

Ni, M., Huang, L., Guo, L. and Zeng, Z., 2010, Hydrogen storage in Li-doped charged single-walled carbon nanotubes, International Journal of Hydrogen Energy., 35(8), 3546–3549pp.

Oliveira, F.M., Barbosa, L.C.A., Fernandes, S.A., Lage, M.R., Carneiro, J.W. D.M. and Kabeshov, M.A., 2016, Evaluation of some density functional methods for the estimation of hydrogen and carbon chemical shifts of phosphoramidates, Computational and Theoretical Chemistry., Elsevier B.V., 1090, 218–224pp.

Perdew, J.P., 1986, Density-functional approximation for the correlation-energy of the inhomogeneous electron-gas, Physical Review B., 33(12), 8822pp.

Perdew, J.P., Burke, K. and Ernzerhof, M., 1996, Generalized Gradient Approximation Made Simple, Physical Review Letters., 77(18), 3865–3868pp.

Perdew, J.P. and Wang, Y., 1992, Accurate and simple analytic representation of the electron-gas correlation energy, Physical Review B., 45(23), 13244–13249pp.

REFERENCES (Continued)

Pham-Huu, C., 2001, The First Preparation of Silicon Carbide Nanotubes by Shape Memory Synthesis and Their Catalytic Potential, Journal of Catalysis., 200(2), 400–410pp.

Pollmann, J., Peng, X., Wieferink, J. and Kroger, P., 2014, Adsorption of hydrogen and hydrocarbon molecules on SiC(001), Surface Science Reports.

Pople, J.A., Krishnan, R., Schlegel, H.B., and Binkley, J.S., 1978, Electron correlation theories and their application to the study of simple reaction potential surfaces, International Journal of Quantum Chemistry., John Wiley & Sons, Inc., 14(5), 545–560pp.

Pople, J.A. and Nesbet, R.K., 1954, Self-Consistent Orbitals for Radicals, The Journal of Chemical Physics., American Institute of Physics, 22(3), 571–572pp.

Pople, J., Head-Gordon, M., and Raghavachari, K. ,1987, Quadratic configuration interaction. A general technique for determining electron correlation energies, The Journal of Chemical Physics., 87(10), 5968pp.

Purvis, G.D. and Bartlett, R.J., 1982, A full coupled-cluster singles and doubles model: The inclusion of disconnected triples, The Journal of Chemical Physics., American Institute of Physics, 76(4), 1910–1918pp.

Rad, A.S. and Ayub, K., 2016, Enhancement in hydrogen molecule adsorption on B12N12 nano-cluster by decoration of nickel, International Journal of Hydrogen Energy., 41(47), 22182–22191pp.

Raghavachari, K., Binkley, J.S., Seeger, R. and Pople, J.A., 1980, Self-Consistent Molecular Orbital Methods. 20. Basis set for correlated wave-functions, Journal of Chemical Physics., 72, 650–654pp.

Řezáč, J., 2016, Cuby: An integrative framework for computational chemistry, Journal of Computational Chemistry., 37(13), 1230–1237pp.

Ritschel, M., Uhlemann, M., Gutfleisch, O., Leonhardt, A., Graff, A., Täschner, C. and Fink, J., 2002, Hydrogen storage in different carbon nanostructures, Applied Physics Letters., 80(16), 2985–2987pp.

REFERENCES (Continued)

Roothaan, C.C.J., 1951, New developments in molecular orbital theory, Rev. Mod. Phys., 23(2), 69pp.

Rubio, A., Corkill, J.L. and Cohen, M.L., 1994, Theory of graphitic boron nitride nanotubes, Physical Review B., 49(7), 5081–5084pp.

Sorensen, R.Z., Hummelshoj, J.S., Klerke, A., Reves, J.B., Vegge, T., Norskov, J.K. and Christensen, C.H., 2008, Indirect, reversible high-density hydrogen storage in compact metal ammine salts, Journal of the American Chemical Society., 130(27), 8660–8668pp.

Sakintuna, B., Lamari-Darkrim, F. and Hirscher, M., 2007, Metal hydride materials for solid hydrogen storage: A review, International Journal of Hydrogen Energy.

Sandrock, G., Reilly, J., Graetz, J., Zhou, W.M., Johnson, J. and Wegrzyn, J., 2005, Accelerated thermal decomposition of AlH3 for hydrogen-fueled vehicles, Applied Physics A: Materials Science and Processing., 80(4), 687–690pp.

Satyapal, S., Petrovic, J., Read, C., Thomas, G. and Ordaz, G., 2007, The U.S. Department of Energy's National Hydrogen Storage Project: Progress towards meeting hydrogen-powered vehicle requirements, Catalysis Today., 120(3–4 SPEC. ISS.), 246–256pp.

Schlapbach, L. and Züttel, A., 2001, Hydrogen-storage materials for mobile applications., Nature., 414(6861), 353–358pp.

Schulz, R., Huot, J., Liang, G., Boily, S. and Van Neste, A., 1999, Structure and hydrogen sorption properties of ball milled Mg dihydride, Materials Science Forum., 312, 615–622pp.

Schüth, F., Bogdanović, B. and Felderhoff, M., 2004, Light metal hydrides and complex hydrides for hydrogen storage., Chemical communications (Cambridge, England)., (20), 2249–2258pp.

Scuseria, G.E., Janssen, C.L. and Schaefer, H.F., 1988, An efficient reformulation of the closed-shell coupled cluster single and double excitation (CCSD) equations, The Journal of Chemical Physics., American Institute of Physics, 89(12), 7382–7387pp.

REFERENCES (Continued)

Scuseria, G.E., Schaefer, H.F. and Schaefer Iii, H.F., 1989, Is coupled cluster singles and doubles (CCSD) more computationally intensive than quadratic configuration interaction (QCISD)?, J. Chem. Phys. Additional information on J. Chem. Phys. Journal Homepage., 90(3700).

Serov, A. and Kwak, C., 2010, Direct hydrazine fuel cells: A review, Applied Catalysis B: Environmental.

Seyller, T., 2004, Passivation of hexagonal SiC surfaces by hydrogen termination, Journal of Physics: Condensed Matter., 16(17), s1755–S1782pp.

Singh, A.K., Singh, S. and Kumar, A., 2015, Hydrogen energy future with formic acid: a renewable chemical hydrogen storage system, Catal. Sci. Technol., Royal Society of Chemistry, 6, 12–40pp.

Singh, S.K. and Xu, Q., 2009, Complete conversion of hydrous hydrazine to hydrogen at room temperature for chemical hydrogen storage, Journal of the American Chemical Society., 131(50), 18032–18033pp.

Solangi, K.H., Islam, M.R., Saidur, R., Rahim, N.A. and Fayaz, H., 2011, A review on global solar energy policy, Renewable and Sustainable Energy Reviews.

Song, N., Wang, Y., Zheng, Y., Zhang, J., Xu, B., Sun, Q. and Jia, Y., 2015, New template for Li and Ca decoration and hydrogen adsorption on graphene-like SiC: A first-principles study, Computational Materials Science., 99, 150–155pp.

Springborg, M., 2000, *Methods of electronic-structure calculations : from molecules to solids*,Wiley.

Staroverov, V.N. and Davidson, E.R., 2001, The cope rearrangement in theoretical retrospect, Journal of Molecular Structure: THEOCHEM.

Staroverov, V.N., Scuseria, G.E., Tao, J. and Perdew, J.P., 2003, Comparative assessment of a new nonempirical density functional: Molecules and hydrogen-bonded complexes, Journal of Chemical Physics., 119(23), 12129–12137pp.

REFERENCES (Continued)

Steffen, C., Thomas, K., Huniar, U., Hellweg, A., Rubner, O. and Schroer, A., 2010, TmoleX-A graphical user interface for TURBOMOLE, Journal of Computational Chemistry.

Stewart, J.J.P., 1990, MOPAC: A semiempirical molecular orbital program, Journal of Computer-Aided Molecular Design.

Stewart, J.J.P., 2009, Application of the PM6 method to modeling proteins, Journal of Molecular Modeling., 15(7), 765–805pp.

Stewart, J.J.P., 2013, Optimization of parameters for semiempirical methods VI: more modifications to the NDDO approximations and re-optimization of parameters, Journal of Molecular Modeling., 19(1), 1–32pp.

Styrov, V.V., Tyutyunnikov, V.I., Sergeev, O.T., Oya, Y. and Okuno, K., 2005, Chemical reactions of atomic hydrogen at SiC surface and heterogeneous chemiluminescence, Journal of Physics and Chemistry of Solids., 513–520.

Sun, Q., Wang, Q. and Jena, P., 2005, Storage of molecular hydrogen in B-N cage: Energetics and thermal stability, Nano Letters., 5, 1273–1277pp.

Tang, C., Bando, Y., Ding, X., Qi, S. and Golberg, D., 2002, Catalyzed collapse and enhanced hydrogen storage of BN nanotubes, Journal of the American Chemical Society., 124(49), 14550–14551pp.

Tokarev, A., Kjeang, E., Cannon, M. and Bessarabov, D., 2016, Theoretical limit of reversible hydrogen storage capacity for pristine and oxygen-doped boron nitride, International Journal of Hydrogen Energy., Elsevier Ltd, 41(38), 16984–16991pp.

Vosko, S.H., Wilk, L. and Nusair, M., 1980, Accurate spin-dependent electron liquid correlation energies for local spin density calculations: a critical analysis, Canadian Journal of Physics., 58(8), 1200–1211pp.

Vydrov, O.A., Heyd, J., Krukau, A.V. and Scuseria, G.E., 2006, Importance of short-range versus long-range Hartree-Fock exchange for the performance of hybrid density functionals, Journal of Chemical Physics., 125(7).

REFERENCES (Continued)

Wang, G., Yuan, H., Kuang, A., Hu, W., Zhang, G. and Chen, H., 2014, High-capacity hydrogen storage in Li-decorated (AlN)n (n = 12, 24, 36) nanocages, International Journal of Hydrogen Energy., 39(8), 3780–3789pp.

Wang, J., Lee, C. H. and Yap, Y.K., 2010, Recent advancements in boron nitride nanotubes, Nanoscale., 2(10), 2028pp.

Wang, L. and Yang, R.T., 2010, Hydrogen Storage on Carbon-Based Adsorbents and Storage at Ambient Temperature by Hydrogen Spillover, Catalysis Reviews., 52(4), 411–461pp.

Wang, P., Hu, Y., Zhan, H. and Chen, J., 2017, Gas-phase conformational preference of the smallest saccharide (glycolaldehyde) and its hydrated complexes with bridged hydrogen bonding, RSC Adv., Royal Society of Chemistry, 7(11), 6242–6250pp.

Wang, Q., Sun, Q., Jena, P. and Kawazoe, Y., 2009, Potential of AlN nanostructures as hydrogen storage materials, ACS Nano., 3(3), 621–626pp.

Wang, X., and Liew, K. M., 2012, Density functional study of interaction of lithium with pristine and Stone-Wales-defective single-walled silicon carbide nanotubes, Journal of Physical Chemistry C., 116(51), 26888–26897pp.

Weigend, F., 2006, Accurate Coulomb-fitting basis sets for H to Rn, Physical Chemistry Chemical Physics., 8(9), 1057pp.

Wu, H., Fan, X. and Kuo, J.L., 2012, Metal free hydrogenation reaction on carbon doped boron nitride fullerene: A DFT study on the kinetic issue, International Journal of Hydrogen Energy., Elsevier Ltd, 37(19), 14336–14342pp.

Wu, H. S., Jiao, H., Cui, X.Y., Qin, X. F. and Strout, D.L., 2006, Boron nitride cages from B12N12to B36N36: Square-hexagon alternants vs boron nitride tubes, Journal of Molecular Modeling.

Xu, X. and Goddard, W.A., 2004, The X3LYP extended density functional for accurate descriptions of nonbond interactions, spin states, and thermochemical properties, Proceedings of the National Academy of Sciences of the United States of America., 101(9), 2673–2677pp.

REFERENCES (Continued)

Yanai, T., Tew, D.P. and Handy, N.C., 2004, A new hybrid exchange-correlation functional using the Coulomb-attenuating method (CAM-B3LYP), Chemical Physics Letters., 393(1–3), 51–57pp.

Yang, F.H. and Yang, R.T., 2002, Ab initio molecular orbital study of adsorption of atomic hydrogen on graphite: Insight into hydrogen storage in carbon nanotubes, Carbon., 40(3), 437–444pp.

Yang, J., Sudik, A., Wolverton, C. and Siegel, D.J., 2010, High capacity hydrogen storage materials: attributes for automotive applications and techniques for materials discovery, Chemical Society Reviews., 39(2), 656–675pp.

Yang, R. T., 2000, Hydrogen storage by alkali-doped carbon nanotubes-revisited, Carbon., 38(4), 623–626pp.

Ye, X., Wang, Y., Hopkins, R.C., Adams, M.W.W., Evans, B.R., Mielenz, J.R. and Zhang, Y.H.P., 2009, Spontaneous high-yield production of hydrogen from cellulosic materials and water catalyzed by enzyme cocktails, ChemSusChem., 2(2), 149–152pp.

Zaluska, A., Zaluski, L. and Strom-Olsen, J.O., 1999, Nanocrystalline magnesium for hydrogen storage, Journal of Alloys and Compounds., 288 (1–2), 217–225pp.

Zaluski, L., Zaluska, A. and Ström-Olsen, J., 1997, Nanocrystalline metal hydrides, Journal of Alloys and Compounds., 253–254, 70–79pp.

Zarkevich, N.A. and Johnson, D.D., 2006, Comment on "structural stability of complex hydrides: LiBH4 revisited," Physical Review Letters.

Zhang, G. and Musgrave, C.B., 2007, Comparison of DFT methods for molecular orbital eigenvalue calculations, Journal of Physical Chemistry A., 111(8), 1554–1561pp.

Zhang, Y.H.P., 2009, A sweet out-of-the-box solution to the hydrogen economy: is the sugar-powered car science fiction?, Energy \& Environmental Science., 2(3), 272pp.

REFERENCES (Continued)

Zhang, Y.H.P., 2011, Simpler is better: High-yield and potential low-cost biofuels production through cell-free synthetic pathway biotransformation (SyPaB), ACS Catalysis.

Zhang, Y., Zheng, X., Zhang, S., Huang, S., Wang, P. and Tian, H., 2012, Bare and Ni decorated Al12N12 cage for hydrogen storage: A first-principles study, International Journal of Hydrogen Energy., 37(17), 12411–12419pp.

Zhao, Y. and Truhlar, D.G., 2006, Density functional for spectroscopy: No long-range self-interaction error, good performance for Rydberg and charge-transfer states, and better performance on average than B3LYP for ground states, Journal of Physical Chemistry A., 110(49), 13126–13130pp.

Zhao, Y. and Truhlar, D.G., 2006b, A new local density functional for main-group thermochemistry, transition metal bonding, thermochemical kinetics, and noncovalent interactions, Journal of Chemical Physics., 125(19).

Zhao, Y. and Truhlar, D.G., 2008, The M06 suite of density functionals for main group thermochemistry, thermochemical kinetics, noncovalent interactions, excited states, and transition elements: Two new functionals and systematic testing of four M06-class functionals and 12 other function, Theoretical Chemistry Accounts., 120(1–3), 215–241pp.

Zhou, L., 2005, Progress and problems in hydrogen storage methods, Renewable and Sustainable Energy Reviews.

Zhou, Z., Zhao, J., Chen, Z., Gao, X., Yan, T., Wen, B. and Schleyer, P.V.R., 2006, Comparative study of hydrogen adsorption on carbon and BN nanotubes., The journal of physical chemistry. B., 110(27), 13363–13369pp.

Zhu, M., Wang, H., Ouyang, L.Z. and Zeng, M.Q., 2006, Composite structure and hydrogen storage properties in Mg-base alloys, International Journal of Hydrogen Energy., 251–257.

Züttel, A., 2004, Hydrogen storage methods, Naturwissenschaften., 91(4), 157–172pp.

ACKNOWLEDGMENT

Sometimes, there are several important breaking points that may cause good change of person life. In my point, one of these breaking points is to meet Prof. Dr. Armağan KINAL. He always aimed me to be a better person having both as academic and social. In addition, He also supported me even when I felt terrible during my thesis period. In my eyes, he is the person who teach me how to learn. Therefore, I would like to thank Prof. Dr. Armağan KINAL due to his friendship, sensibility, humanity and being good supervisor. I am extremely pleased to work together and always I will be.

I also thank to Assoc. Prof. Dr. Nursel ACAR SELÇUKİ and Prof. Dr. Cenk SELÇUKİ. They made me think differently and freely during my thesis period and they did not never avoid to share their academic experience with me.

I would like to send a special thank to my dear wife, Eylül Başkurt SAYHAN because of her patience, love, countless help. I owe her a great deal.

I also thank to my special friends Yaşar DIKICI and Uğur USLU because of their moral support.

Finally, I thank to TUBITAK because they provided me to National Scholarship for priority fields in science (2211-C) and most of the calculations reported in this thesis were performed at High Performance and Grid Computing Center (TRUBA resources), ULAKBIM in TUBITAK.

CURRICULUM VITAE

Name Surname   **:** Sinan Sayhan

Profession   **:** Chemist

Date/Place of Birth   **:** 05.07.1985 / İZMİR

Nationality   **:** Turkish

Gender   : Male

Marital Status   **:** Married

Adress   **:** Ege University, Faculty of Science Department of Chemistry Division of Physical Chemistry, 35100 Bornova-İzmir/Turkey

e-mail   **:** sinansayhan@hotmail.com

EDUCATIONAL BACKGROUND

Bachelor Study.   In Chemistry, 2008, Brno University of Technology Brno-Czech Republic, 2009, Selcuk University Konya-Turkey

MS Study, 2011-2013   Ege University Institue of Naturel and Applied Science Deparment of Chemistry

LIST OF PUBLICATIONS

1. **S. Sayhan** and A. Kınal, Computational investigation and comparison of hydrogen storage properties of $B_{24}N_{24}$ and $Al_{24}N_{24}$ nanocages; *International journal of hydrogen energy* 42 (2017) 14166-14180.

2. **S.Sayhan** and A.Kınal Accurate Prediction of Hydrogen Storage Capacity of Small Boron NitrideNanocages by Dispersion Corrected Semi-empirical PM6-DH2 Method, *International Hydrogen Energy*, 2016.

3. **S.Sayhan** and A.Kınal, Stability of Endohedral Hydrogen Doped Boron Nitride Nanocages: A Density Functional Theory Study, *Asian Journal of Chemistry*, Vol. 26, No.18 (2014), 5935-5939.

4. **S.Sayhan** and A.Kınal, Computational Investigation of Hydrogen Storage Capacity Boron Nitride Nanocages by Newly Developed PM7 method, *Asian Journal of Chemistry*, Vol. 27, No.2 (2015), 667- 670.